โครงสร้างซุปราโมเลคิวลาร์ของสารประกอบอะไซโคลเวียร์ยาต้านไวรัสเฮอร์พีทและสารประกอบที่เกี่ยวข้อง

นางสาวมณฑา หมีไพรพฤกษ์

SUPRAMOLECULAR STRUCTURE OF THE HERPES

ANTIVIRAL AGENT ACYCLOVIR AND

RELATED COMPOUNDS

Montha Meepripruk

A Thesis Submitted in Partial Fulfillment of the Requirements for the

Degree of Doctor of Philosophy in Biochemistry

Suranaree University of Technology

Academic Year 2012

SUPRAMOLECULAR STRUCTURE OF THE HERPES

ANTIVIRAL AGENT ACYCLOVIR AND

RELATED COMPOUNDS

Suranaree University of Technology has approved this thesis submitted in partial fulfillment of the requirements for the Degree of Doctor of Philosophy.

Thesis Examining Committee
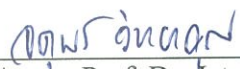
_____
(Assoc. Prof. Dr. Jatuporn Wittayakun)

Chairperson

_____
(Assoc. Prof. Dr. Kenneth J. Haller)

Member (Thesis Advisor)

_____
(Prof. Dr. James R. Ketudat-Cairns)

Member
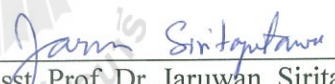
_____
(Asst. Prof. Dr. Jaruwan Siritapetawee)

Member

_____
(Dr. Samroeng Krachodnok)

Member

_____
(Prof. Dr. Sukit Limpijumnong)

Vice Rector for Academic Affairs

_____
(Assoc. Prof. Dr. Prapun Manyum)

Dean of Institute of Science

นางสาวมณฑา หมีไพรพฤกษ์ : โครงสร้างซุปราโมเลคิวลาร์ของสารประกอบอะไซโคล
เวียร์ยาต้านไวรัสเฮอร์พีทและสารประกอบที่เกี่ยวข้อง (SUPRAMOLECULAR
STRUCTURE OF THE HERPES ANTIVIRAL AGENT ACYCLOVIR AND
RELATED COMPOUNDS) อาจารย์ที่ปรึกษา : รองศาสตราจารย์ ดร. เค็นเนท เจ
แฮลเลอร์, 158 หน้า.

อะไซโคลเวียร์เป็นยาต้านไวรัสเฮอร์พีทชนิด 1 และ 2 และวาริเซลลาซอสเตอร์ ข้อดีของอะ
ไซโคลเวียร์คือมีพิษน้อยและไวรัสเฮอร์พีทมีความต้านทานต่ออะไซโคลเวียร์ต่ำ ซึ่งผลเสียของอะ
ไซโคลเวียร์คือมีการออกฤทธิ์ทางชีวภาพต่ำเนื่องจากมีข้อจำกัดในการละลายของตัวยา สูตร
โครงสร้างของอะไซโคลเวียร์ $C_8H_{11}N_5O_3$ ได้จากการแยกสารอะไซโคลเวียร์ออกจากอะไซโคลเวียร์
ยาต้านไวรัสเฮอร์พีท ผลึกมีลักษณะเป็นแผ่นบางๆโดยใช้น้ำเป็นตัวทำละลายและผลึกเดี่ยวจัดอยู่ใน
ระบบไตรคลินิกหมู่ $P\bar{1}$ มีแกนเอยาว 6.8996(6) อังสตรอม แกนบียาว 11.4170(9) อังสตรอม และ
แกนซี ยาว 15.0806(13) อังสตรอม ทำมุมแอลฟา 82.595(7) องศา มุมเบต้า 82.395(6) องศา มุม
แกมมา 89.368(6) องศา ที่อุณหภูมิ 293(2) เคลวิน โครงสร้างของผลึกประกอบด้วยอะไซโคลเวียร์
สองโมเลกุลคือโมเลกุลเอและบี และน้ำสี่โมเลกุลต่อหนึ่งหน่วยเซลล์ โดยที่วงแหวนของเบสกัวนีน
เชื่อมต่อกันโดยใช้พันธะไฮโดรเจนของ C–H···O, N–H···N และ N–H···O ทำให้เกิดสายคลื่นที่ยาว
ไม่มีที่สิ้นสุดในหนึ่งมิติทิศทางตั้งฉากกับแกนเอ ส่วนหางของอะไซโคลเวียร์ โมเลกุลบีในสายคลื่น
เชื่อมต่อกับส่วนหางของอะไซโคลเวียร์โมเลกุลบีในสายคลื่นที่ใกล้กันด้วยพันธะไฮโดรเจนแบบ
แยกเป็นสองทิศทางทำให้เกิดโครงสร้างสองมิติ โดยที่โครงข่ายสองมิติที่ใกล้กันเชื่อมต่อกันโดย
การเรียงซ้อนผ่านกัวนีนเพื่อสร้าง โครงสร้างสามมิติ โดยที่ระยะห่างระหว่างวงแหวนกัวนีนของ
โมเลกุลเอ/บีเท่ากับ 3.2950 (13) อังสตรอม และโมเลกุลบี/เอเท่ากับ 3.3925(18) อังสตรอม กลุ่มของ
น้ำจัดเรียงตัวแบบสายริบบิ้นยาวไม่มีที่สิ้นสุดเกิดจากการเชื่อมต่อเป็นสายโซ่ยาว ·[·O2–H···O1–
H···O3–H···O4–H·]∞ ของน้ำและอะไซโคลเวียร์ในรูปวงแหวนห้าเหลี่ยมสลับกันผ่านเข้าไปใน
ช่องว่าง สายของวงแหวนห้าเหลี่ยมประกอบด้วยลวดลายที่สลับกันแบบ $R_5^5(10)$ ของพันธะ
ไฮโดรเจนที่แข็งแรงซึ่งในวงห้าเหลี่ยมประกอบด้วยหนึ่งออกซิเจนของกลุ่มคาร์บอนิลหรือกลุ่มไฮ
ดรอกซิล การเกิดรูปแบบวงแหวนห้าเหลี่ยมที่มั่นคงทำให้เกิดโครงสร้างซุปราโมเลคิวลาร์ในสาม
มิติ

ไตรไซคลิกอะไซโคลเวียร์มีสูตรโมเลกุลคือ $C_{11}H_{13}N_5O_3$ มีการรายงานว่าประกอบด้วยน้ำ
สองโมเลกุล ซึ่งในการนำโครงสร้างเดิมของไตรไซคลิกอะไซโคลเวียร์ถูกนำมาปรับปรุงให้มี
รูปแบบของโครงสร้างที่ดีขึ้นโดยใช้ข้อมูลจากเอกสารอ้างอิง โดยการอธิบายเพิ่มเติมในส่วนของ

ความผิดปกติของไฮโดรเจนอะตอม ไตรไซคลิกอะไซโคลเวียร์กับสองโมเลกุลของน้ำเชื่อมขยายไป
ในทุกทิศทางด้วยพันธะไฮโดรเจนที่แข็งแรงประกอบเป็นโครงสร้างซุปราโมเลคิวลาร์ โมเลกุลของ
น้ำโดยจัดเรียงตัวเป็นกลุ่มของน้ำทั้งหมดแปดโมเลกุลด้วยพันธะไฮโดรเจนระหว่างน้ำสองโมเลกุล
ที่มีความยาวพันธะ [O⋯O] เท่ากับ 2.81 อังสตรอม เชื่อมต่อกันผ่านจุดผกผัน กลุ่มของน้ำมีปฏิกิริยา
กับโครงข่ายไตรไซคลิกอะไซโคลเวียร์ด้วยพันธะไฮโดรเจน O–H⋯O และ O–H⋯N กลายเป็นส่วน
หนึ่งของโครงข่ายสามมิติ ความผิดปกติอย่างไม่เป็นไปตามสถิติในองค์ประกอบหลักสามารถ
อธิบายได้โดยเกิดจากพันธะไฮโดรเจน C–H⋯O ที่ตำแหน่งของอะตอมที่ผิดปกติและเกิดพันธะ
ไฮโดรเจนที่ไม่ชัดเจนที่ออกซิเจนในตำแหน่งอื่น และเกิดพันธะไฮโดรเจนที่อ่อน   C–H⋯O ที่
ตำแหน่งของอะตอมที่ผิดปกติในองค์ประกอบรองของส่วนหาง

สาขาวิชาชีวเคมี   ลายมือชื่อนักศึกษา_____

ปีการศึกษา 2555   ลายมือชื่ออาจารย์ที่ปรึกษา_____

MONTHA MEEPRIPRUK : SUPRAMOLECULAR STRUCTURE OF THE
HERPES ANTIVIRAL AGENT ACYCLOVIR AND RELATED
COMPOUNDS. THESIS ADVISOR : ASSOC. PROF. KENNETH J.
HALLER, Ph.D. 158 PP.

SUPRAMOLECULAR STRUCTURE/ HERPES ANTIVIRAL AGENT/
DISORDER/ REREFINEMENT

Acyclovir is an antiviral drug used to treat herpes simplex virus type 1 (HSV-1), herpes simplex virus type 2 (HSV-2), and varicella-zoster virus (VZV) infections. Advantages of acyclovir are low cytotoxicity and low HSV resistance to acyclovir. One disadvantage is low bioavailability, perhaps partially due to low solubility. Acyclovir, $C_8H_{11}N_5O_3$ was separated from acyclovir drug. Thin plates of the dihydrate, obtained from water solvent, crystallized in the triclinic space group $P\bar{1}$, with cell dimensions, $a = 6.8996(6)$ Å, $b = 11.4170(9)$ Å, $c = 15.0806(13)$ Å, $\alpha = 82.595(7)°$, $\beta = 82.395(7)°$, $\gamma = 89.368(7)°$, $V = 1167.65(17)$ Å^3 at 293(2) K. The crystal lattice contains two crystallographically independent acyclovir molecules and four water molecules in the asymmetric unit. The guanine bases of the two independent molecules join via C–H⋯O, N–H⋯N, and N–H⋯O hydrogen bonds into 1–D infinite wave-like chains. The chains interconnect to create 2–D sheet networks perpendicular to the a axis via bifurcated hydrogen bonds to the side chain of one of the independent acyclovir molecules. The adjacent 2–D sheet networks connect together to create 3–D networks through guanine stacking with average distances of 3.2950(13) Å for A/B and 3.3925(18) Å for B/A. The water molecules

form infinite serpentine chains, $\cdot[\cdot \text{O2–H}\cdots\text{O1–H}\cdots\text{O3–H}\cdots\text{O4–H}\cdot]_\infty$, that propagate through channels parallel to the *a* axis in the network. The chains consist of alternating $R_5^5(10)$ motifs containing one oxygen atom of a carbonyl group and one hydroxyl group, respectively, to make stable pentagonal forms which further stabilize the strongly hydrogen bonded 3–D supramolecular network.

Tricyclic acyclovir, $C_{11}H_{13}N_5O_3$, has been reported as the dihydrate. The structure has been rerefined based on the literature data, and an improved model describing additional hydrogen atom disorder is presented. Tricyclic acyclovir dihydrate assembles into a supramolecular structure utilizing both drug and water molecules with extensive, strong hydrogen bond interactions in all directions. The solvent water molecules form an $(H_2O)_8$ cluster through a strong hydrogen bond $(d[\text{O}\cdots\text{O}] = 2.81$ Å$)$ between two water molecules across an inversion center. The water clusters interact with the tricyclic acyclovir network using strong O–H$\cdots$O and O–H$\cdots$N interactions, thereby becoming an integral part of the 3–D hydrogen bonded network. A nonstatistical disorder in the side chain can be explained by clear C–H$\cdots$O preferences for the major component at two atom sites, no clear preference at the other oxygen atom site, and a weak C–H$\cdots$O preference at one minor component site.

School of Biochemistry   Student's Signature_____

Academic Year 2012   Advisor's Signature_____

ACKNOWLEDGEMENTS

at the XXII Congress and General Assembly of the International Union of Crystallography (IUCr'11) in Spain.

I would also like to thank all of my colleagues at KPRU, Dr. Haller's research group members, and my other friends at SUT for all their support, help, and encouragement throughout the time of my studies.

Finally, I would like to take this opportunity to express my deepest appreciation and sincerest gratitude to my dear parents, sister, and my best friend for their love, devotion, understanding, consolation, and encouragement throughout the long years of my study. Without their love and understanding this work would not have been successful.

Montha Meepripruk

CONTENTS

CONTENTS (Continued)

CONTENTS (Continued)

LIST OF TABLES

LIST OF TABLES (Continued)

LIST OF TABLES (Continued)

LIST OF FIGURES

LIST OF FIGURES (Continued)

LIST OF FIGURES (Continued)

LIST OF ABBREVIATIONS

Å	Ångstrom unit (10^{-10} m)
δ	vibrational frequency (cm^{-1}) of bending mode
Δρ	difference electron density
μ	linear absorption coefficient
μg	microgram
μM	micromole
λ	an average wavelength
α, β, γ	interaxial angles between b and c, a and c, and a and b, respectively (alpha, beta, gamma)
θ	Bragg angle or scattering angle
$G_d^a(n)$	graph-set notation pattern
a, *b*, *c*	unit cell axial lengths
a	the number of hydrogen bond acceptors
ab <u>initio</u>	computational chemistry methods base on quantum chemistry
ACV	acyclovir
API	active pharmaceutical ingredient
cm^{-1}	wave number (per centimeter)
C	chains
Calc	calculated

LIST OF ABBREVIATIONS (Continued)

CSD	Cambridge Structural Database
1–D	one-dimension(al)
2–D	two-dimension(al)
3–D	three-dimension(al)
d	the number of hydrogen bond donors
D	finite complexes (dimers)
D_{calc}	calculated density
DSC	differential scanning calorimetry
FCV	famciclovir
FTIR	infrared spectroscopy
F_o and F_c	measured and calculated the structure factors
F_o^2 and F_c^2	measured and calculated intensities
fw	molecular weight
g	gram
GCV	ganciclovir
GRAS	generally recognized as safe
GVACV	glycine-valine-acyclovir
h,k,l	the reflection data
HSV	herpes simplex virus
HSV-1	herpes simplex virus type 1
HSV-2	herpes simplex virus type 2

LIST OF ABBREVIATIONS (Continued)

in vitro	outside of living organisms
IFN-α	interferon-Alpha
IU	international unit
kJ	kilojoules
kg	kilogram
mol	mole
mg	milligram
mL	milliliter
mM	millimole
M	molarity
MO	molecular-orbital
n	number of atoms in each pattern
NF	National Formulary
PCV	penciclovir
PXRD	powder X-ray diffraction
r_{Cg}	radius of ring centroid
r_H	radius of hydrogen atom
R_1	conventional discrepancy index = $R_1 = \dfrac{\sum\limits_{hkl}\left\lVert F_o\rvert - \lvert F_c\right\rVert}{\sum\limits_{hkl}\lvert F_o\rvert}$
R	ring

LIST OF ABBREVIATIONS (Continued)

S	the goodness of fit
S	intramolecular (self) hydrogen bonds
TFT	trifluorothymidine
TGA	thermogravimetric analysis
wR	the weighted R-factor
U	isotropic and anisotropic vibration parameters
USP	United States Pharmacopeial Convention
v_s and v_{as}	vibrational frequency (cm^{-1}) of symmetric and asymmetric stretching modes, respectively
V	the volume of the unit cell
VACV	valacyclovir
VVACV	val-val acyclovir
VZV	varicella-zoster virus
Z	number of formula units or molecules in the unit cell
%	percent

CHAPTER I

INTRODUCTION

1.1 Herpes Simplex Viruses

Herpes viruses are DNA viruses mostly associated with herpes simplex (HSV) and chicken pox. Herpes simplex is an incurable viral disease, consisting of herpes simplex virus types 1 (HSV-1), and 2 (HSV-2). HSV-1 is mainly localized around the oral region and HSV-2 around the genital region. Symptoms of HSV infection can be pain, fever, and lesions. In extreme cases, outbreaks can appear in and about the eyes, esophagus, trachea, brain, arms, and legs (Slonczewski and Foster, 2010). It is quite possible to transmit the virus from either region to either region. Varicella-zoster virus (VZV) is associated with the conditions of chicken pox, usually in children, and shingles in older individuals (who had chicken pox previously). Chicken pox is a common contagious childhood disease that produces itchy blisters. Infecting particles can be found in secretions of the upper airways and fluid secretions from the vesicles of patients with active chicken pox disease. Shingles symptoms are usually one-sided pain, tingling, or burning; the pain and burning may be severe and is usually present before any rash appears. HSV infections in humans are common worldwide with HSV-1 more common than HSV-2 (Chayavichitsilp, Buckwalter, Krakowski, and Friedlander, 2009) with rates of both increasing as people age (Smith and Robinson, 2002). Worldwide rates of HSV-1 infection are between 60% and 90% infection in older adults (Roizman and Sears, 1990; Smith and Robinson, 2002). In the Americas

17.2% of the population is HSV-2 seropositive with only 14.5% of the seropositive population aware that they are infected (Xu, Sternberg, Kottii, McQuillan, Lee, Nahmias, Berman, and Markowitz, 2006).

Acyclovir is the active pharmaceutical ingredient (API) in the most common antiviral drug used for treatment of HSV and VZV infections. Advantages for acyclovir are low cytotoxicity and low HSV resistance, as well as availability of low cost generic forms. Disadvantages are low bioavailability and lower effectivesness than that of valacyclovir, famciclovir, and fascarnet for HSV infection. As with many viral diseases, after several decades of acyclovir use, resistant strains of the virus are beginning to develop, especially in immunocompromised patients (Greco, Diaz, Thouvenot, and Morfin, 2007). Thus, many researchers are trying to improve properties of acyclovir to increase dissolution rate, and searching for synergistic effects between acyclovir and other materials used in treating herpes infections. Results of these studies may be important in the development of new pharmaceutical products or therapies.

Supramolecular chemistry, which is based on noncovalent bonds, is the chemistry of molecular assemblies. The results of supramolecular chemistry have been exploited to provide encapsulation and targeted release mechanisms for pharmaceutical agents. Supramolecular systems have also been designed to disrupt protein-protein interactions that are important to cellular function (Bertrand, Guathier, Bouvet, Moreau, Petitjean, Leroux, and Leblond, 2011). Understanding the supramolecular structures of a drug is an important part of understanding the interactions of the drug at a binding site.

1.2 Therapeutic agents used to treat HSV-1 and HSV-2

HSV infections have been treated with antiherpes virus drugs such as acyclovir (Zovirax), valacyclovir (Valtrex), penciclovir (PCV) or famciclovir (FCV), foscarnet, and trifluridine (Viroptic) (Elion, Furman, Fyfe, de Beauchamp, and Schaeffe, 1977). Acyclovir is the first of second-generation nucleoside analogues, which are the most commonly used antiviral drugs for treatment of HSV-1, HSV-2, and VZV infections. They are highly selective inhibitors and safe for oral administration (de Clerk and Field, 2006). Current treatment agents for HSV-1 and HSV-2 are summarized in Table 1.1.

Table 1.1 Drugs, dietary supplements, and natural products used for treatment of HSV-1 and HSV-2.

Drugs/Structures	Activity
Acyclovir Family	
Acyclovir (ACV)[a1,a2,a3,a4,a5]	Exhibits anti-herpetic activity after phosphorylation by viral thymidine kinase (TK). Acyclovir triphosphate interferes with viral DNA polymerization through competitive inhibition with guanosine triphosphate inhibiting DNA synthesis by obligatory chain termination.
1-methyl acyclovir[b1]	Inhibits HSV-1 and HSV-2. Antiviral activity on a specific phosphorylation by the virus-encoded thymidine kinase.
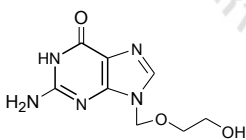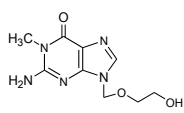
a1. Naesens *et al*. (2001); a2. Biron *et al*. (1980); a3. Coen *et al*. (1980); a4. Elion *et al*. (1977); a5. Larder *et al*. (1986); b1. Boryski *et al*. (1988); c1. de Clerk *et al*. (2006).

Table 1.1 (Continued).

Drugs/Structures	Activity
Valacyclovir (VACV)[c1]	Inhibits viral DNA polymerase
Penciclovir (PCV)[a1, d1]	Inhibits viral DNA polymerase.
Famciclovir (FCV)[e1]	In murine model (mice and rats), prevents viral recurrence of HSV-2 infection and prevents HSV-1 latency in mice.
Ganciclovir (GCV)[c1]	Inhibits viral DNA polymerase.
Val-Val acyclovir (VVACV)[fi, f2]	Lower cytotoxic and highly water soluble prodrug showing excellent *in vivo* activity against HSV-1 in rabbit epithelial and stromal keratitis.
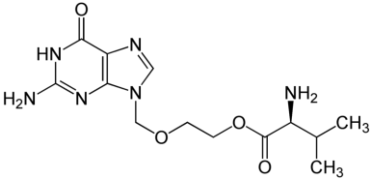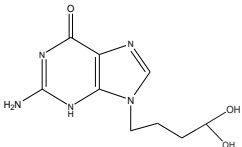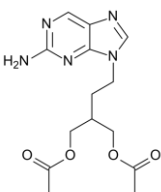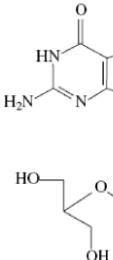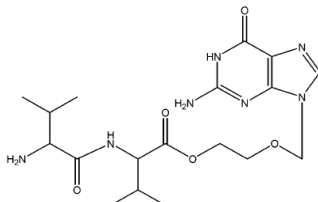
d1. Perry *et al.* (1995); e1. Crumpacker (1996); f1. Anand *et al.* (2003); f2. Anand *et al.* (2004).

Table 1.1 (Continued).

Drugs/Structures	Activity
Glycine-valine-acyclovir (GVACV)[f2]	Treatment of ocular HSV infections.
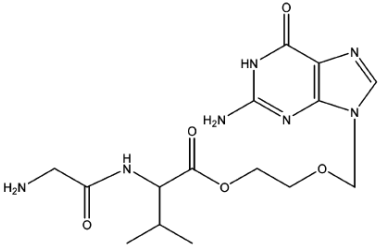
Acyclovir derivative

Tricyclic acyclovir[b1, g1,g2, g3]	Exhibits a marked antiherpetic activity and lower cytotoxicity with potent and selective activity against HSV-1 and HSV-2, VZV, and cytomegalovirus.
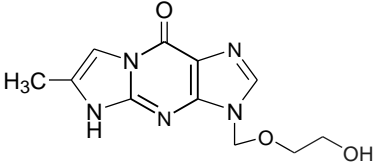
Other Substances
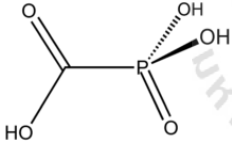
Foscarnet[h1]	Inhibits the pyrophosphate binding site on viral DNA polymerases.

Trifluorothymidine (TFT)[i1]	Exhibits antiviral activity against acyclovir-susceptible HSV-1 strains but associated with severe cytotoxicity and mutagenicity in long-term treatment.
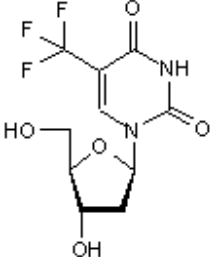
g1. Boryski *et al*. (1991).; g2. Balzarini *et al*. (2002); g3. Suwińśka *et al*. (2001); h1. Chrisp *et al*. (1991);

i1. Beers *et al*. (1999).

Table 1.1 (Continued).

Drugs/Structures	Activity
Cidofovir[i1, i2]	Inhibits viral DNA polymerase.
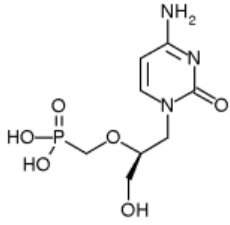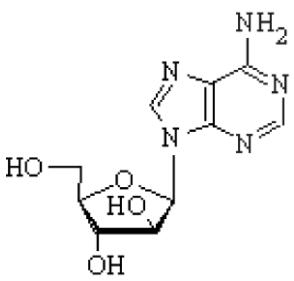
Vidarabine[k1, k2]	Inhibitor and a substrate of viral DNA polymerase HSV encephalitis. Thymidine kinase inhibitor that prevents encephalitic death in mice caused by HSV-1 and HSV-2.

2-Phenylamino-6-oxo-9-(4-hydroxybutyl)purine[k2]	Thymidine kinase inhibitor that prevents encephalitic death in mice caused by HSV-1 and HSV-2.
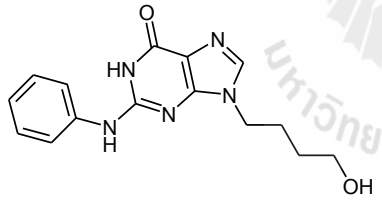
Natural products

Caffeic acid[l1, l2, l3, l4]	Inhibits HSV-1 before the completion of viral DNA replication.
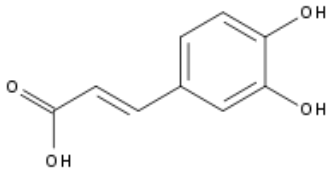
i2. de Clercq *et al*. (1996); j2. Ho *et al*. (1992); k1. Whitley *et al*. (1980); k2. Bryan *et al*. (2009);

l1. Mundinger *et al.* (2008); l2. Bourne *et al*. (1999); l3. Dimitrova *et al*. (1993); l4. Chiang *et al*. (2002).

Table 1.1 (Continued).

Drugs/Structures	Activity
Curcumin[ll m1]	Inhibits immediate-early genes of HSV-1 by interference with HSV-1 replication and protects from HSV-2 infection.
Cineole[ll m1]	Inhibits immediate-early genes of HSV-1 by interference with HSV-1 replication and protects from HSV-2 infection.
Eugenol[ll, l2, n1, n2]	Inhibits immediate-early genes of HSV-1 by interference with HSV-1 replication and protects from HSV-2 infection in a mouse model.
Cis-capsaicin or Civamide[ll, l2]	Reduces the recurrence of latent infections when weekly treatment is continued as a suppressive maintenance therapy.
Galangin[ll, o1, o2]	Inhibits HSV-1 activity in the step before viral entry into the host cells.
Kaempferol[ll, o1, o2]	Shows highest anti-HSV activity *in vitro* than quercetin.
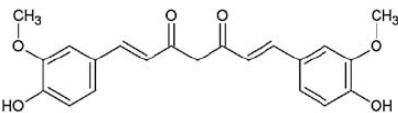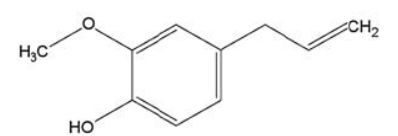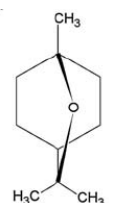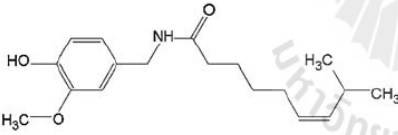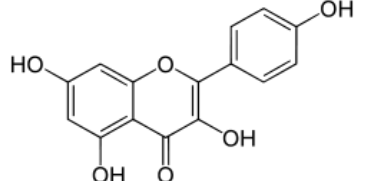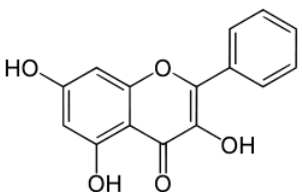
m1. Kutluay *et al*. (2008); n1. Benencia *et al*. (2000); n2. Serkedjieva *et al*. (1992); o1. Amoros *et al*. (1992); o2. Lyu *et al*. (2005);

Table 1.1 (Continued).

Drugs/Structures	Activity
Isoborneol[ll, p1]	A promising new candidate for HSV treatment.
Moronic acid[ll, q1]	Reduces skin lesions and increases survival time for mice with cutaneous HSV-1.
Alkaloid FK3000[ll, r1, r2]	Reduces skin lesions and prolongs survival time for mice with herpes simplex keratitis.
Meliacine[ll, l2, s1, s2]	Reduces viral replication and prevented tissue damage in the corneas in mice model.
λ-Carrangeenans [ll, t1]	Antiviral activity against HSV-1 and HSV-2 in replication process.
Rhamnan sulfate[ll, u1, u2]	Inhibits virus replication in the later stages of HSV-1 infection
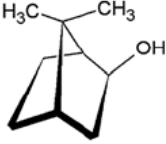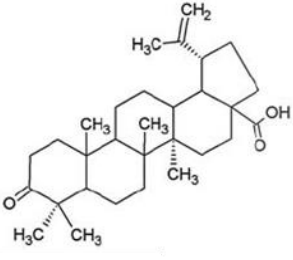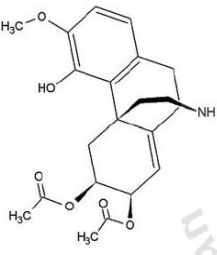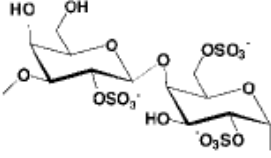
p1. Armaka *et al.* (1999); q1. Nawawi *et al.* (2001); r1. Alche *et al.* (2002); r2. Alche *et al.* (2000); s1. Talarico *et al.* (2004); s2. Pujol (2006); t1. Lee *et al.* (1999); u1. Ponce *et al.* (2003); u2. Thompson *et al.* (2004).

Table 1.1 (Continued).

Drugs/Structures	Activity
Galactofucanes[ll, v1, v2]	Inhibits viral penetration into the host cell.
Calcium spirulan[w1]	Interferes in the later stages of replication. Replacing Ca^{2+} with Na^+ or K^+ maintains antiviral activity.
Echinacea[x1]	Reduces frequency of herpes outbreaks or the time it takes for the sores to heal.
Bee products [x1, o1, y1]	Both antibacterial and antiviral, including having activity against HSV.
Aloe vera [z1]	Antiviral activity against HSV-2 before attachment and entry of virus to the vero cells and post attachment stages of virus replication.

Alternative medicine

L-lysine[aa1]	Reduces the frequency of recurrences, and prevents and treats HSV outbreaks.
Vitamin C [aa1, ab1]	Massive parenteral doses of vitamin C accelerates the healing of herpes lesions.
Vitamin E[aa1, ac1, ac2, ac3, ac4]	Vitamin E relieves pain and aids in the healing of oral herpetic lesions (gingivostomatitis or herpetic cold sores).
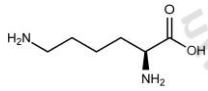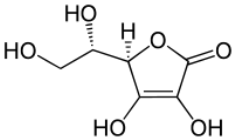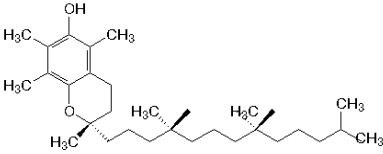
v1. Hayashi *et al.* (1996); v2. Lee *et al.* (2001); w1. Ren *et al.* (2010); x1. Perfect *et al.* (2005); y1. Amoros *et al.* (1994); z1. Zandi *et al.* (2007); aa1. Gaby (2006); ab1. Klenner (1949); ac1. Shlomai *et al.* (1975); c2. Fridlender *et al.* (1978); ac3. Gupta *et al.* (1976); ac4. Gordon *et al.* (1975).

Table 1.1 (Continued).

Drugs/Structures	Activity
Zinc[aa1, ad1, ad2, ad3, ad4]	The inhibition was almost complete and appears to result from selective inhibition of the viral DNA polymerase of HSV-1 and HSV-2 *in vitro* and, reduces the frequency and severity of herpes outbreaks.
Lithium[aa1, ad1, ad2, ad3, ad4]	Inhibits the replication of HSV-1 and HSV-2 *in vitro*. Lithium carbonate for depression or other psychiatric problems is associated with a reduction in the frequency of HSV outbreaks.

ad1. Skinner *et al*. (1980); ad2. Bschor (1999); ad3. Amsterdam *et al*. (1990); ad4. Lieb (1981).

Acyclovir is commonly marketed as tablets (200 mg, 400 mg, 800 mg, and 1 g), topical cream (5%), intravenous injection solution (25 mg/mL), and ophthalmic ointment (3%). Cream preparations are used primarily for labial HSV. Intravenous injection is used when high concentrations of acyclovir are required. Ophthalmic ointment is only used for herpes simplex keratitis. The recommended dose for treating an initial HSV-2 infection is 200 mg of acyclovir five times a day (about every four hours) for 10 days. Later outbreaks of HSV-2 are treated with 200 mg of acyclovir five times a day for five days, starting at the first signs of an outbreak. Adverse effects of high doses include coma, confusion, delirium, encephalopathy, hallucinations, paresthesias, psychosis, seizures, or tremor (Ellenhorn, 1997).

Several natural remedies for HSV including lysine, vitamin C, zinc, vitamin E, adenosine monophosphate, lemon balm, and lithium have been discussed (Gaby, 2006). They are dietary modifications and natural substances, and useful for treating HSV lesions or preventing recurrences.

1.3 Combination of acyclovir with other compounds

Because of the low solubility and resistance of some viral strains of herpes to acyclovir, researchers are trying to improve the physical properties to optimize administration of the drug and/or the chemistry to design bioreversible prodrugs that may be useful in the optimization of drug absorption properties (Stella, Charman, and Naringrekar, 1985). Combinations of acyclovir with other compounds, some of which have demonstrated antiviral activity, have been demonstrated to possess synergistic effects against HSV. Examples of such combinations of acyclovir with other compounds for treatment of HSV infection are summarized in Table 1.2.

Table 1.2 Synergistic combination therapies of acyclovir with other compounds for treatment of HSV infection.

Synergistic Combination Studies		Activity/Target site
5 mM acyclovir	100 IU/mL IFN-α[a]	Inhibits two pathways of viral DNA polymerase and reduces the amount of dGTP which competes with acyclovir triphosphate for incorporation into viral DNA on Vero or corneal cells.
50 mg/kg acyclovir	100 mg/kg 2-Phenylamino-6-oxo-9-(4-hydroxybutyl) purine[b]	Prevents encephalitic death in mice caused by HSV-1 infection gave 100% survival.
Acyclovir	Chlorhexidine[c]	Synergistically inhibits viral replication by enhancing in part the reduction of viral DNA synthesis *in vitro* that might be beneficial for the control of intraoral herpetic infections.

a.Taylor *et al.* (1998); b. Gebhard *et al.* (2009); c. Park *et al.* (1991).

Table 1.2 (Continued).

Synergistic Combination Studies		Activity/Target site
Acyclovir	Benzo[*a*]phenothiazines[d]	Might enhance their antiviral activity probably by reduction of the mutagenic rate in the virus populations in vero cell.
Acyclovir	vidarabine[e]	Alteration of herpes viral DNA polymerase causes a change of substrate specificity for both acyclovir and vidarabine which the triphosphate forms of both acyclovir and vidarabine are essential for their synergism and the nature of their binding sites on DNA polymerase is important for their synergistic antiviral effects against herpes viruses.
0.45 µg/mL acyclovir	8.4 µg/mL betulin[f]	Synergistic antiviral effect was found only at higher concentrations of the compounds tested.
0.3 µM acyclovir	0.25 M 5-fluorodeoxyuridine + 3.6 µM 2-acetylpyridine thiosemicarbazone[g.]	Increase the apparent potency of acyclovir against HSV synergistically by inhibiting replication of HSV.

d. Mucsi, *et al.* (2001); e. Suzuki, *et al.* (2006); f. Gong, *et al.* (2004); g. Prichard, *et al.* (1993).

Treatment with 50 mg/kg acyclovir and 100 mg/kg 2-phenylamino-6-oxo-9-(4-hydroxybutyl) purine shows synergistic activity against HSV encephalitis in mice. The development of a potent and safe combination therapy for the prevention and/or treatment of HSV infection of the central nervous system could improve the outcome of this infection in humans (Gebhardt, Focher, Eberle, Manikowski, and Wright, 2009).

Organotin polyamine ethers containing acyclovir in their backbone with diethyltin, dibutyltin, and diphenyltin exhibit the ability to inhibit both RNA and DNA viruses, particularly the HSV-1 and VZV viruses responsible for herpes, chicken pox, and shingles (Carraher, Sabir, and Roner, 2006).

Treatment with 5 mM acyclovir and 100 IU/mL human interferon-α (IFN-α) reduced HSV-1 DNA levels more than 8-fold compared to cells treated with acyclovir alone. The synergistic anti-HSV activities of human interferon-α (IFN-α) with acyclovir could be mediated, in part, through some post-transcriptional mechanism induced by IFN-α treatment, leading to the reduction in production of viral early enzymes, especially DNA polymerase (Taylor, Tom, and O'Brien, 1998).

1.4 Chemistry and Biochemistry of Acyclovir

Acyclovir is 9-[(2-hydroxyethoxy)methyl]guanine or acycloguanosine. Solid state acyclovir is a white, crystalline powder with the molecular formula $C_8H_{11}N_5O_3$, molecular weight 225.21 g/mol, and melting point at 256 °C (USP 27-NF 22, 2006). It has maximum solubility in water of 2.5 mg/mL at 37 °C, very slight solubility in ethanol, good solubility in dilute aqueous alkali hydroxide and mineral acid solutions, and is freely soluble in dimethyl sulfoxide. Acyclovir contains alcohol and amine functional groups with pKa of the monocation at 2.27 and of the alcohol at 9.25, as represented in Figure 1.1 (McEvoy, Miller, and Litvak, 2004).
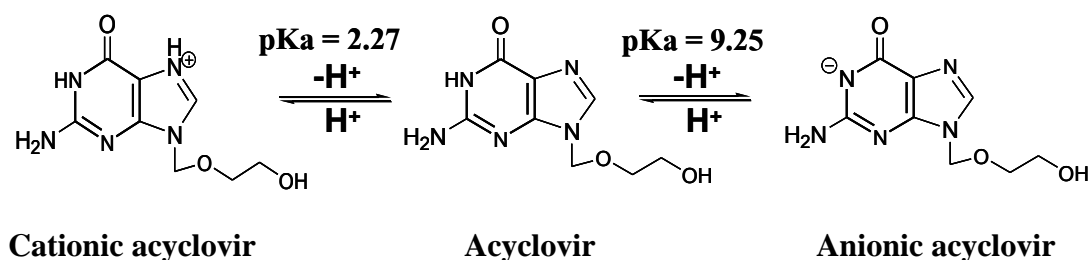
Figure 1.1 Formal diagram demonstrating speciation of acyclovir.

Pharmaceutical acyclovir is normally present in a hydrated crystalline form consisting of three acyclovir molecules and two water molecules in the crystallographic asymmetric unit (Kristl, Srcic, Vrecer, Sustar, and Vojnovic, 1996) corresponding to a theoretical water content of about 5%. Dose and solubility are normally expressed in units of anhydrous acyclovir. Two anhydrous polymorphs and an unstable hydrate of acyclovir have also been reported. A stable anhydrous form can be obtained by drying hydrated acyclovir at temperatures above 150 °C (Kristl, Srcic, Vrecer, Sustar, and Vojnovic, 1996). Conformation features have been compared with those in other known acyclonucleosides and examined in relation to the behavior of acyclonucleosides in various enzymatic systems, including those related to antiviral activity (Birnbaum, Cygler, and Shugar, 1984).

Previous studies have characterized the crystalline forms by infrared spectroscopy (FTIR), solubility, dissolution rate, X-ray powder diffraction (Kristl, Srcic, Vrecer, Sustar, and Vojnovic, 1996; Sohn and Kim, 2008), and by the thermal techniques, differential scanning calorimetry (DSC) and thermogravimetric analysis (TGA) (Sohn and Kim, 2008); both polymorphic and pseudo polymorphic forms have been studied (Kristl, Srcic, Vrecer, Sustar, and Vojnovic, 1996). Some research

focused on the compatibility and stability of the drug ingredients; acyclovir API and mixtures of acyclovir with excipients, has been carried out using DSC, powder X-ray diffraction (PXRD), and FTIR techniques for the purpose of development of acyclovir extended release formulations, because potential physical and chemical interaction between drugs and excipients can affect the characteristics of chemical nature, the stability and bioavailability of the drug, and consequently, their therapeutic efficacy and safety. Acyclovir only exhibited interactions that could influence the stability of the product in the binary mixture of acyclovir with magnesium stearate (Barboza, Vecchia, Tagliari, Silva, and Stulzer, 2009).

Mechanism of Action

Acyclovir competes with deoxyribonucleosides for viral thymidine kinase or cellular kinases. The thymidine kinase encoded by HSV, VZV, and Epstein-Barr virus converts acyclovir into acyclovir monophosphate. Acyclovir monophosphate is subsequently converted to the diphosphate by cellular guanylate kinase and into the triphosphate by a number of cellular enzymes (Miller and Miller, 1980; O'Brien and Campoli-Richards, 1989). Acyclovir triphosphate incorporates in the growing viral DNA chain, leading to the termination of DNA synthesis because of its lack of a 3´-hydroxyl moiety. Acyclovir triphosphate interferes with herpes simplex virus DNA polymerase and inhibits viral DNA replication. The pathway of the mechanism of acyclovir action is shown in Figure 1.2.

In vitro, acyclovir triphosphate stops replication of herpes viral DNA in three ways. First, acyclovir triphosphate competes with the natural nucleoside deoxyguanosine triphosphate to bind to HSV DNA polymerase. Second, acyclovir incorporates into and terminates the growing viral DNA chain. Third, acyclovir

inactivates viral DNA polymerase, thus preventing further elongation of the DNA chain (Furman, St. Clair, and Spector, 1984; Elion, 1993).
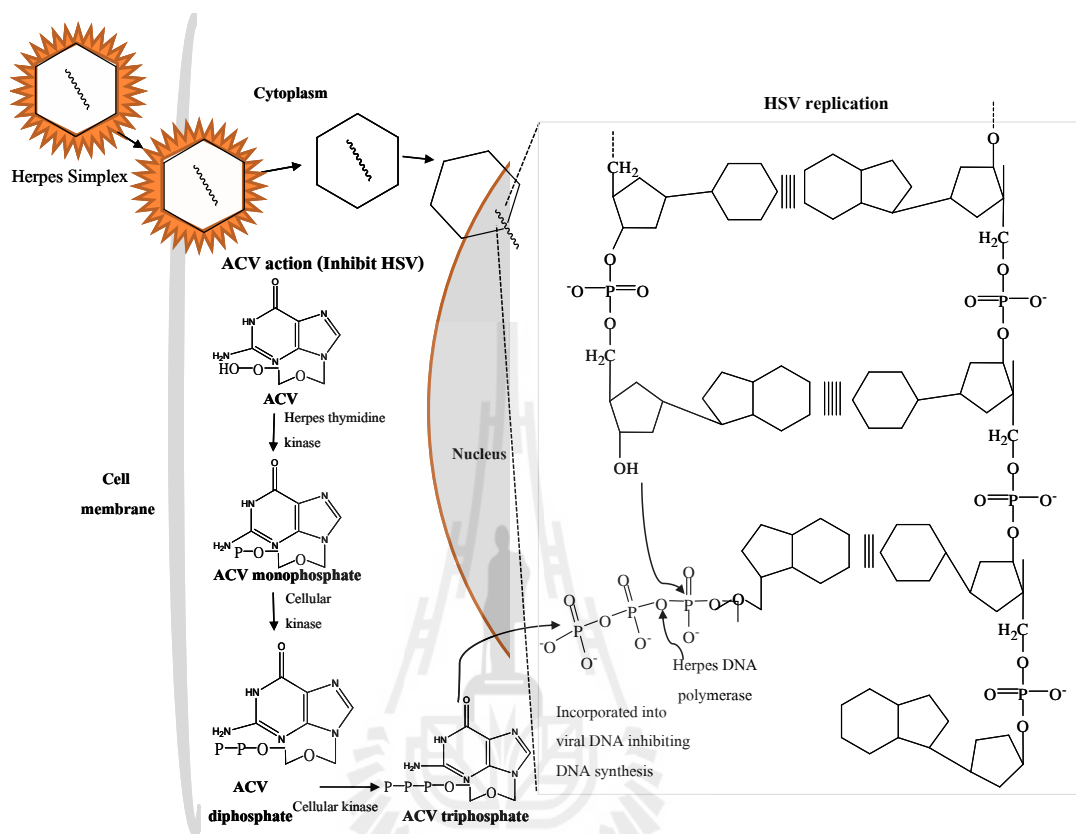
Figure 1.2 Mechanism of action of acyclovir in cells infected by HSV (redrawn from Brunton, Chabner, and Knollmann, 2010).

Acyclovir is much less toxic *in vitro* for normal uninfected cells because less is taken up, less is converted to the active form, and cellular α-DNA polymerase is less sensitive to the effect of the active form. Acyclovir is widely distributed into most body tissues, including the brain, kidney, lung, liver, heart, muscle, spleen, placenta, uterus, and vaginal mucosa and in many bodily fluids including semen, saliva, amniotic fluid, aqueous humor, and cerebrospinal fluid. Furthermore, acyclovir

demonstrates minimal protein binding (9-33%) at therapeutic plasma concentrations (Thomson and Dragar, 2004; McEvoy, Miller, and Litvak, 2004). However, most of a single acyclovir dose (62-91% of an intravenous dose) is excreted unchanged in urine via glomerular filtration and tubular secretion in adults with normal renal function (McEvoy, Miller, and Litvak, 2004). Acyclovir is metabolized in the liver, partially to 9-[(carboxymethoxy)methyl]guanine and minimally to 8-hydroxy-9-(2-hydroxy-ethoxymethyl)guanine (Thomson and Dragar, 2004; McEvoy, Miller, and Litvak, 2004).

The pharmacokinetic disposition of the drug is not affected by dose, duration, or frequency of administration. Mean plasma acyclovir concentrations at steady state (6.7-20.6 mg/L) after intravenous administration in immunocompromised patients (2.5-15 mg/kg every 8 h) are similar to the peak plasma concentrations obtained with equivalent single doses (Whitley, Blum, Barton, and de Miranda, 1982). Absorption of oral acyclovir across the small intestine appears to be passive (Tanna, Wood, and Lawrence, 1992; Lewis, Fowle, Bittiner, Bye, and Isaacs, 1986) and is incomplete, resulting in 15-30% bioavailability and mean peak plasma concentrations 1.5-2.5 h post dose (Loregian, Gatti, Palù, and de Palo, 2001).

1.5 Crystallographic Data

Acyclovir

Acyclovir crystallized from aqueous dimethylformamide gives thin plates of a 3:2 hydrate with monoclinic space group $P2_1/n$: $C_8H_{11}N_5O_3 \cdot 2/3H_2O$, $fw = 237.23$, $a = 25.459(1)$, $b = 11.282(1)$, $c = 10.768(1)$ Å, $\beta = 95.16(1)°$ (Birnbaum, Cygler, and Shugar, 1984). The asymmetric unit consists of three independent molecules of

acyclovir and two molecules of water. All of the guanine bases join together into infinite sheets using hydrogen bonds. Each base is connected to two adjacent bases by N–H···N and N–H···O hydrogen bonds forming ribbons of acyclovir molecules. There are two unique ribbons in the crystal structure; one formed by a 2_1 screw axis in the ribbon relating A molecules and the other by alternating B and C molecules. The unit cell thus contains three ribbons, one with only A molecules and two others containing alternating B and C molecules related by the 2_1 screw axis through the A molecules. The side chains of two molecules A and B are partially folded and the third (molecule C) is fully extended (Birnbaum, Cygler, and Shugar, 1984) and almost perpendicular to the guanine base, the glycosidic torsion angles are in the range 91.4-104.3º.

Acyclovir Derivative

Tricyclic acyclovir, 3-[(2-hydroxyethoxy)-methyl]-6-methyl-3*H*-imidazolo[1,2-*a*]purin-9(5*H*)-one, was expected to be inactive when the NH_2 group at C-2 of acyclovir was blocked by the closure of the third ring (Boryski, Golankiewicz, and de Clerk, 1988), but instead it exhibits a marked antiherpetic activity with potent and selective activity against HSV-1 and HSV-2, varicella-zoster virus, and cytomegalovirus. At the same time, it has lower cytotoxicity, which results in a higher selectivity index than that of acyclovir (Boryski, Golankiewicz, and de Clercq, 1991; Balzarini and McGuigan, 2002). Many studies focused on the potent and selective antiherpetic activity and it was also noted that the new compound had a higher dissolution rate than acyclovir (Boryski, Golankiewicz, and de Clercq, 1991). The structure of tricyclic acyclovir has also been reported as the dihydrate, $C_{11}H_{13}N_5O_3 \cdot 2H_2O$, and the complex hydrogen bond network of water and tricyclic

acyclovir molecules was suggested to be related to the solvation of the molecules in solution (Suwińska, Golankiewicz, and Zielenkiewicz, 2001). The $Z = 2$ structure contains four independent solvent water molecules, forming an $(H_2O)_8$ cluster through a strong hydrogen bond between two water molecules across an inversion center. The solid state structure contains two crystallographically independent molecules A and B, with different side-chain conformations. Additionally, the (2-hydroxyethoxy)methyl side chain in molecule B is conformationally disordered with two different conformations, designated B and C, observed as shown in Figure 1.3.
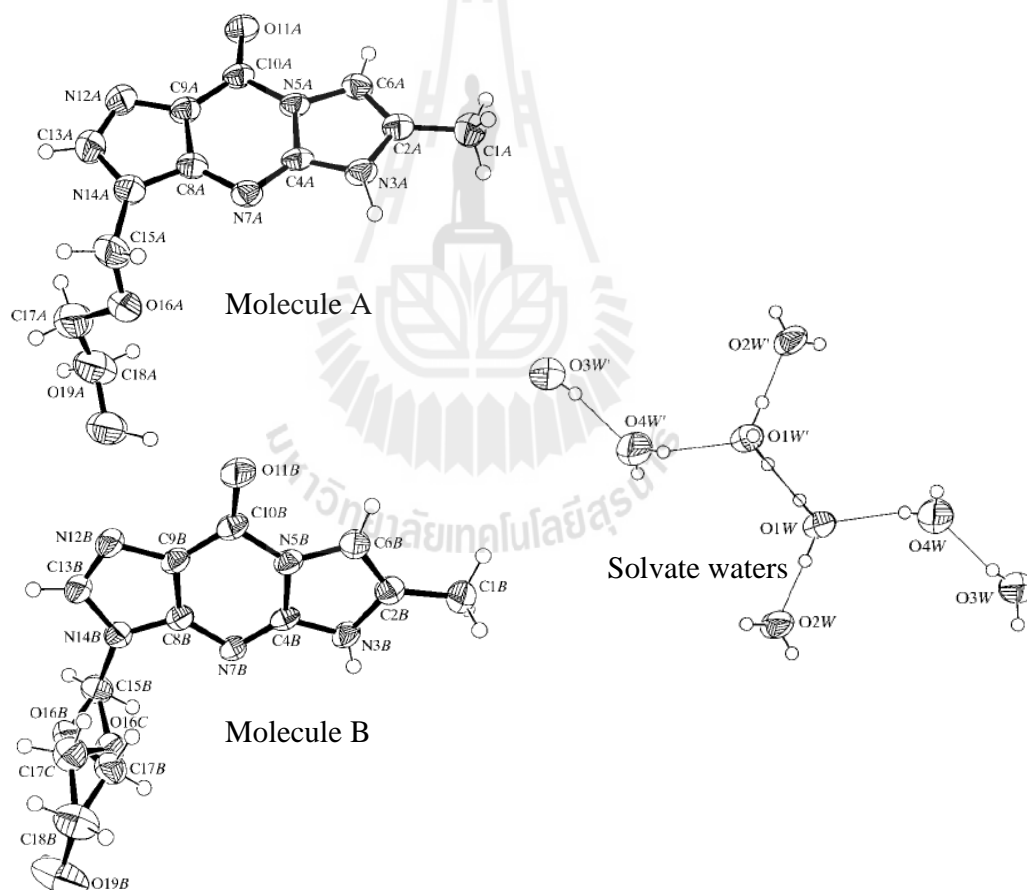
Figure 1.3 The molecular structure of molecule A, molecule B, and the disordered conformer C, and the $(H_2O)_8$ cluster in tricyclic acyclovir (redrawn from Suwińska, Golankiewicz, and Zielenkiewicz, 2001).

1.6 Supramolecular Interactions

Supramolecular assembly occurs in a multicomponent system of atoms, ions, and/or molecules which are held together by supramolecular interactions. Supramolecular chemistry has been defined by Lehn (1993), who won the Nobel prize in 1987 for his work in the area,

Supramolecular chemistry is 'chemistry beyond the molecule', whose goal is to gain control over the intermolecular noncovalent bond. It is concerned with the entities of higher complexity than molecules themselves-supramolecular species and assemblies held together and organized by means of intermolecular binding interactions. It is a highly interdisciplinary field of science and technology bridging chemistry with biology and physics.

In molecular chemistry, the forces responsible for the spatial organization may vary from weak (inter- and intra-molecular forces that are primarily electrostatic, especially hydrogen bonding) to strong (covalent bonding), provided that the degree of electronic coupling between the molecular components remains small with respect to relevant energy parameters of the component of interest (Lehn, 1993).

Recrystallization

Recrystallization is a purification technique of organic molecules in which the crystallization process from solution are evolutes or melts of the crystalline state. Key issues for recrystallization include the formation of crystal nuclei, the influence of crystallization conditions, and the overlap between concepts of the growth unit. The notion of growth unit has a distinct link with the supramolecular concept of a synthon.

The term 'synthon' was originally introduced to describe synthetic organic structural features. The supramolecular synthon (Desiraju, 1995) is defined as:

'structural units within supermolecules which can be formed and/or assembled by known conceivable synthetic operations involving intermolecular interaction'.

Supramolecular synthons are the smallest units which contain all the information inherent in directing the process of assembling the molecules into the supramolecular structure. They are made up of spatial arrangements of potential intermolecular interactions that are realized in crystals and are significant in crystal engineering (Reddy, Craig, and Desiraju, 1996; Reddy, Ovchinnikov, Shishkin, Struchkov, and Desiraju, 1996). A first step in forming a supramolecular framework is to choose appropriate synthons that ensure generality, ultimately leading to the predictability of 1–D, 2–D, and 3–D patterns formed by intermolecular interactions as supramolecular interactions. Supramolecular chemistry is the study of the nature of supramolecular interactions, concerning noncovalent bonding interactions. Types of supramolecular interactions include carbonyl–carbonyl dipole interactions, hydrogen bonding, and aromatic–aromatic interactions, as the supramolecular nature of APIs dictates that their properties are modulated by the intramolecular and intermolecular interactions, manifested as the unique molecular conformation and crystal packing.

Carbonyl–Carbonyl Interactions

Carbonyl-carbonyl interactions are noncovalent interactions between carbonyl groups ($>C(\delta^+) \cdots O(\delta^-)$) that can be derived from small molecules. *Ab initio* molecular-orbital (MO) calculations show that carbonyl–carbonyl dipole interaction energies can be up to –22.3 kJ mol^{-1} for the perfect rectangular antiparallel motif with d[C$\cdots$O] an optimum 3.02 Å and the range 2.92–3.32 Å for attractive energies <–20 kJ mol^{-1} separation between the $>C(\delta^+)$ of one carbonyl dipole to the oxygen of

another. This is comparable to medium hydrogen bond interactions (*ca* −20 to −30 kJ mol^{-1}) (Allen, Baalham, Lommerse, and Raithby, 1998).

Allen and coworkers (Allen, Baalham, Lommerse, and Raithby, 1998) analyzed carbonyl–carbonyl interactions using crystallographic data that is available in the Cambridge Structure Database (CSD: Allen, Davies, Galloy, Johnson, Kennard, Macrae, Mitchell, Smith, and Watson, 1991) and *ab initio* molecular orbital (MO) calculations.

Crystallographic data for 9049 carbon-substituted >C=O groups was used and shows that 1328 (15%) form contacts with other >C=O groups, in which d[C⋯O]< 3.6 Å. Three limiting motifs (Figure 1.4) are observed in the crystal structures, (a) a slightly sheared antiparallel motif involving a pair of short C⋯O interactions, −22.3 kJ mol^{-1} (b) a perpendicular motif, −20 kJ mol^{-1} and (c) a highly sheared parallel motif, −7.6 kJ mol^{-1}, which involves a single short C⋯O interaction. The remaining 383 interactions all have torsional angles in the range of 20-160°, and frequently have only one of the C⋯O distances within the 3.6 Å limit. The value of 3.6 Å was chosen as twice the sum of the van der Waals radii of carbon and oxygen, with an unreported tolerance value of 0.2 Å (Bondi, 1996).

Previous work in our group noted strong >C(δ^+)⋯O(δ^-) carbonyl–carbonyl interactions in the molecular structure of Co(picoline)$_3$·H$_2$O (Chainok and Haller, 2004) and in the structure of pyridine-3,5-dicarboxylic acid (Krachodnok and Haller, 2005).

Hydrogen Bond Interactions

Hydrogen Bond Interactions are the masterkey interaction in supramolecular chemistry (Steed and Atwood, 2000). They focus on the interactions between, rather

than within, molecules and enable a chemistry using molecules rather than atoms as building blocks. George Jeffrey (1997) classified hydrogen bonds into three general categories, strong, medium, and weak hydrogen bond interactions, according to the energies of the interactions (Steed and Atwood, 2000), with weaker and stronger interactions often acting in concert.
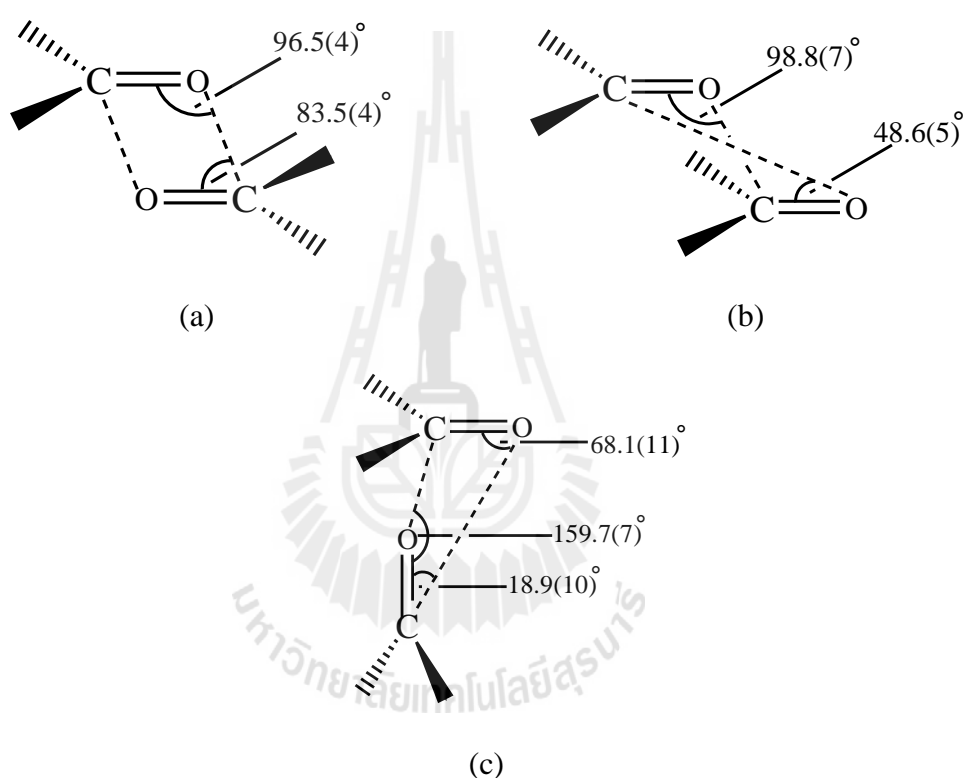
Figure 1.4 Average geometries for the three most common carbonyl–carbonyl interaction motifs. Determined from database analysis (a) anti-parallel, (b) sheared-parallel, and (c) perpendicular motif (Allen, Baalham, Lommerse, and Raithby, 1998).

Hydrogen bonds may be regarded as a special type of dipole-dipole interaction in which a hydrogen atom attached to a negatively charged or negatively polarized

atom forms an X–H⋯A interaction with (or without) lone pairs, which is called a hydrogen bond if X is a hydrogen atom donor (D) and A is an acceptor (A) as shown in Figure 1.5. The distance of X–H⋯A interactions for possible hydrogen bonding (Jeffrey, 1997) with H⋯A distance limits up to 3.0 Å, or even 3.2 Å with angular cut off >90° or > 110° for somewhat more conservative criteria (Steiner, 2002). Hydrogen bonds can be classified into 3 types, (1) strong hydrogen bond with H⋯A distance about 1.2–1.5 Å and bond angle 175–180º, (2) medium hydrogen bonds with H⋯A distance about 1.5–2.2 Å and bond angle 130–180º, and (3) weak hydrogen bonds with H⋯A distance about 2.2–3.2 Å and bond angle 90–150º.
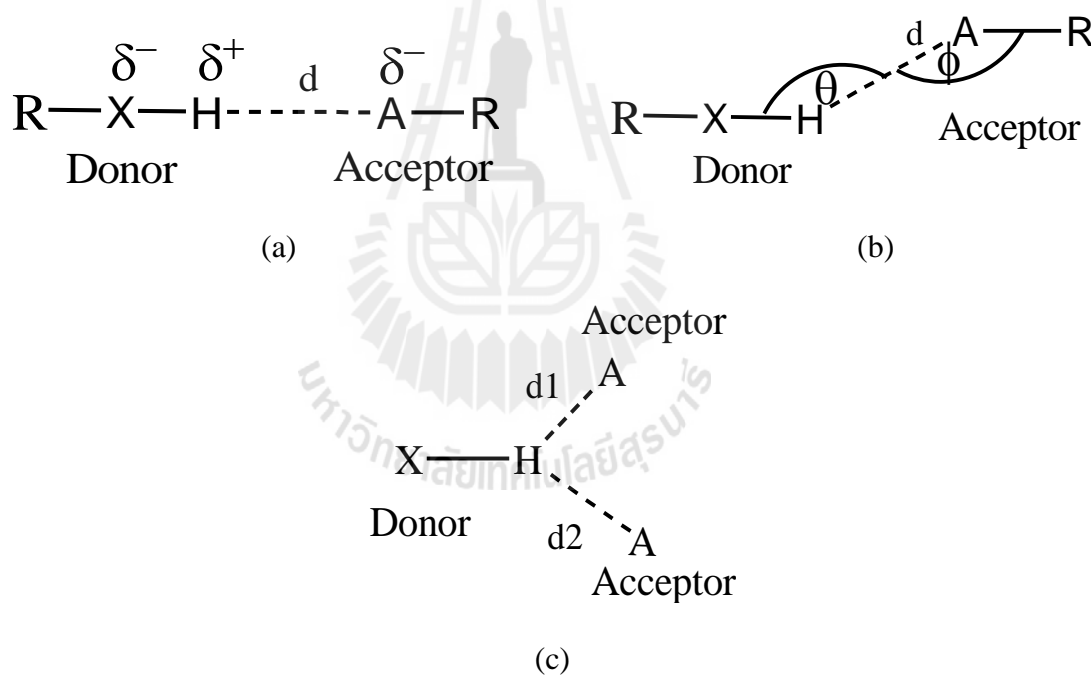
Figure 1.5 Hydrogen bond geometry and partial charges. (a) Donor and acceptor atoms, (b) the angular dependence in hydrogen bonds, and (c) bifurcated hydrogen bond in which the two H⋯A separations may be distinctly different.

In simple hydrogen bonds the donor interacts with one acceptor. If the donor hydrogen atom interacts with two acceptors, a bifurcated hydrogen bond forms and

the two H⋯A separations may be distinctly different, the short interaction is called the major component and the longer interaction is called the minor component of the bifurcated bond (Steiner, 2002) as in Figure 1.5(c). The analysis of hydrogen bond patterns using graph-set notation provides a new way to analyze and understand different hydrogen bonding systems, as well as to establish an efficient basis for creating supramolecular networks using supramolecular synthons as hydrogen bonding motifs, as suggested by the late Margaret Etter (Etter, MacDonald, and Bernstein, 1990). The graph-set notation description uses a combination of four simple patterns: chains (C), rings (R), finite complexes (dimers) (D), and intramolecular (self) hydrogen bonds (S). The number of hydrogen bond donors, d (subscript), and acceptors, a (superscript), and number of atoms, n, in each pattern (the degree of the pattern) are indicated after the pattern designation to give a graph-set notation, $G_d^a(n)$, where G represents one of the above-mentioned four possible patterns (C, R, D, or S) (Grell, Bernstein, and Tinhofer, 1999; Etter, MacDonald, and Bernstein, 1990).

Many studies have used graph-set notation to describe the hydrogen bonding motifs in their work. Molecules of N-(2-formamido-ethyl)formamide, $C_4H_8N_2O_2$, are connected together by N–H⋯O hydrogen bonds that define graph-set motif $R_4^4(22)$ in a centrosymmetric array by the association of four molecules resulting in the formation of a 2–D infinite network parallel to the (010) plane (Yang, Chen, Wang, and Wang, 2008). (E)-4-nitrobenzaldehyde oxime, $C_7H_6N_2O_3$, structure includes intermolecular O–H⋯N hydrogen bonds linking the molecules into centrosymmetric dimers with an $R_2^2(6)$ graph-set motif. The planes containing the CNO and ONO atoms subtend dihedral angles of 5.47(5)° and 8.31(5)°, respectively. (Abbas, Hussain,

Hafeez, Badshah, Hasan, and Lo, 2010). The crystal structure of 4-methylbenzenecarbothioamide C_8H_9NS, is stabilized by intermolecular N–H⋯S hydrogen bonds representing $R_2^2(8)$ and $R_2^4(8)$ motifs resulting in the formation of eight-membered rings lying about inversion centers with the hydrogen bonds building up chains parallel to the *b* axis (Ali, Hameed, Luqman, Akhtar, and Parvez, 2010).

Two types of supramolecular motifs were formed in the cocrystallisation of nicotinic acid hydrazide (niazid) with carboxylic acids. Conventional supramolecular synthesis to form 1–D ribbon and 2–D sheet structures utilizing the similar hydrogen bonds of the ring-type $R_2^2(7)$ heterosynthon and chain-type C(4) homosynthon gave nearly identical crystal packings (Lemmerer, Bernstein, and Kahlenberg, 2011). In 2-[(*Z*)-4,7-dichloro-3,3-dimethyl-2,3-dihydro-1*H*-indol-2-yl-idene]-3-oxopropane-nitrile, $C_{14}H_{14}C_lN_3O$, orientation of the acetamide group arises from intramolecular hydrogen bonding between the indole N–H and carbonyl groups forming N–H⋯O hydrogen-bonded dimers in $R_2^2(8)$ motifs through inversion-related acetamide groups, whilst dimers are also formed by pairs of amine–nitrile N–H⋯N hydrogen bonds in $R_2^2(12)$ motifs. Together these interactions generate ribbons propagating along the b-axis direction (Helliwell, Baradarani, Alyari, Afghan, and Joule, 2012).

π–π Interactions or Aromatic–Aromatic Interactions

Aromatic–aromatic interactions are noncovalent interactions that occur between aromatic rings, often in situations where one is relatively electron rich and the other relatively electron poor, combining weak electrostatic and weak van der Waals interactions.. Aromatic stacking interactions are widespread in nature and are believed to provide stability to these natural structures. A heteroatom in an aromatic ring can be

electron neutral, electron rich, or electron deficient. An electron deficient π-system stabilizes the interaction by decreasing the repulsion (Hunter, Lawson, Perkins, and Urch, 1991).

Analysis of X–H$\cdots\pi$ bonding is not standardized. Many researchers follow the simple expedient of calculating the contacts between hydrogen atom positions, often without correcting for the apparent shortening of the X–H bond that occurs in X-ray crystallographic analysis, and the atoms of the aromatic moiety. Other researchers calculate the perpendicular distance from the hydrogen atom positions to the best mean plane through the aromatic moiety. A recent review of hydrogen bonds between carbon based aromatic rings (Nangia, 2002) defined the centroid of the ring, Cg, and calculated distances $D = $ [donor$\cdots Cg$], d = [H$\cdots Cg$], and the angle $\theta = $ [X–H$\cdots Cg$] relative to the ring centroid as illustrated in Figure 1.6.
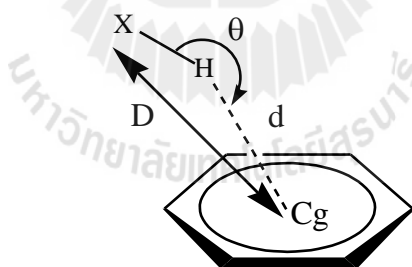
Figure 1.6 Geometrical parameters used for analysis of the model π-system of an aromatic ring (Nangia, 2002).

A recent study of hydrogen bonds between nitrogen containing heterocyclic rings (isoxazole, imidazole, and indole) used the same system, defining the centroid of the heterocyclic ring, Cg, and calculating distances $D = $ [donor$\cdots Cg$], d = [H$\cdots Cg$],

and the angle θ = [X–H⋯Cg] relative to the ring centroid (Malathy and Ponnuswamy, 2005) similar to that illustrated in Figure 1.6. They searched nonbonded contacts from atoms surrounding the ring centroid (Cg) with intermolecular interaction distance up to 4.0 Å for D and 3.0 Å for d. Lower limits with Cg were set at 2.8 Å for D and 1.8 Å for d distances to avoid false contacts within the molecule. Distance and directionality characteristics of hydrogen bonds can be conveniently studied in scatter plots of hydrogen-bond angles versus d and/or D distances (Olovsson, Jonsson, Schuster, Zundel, and Sandorfy, 1976).

To compare the different (X–H⋯π) systems, the distances d were normalized according to the sum of the van der Waals radii:

$$R = \frac{d(H \cdots Cg)}{\sum (r_{Cg} + r_H)},$$ (1)

where r_{Cg} is radius of ring centroid and r_H is radius of hydrogen atom. The centroid of the π-system is assumed to be involved in the interaction and heteroatoms are presented and the van der Waals radii for the ring is taken as the average van der Waals radii of all the atomic species. The result in this study showed that carbon donors participate in relatively large numbers for X–H⋯π interactions, and they adopt T-shaped geometry. The aromatic–aromatic interaction analysis was categorized into three types of geometry, the edge-to-face (T-shaped) geometry (that is, a C–H⋯π interaction), the offset stacked (parallel displaced) orientation, and the face-to-face stacked orientation that occurs with opposite quadrupole moments based on the involvement of the heterocyclic π-systems as illustrated in Figure 1.7. The π-systems in all three categories prefer to form offset stacking C–H⋯π interaction geometry. The heterocyclic aromatic rings which normally favor the formation of T-shaped

geometry are also found to prefer offset stacking geometry, which may be due to the influence of the heteroatom.
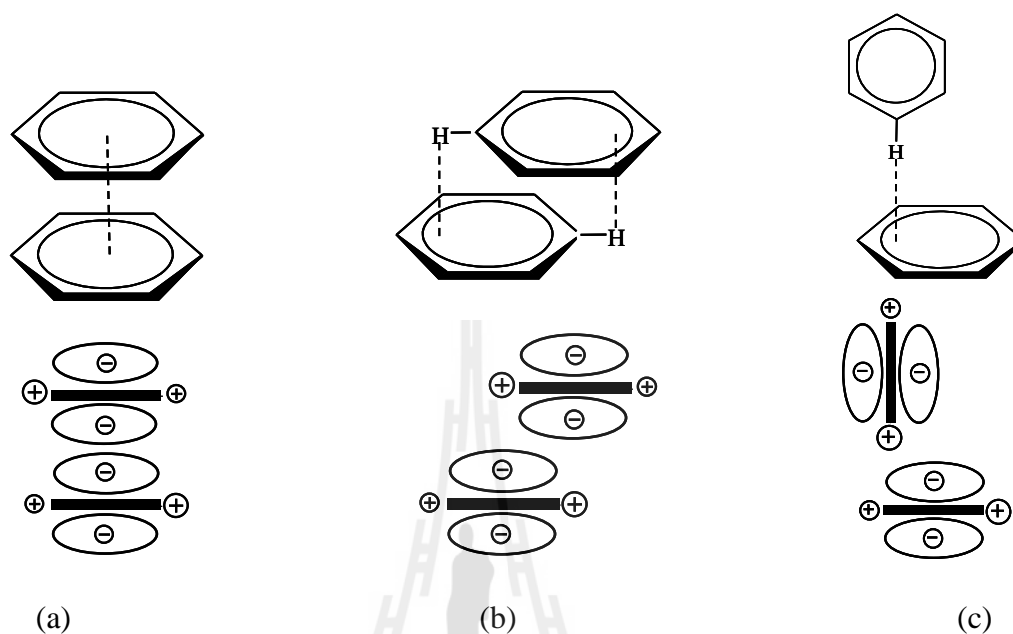
Figure 1.7 Geometries of aromatic interactions. (a) face-to-face (*ff*), (b) offset stacked (*off*), and (c) edge-to-face (*ef*) stacked.

1.7 Research Objectives

(1) Separate acyclovir from the excipients and recrystallize the separated material and/or crystal screening from different solvents to prepare suitable single crystals that contain acyclovir in the crystal lattice.

(2) Evaluate the crystalline materials by optical microscopy and Fourier transform infrared spectroscopy to identify the functional groups in the material and by thermogravimetric analysis to check weight loss of water. Determine single crystal X-ray crystal structure to study the 3−D crystal structure and atomic species.

(3) Analyze supramolecular interactions of acyclovir and tricyclic acyclovir including interatomic distances, angles, and torsional angles, especially to improve understanding of hydrogen-bonding and other inter- and intra-molecular interactions in their crystal structures.

1.8 References

Abbas, A., Hussain, S., Hafeez, N., Badshah, A., Hasan, A., and Lo, K. M. (2010). (E)-4-nitrobenzaldehyde oxime. **Acta Crystallographica Section E**. 66: o1130.

Alche, L. E, Berra, A., Veloso, M. J., and Coto, C. E. (2000). Treatment with meliacine, a plant derived antiviral, prevents the development of herpetic stromal keratitis in mice. **Journal of Medical Virology**. 61: 474–480.

Alche, L. E., Barquero, A. A., Sanjuan, N. A., and Coto, C. E. (2002). An antiviral principal present in a purified fraction from *malia azedarach* L. leaf aqueous extract restrains herpes simplex virus type 1 propagation. **Phototherapy Research**. 16: 348–352.

Ali, S., Hameed, S., Luqman, A., Akhtar, T., and Parvez, M. (2010). 4-Methylben-zenecarbothioamide. **Acta Crystallographica Section E**. 66: o1271.

Allen, F. H., Davies, J. E., Galloy, J. J., Johnson, O., Kennard, O., Macrae, C. F., Mitchell, G. F., Smith, J. M., and Watson, D. G. (1991). The development of versions 3 and 4 of the Cambridge Structural Database System. **Journal of Chemical Information and Computer Sciences**. 31: 187–204.

Allen, F. H., Hoy, V. J., Howard, J. A. K., Thalladi, V. R., Desiraju, G. R., Wilson, C. C., and McIntyre, G. J. (1998). Carbonyl-carbonyl interactions can be

competitive with hydrogen bonds. **Journal of the American Chemical Society**. 119: 3477–3480.

Amoros, M., Simoes, C. M., Girre, L., Sauvager, F., and Cormier, M. (1992). Synergistic effect of flavones and flavonols against herpes simplex virus type 1 in cell culture. Comparison with the antiviral activity of propolis. **Journal of Natural Products**. 55: 1732–1740.

Amoros, M., Lurton, E., Boustie, J., Girre, L., Sauvager, F., and Cormier, M. (1994). Comparison of the antiherpes simplex virus activities of propolis and 3-methyl-but-2-enyl caffeate. **Journal of Natural Products**. 57: 644–647.

Amsterdam, J. D., Maislin, G., and Rybakowski, J. (1990). A possible antiviral action of lithium carbonate in herpes simplex virus infections. **Biological Psychiatry**. 27: 447–453.

Anand, B. S., Hill, J. M., Dey, S., Maruyama, K., Bhattacharjee, P. S., Myles, M. E., Nashed, Y. E., and Mitra, A. K. (2003). *In vivo* antiviral efficacy of a dipeptide acyclovir prodrug, val-val-acyclovir, against HSV-1 epithelial and stromal keratitis in the rabbit eye model. **Investigative Ophthalmology & Visual Science**. 44(6): 2529–2534.

Anand B. S., Katragadda S., and Mitra, A. K. (2004). Pharmacokinetics of novel dipeptide ester prodrugs of aciclovir after oral administration: Intestinal absorption and liver metabolism. **Journal of Pharmacology and Experimental Therapeutics**. 311: 659–667.

Armaka, M., Papanikolaou, E., Sivropoulou, A., and Arsenakis, M. (1999). Antiviral properties of isoborneol, a potent inhibitor of herpes simplex virus type 1. **Antiviral Research**. 43: 79–92.

Balzarini, J. and McGuigan, C. (2002). Bicyclic pyrimidine nucleoside analogues (BCNAs) as highly selective and potent inhibitors of varicella-zoster virus replication. **Journal of Antimicrobial Chemotherapy**. 50: 5–9.

Barboza, F., Vecchia, D. D., Tagliari, M. P., Silva, M. A. S., and Stulzer, H. K. (2009). Differential scanning calorimetry as a screening technique in compatibility studies of acyclovir extended release formulations. **Journal of Pharmaceutical Chemistry**. 43(6): 363–368.

Beers, M.H. and Berkow, R. (1999). Antiviral Drugs. In: Beers MH, Berkow R, editors. The Merck Manual of Diagnosis and Therapy. 17th edition. John Wiley & Sons, New York, 1127–1131.

Benencia, F. and Courreges, M. C. (2000). *In vitro* and *in vivo* activity of eugenol on human herpes virus. **Phytotherapy Research Journal**. 14: 495–500.

Bertrand, N., Gauthier, M. A., Bouvet, C., Moreau, P., Petitjean, A., Leroux, J-C., and Leblond, J. (2011). New pharmaceutical applications for macromolecular binders. **Journal of Controlled Release**. 155(2): 200–210.

Birnbaum, G. I., Cygler, M., and Shugar, D. (1984). Conformational features of acyclonucleosides: Structure of acyclovir. **Canadian Journal of Chemistry**. 62: 2646–2651.

Birnbaum, G. I., Johansson, N. G., and Shugar, D. (1987). Conformation of acyclonucleosides: Crystal structure of 9-(4-hydroxybutyl)guanine, an analogue of acyclovir. **Nucleosides and Nucleotides**. 6(4): 775–783.

Biron, K. K. and Elion, G. B. (1980). In vitro susceptibility of varicella-zoster virus to acyclovir. **Antimicrobial Agents and Chemotherapy**. 18(3): 443–447.

Bondi, A. (1964). van der Waals volumes and radii. **Journal of Physical Chemistry**. 68(3): 441–451.

Boryski, J., Golankiewicz, B., and de Clerk, E. (1988). Synthesis and antiviral activity of novel N-substituted derivatives of acyclovir. **Journal of Medicinal Chemistry**. 31(7): 1351–1355.

Boryski, J., Golankiewicz, B., and de Clerk, E. (1988). Synthesis and antiviral activity of novel N-substituted derivatives of acyclovir. **Journal of Medicinal Chemistry**. 31(7): 1351–1355.

Boryski, J., Golankiewicz, B., and de Clerk, E. (1991). Synthesis and antiviral activity of 3-substituted derivatives of 3,9-dihydro-9-oxo-5H-imidazo[1,2-a]purines, tricyclic analogs of acyclovir and ganciclovir. **Journal of Medicinal Chemistry**. 34(8): 2380–2383.

Bourne, N., Bernstein, D. I., and Stanberry, L. R. (1999). Civamide (ciscapsaicin) for treatment of primary or recurrent experimental genital herpes. **Antimicrobial Agents and Chemotherapy**. 43: 2685–2688.

Brunton, L., Chabner, B. A., and Knollmann, B. C. (2010). Handbook of Goodman & Gilman's. **The Pharmacological Basis of Therapeutics**. 12th edition, McGraw-Hill: New York, Chapter 58.

Bschor, T. (1999). Complete suppression of recurrent herpes labialis with lithium carbonate. **Pharmacopsychiatry**. 32: 158.

Carraher, C. E., Sabir, T. S., and Roner, M. R. (2006). Synthesis of organotin polyamine ethers containing acyclovir and their preliminary anticancer and antiviral activity. **Journal of Inorganic and Organometallic Polymers and Materials**. 16(3): 249–257.

Chainok, K. and Haller K.J. (2004). Hydrothermal synthesis, characterization, and supramolecular structure of [Co(C$_6$H$_4$O$_2$N)$_3$]·H$_2$O. **5th Asian Crystallographic Association Meeting**, Hong Kong.

Chang, Y.-C., Chen, Y.-D., Chen, C.-H., Wen, Y.-S., Lin, J.-T., Chen, H.-Y, Kuo, M.-Y., and Chao, I. (2008). Crystal engineering for π-π stacking via interaction between electron-rich and electron-deficient heteroaromatics. **Journal Organic Chemistry**. 73: 4608–4610.

Chatkon, A. (2001). **Structural studies of supramolecular microporous materials**. M.Sc. Thesis. Suranaree University of Technology, Thailand.

Chatkon, A. and Haller K. J. (2011). Water dimer in the structure of NiV$_2$O$_6$·2H$_2$O. **American Crystallographic Association Meeting**, New Orleans, USA.

Chayavichitsilp, P., Buckwalter, J. V., Krakowski, A. C. and Friedlander, S. F. (2009). Herpes simplex. **Journal of the American Academy of Pediatrics**. 30(4): 119–129.

Chiang, L. C., Chiang, W., Chang, M. Y., Ng, L. T., and Lin, C. C. (2002). Antiviral activity of plant ago major extracts and related compounds *in vitro*. **Antiviral Research**. 55: 53–62.

Chrisp, P. and Clissold, S. P. (1991). Foscarnet. A review of its antiviral activity, pharmacokinetic properties and therapeutic use in immunocompromised patients with cytomegalovirus retinitis. **Drugs**. 41: 104–129.

Coen, D. M. and Schaffer, P. A. (1980). Two distinct loci confer resistance to acycloguanosine in herpes simplex virus type 1. **Proceedings of the National Academy of Sciences**. U.S.A. 77: 2265–2269.

Crumpacker, C. S. (1996). Ganciclovir. **The New England Journal of Medicine**. 335(10): 721–729.

Dimitrova, Z., Dimov, B., Manolova, N., Panchev, S., Ilieva, D., and Shishkov, S. (1993). Antiherpes effect of *Melissa officinalis* L. extracts. **Acta Microbiological Bulgarica**. 29: 65–72.

de Clercq, E. (1996). Therapeutic potential of cidofovir (HPMPC, Vistide) for the treatment of DNA virus (*i.e.* herpes-, papova-, pox- and adenovirus) infections. **Verhandelingen-Koninklijke Academie voor Geneeskunde van Belgie**. 58: 19–49.

de Clerk, E. and Field, H. J. (2006). Antiviral prodrugs–the development of successful prodrug strategies for antiviral chemotherapy. **Journal of Pharmacology**. 147(1): 1–11.

Desiraju, G.R. (1995). Supramolecular synthons in crystal engineering–a new organic-synthesis. **Angewandte Chemie International Edition**. 34: 2311–2327

Duncan, A. M., Ball, R. O., and Pencharz, P. B. (1996). Lysine requirement of adult males is not affected by decreasing dietary protein. **Journal of the American College of Nutrition**. 64: 718–725.

Elion, G. B. (1993). The George Hitchings and Gertrude Elion Lecture. The pharmacology of azathioprine. **Annals of the New York Academy of Sciences**. 685: 400–407.

Elion, G. B., Furman, P. A., Fyfe, J. A., De Miranda, P., Beauchamp, L., and Schaeffer, H. J. (1977). Selectivity of action of an antiherpetic agent, 9-(2-hydroxyethoxymethyl) guanine. **Proceedings of the National Academy of Sciences**. 74: 5716–5720.

Elion, G. B., Furman, P. A., Fyfe, J. A., de Miranda, P., Beauchamp, L., and Schaeffe, H. J. (1977). Selectivity of action of an antiherpetic agent, 9-(2-hydroxyethoxymethyl)guanine. **Proceedings of the National Academy of Sciences**. USA 74(12): 5716–5720.

Ellenhorn, M. J. (1997). **Medical Toxicology. Diagnosis and Treatment of Human Poisoning. 2nd ed**. Williams & Wilkins, Baltimore, USA. pp 296–300.

Etter, M. C., MacDonald, J. C., and Bernstein, J. (1990). Graph-set analysis of hydrogen-bond patterns in organic crystals. **Acta Crystallographica Section B**. 46: 256–262.

Finnerty, E. F. (1986). Topical zinc in the treatment of herpes simplex. **Cutis**. 37(2): 130–131.

Flodin, N. W. (1997). The metabolic roles, pharmacology, and toxicology of lysine. **Journal of the American College of Nutrition**. 16: 7–21.

Fridlender, B., Chejanovsky, N., and Becker, Y. (1978). Selective inhibition of herpes simplex virus type I DNA polymerase by zinc ions. **Virology**. 84: 551–554.

Furman, P. A., St. Clair, M. H., and Spector, T. (1984). Acyclovir triphosphate is a suicide inactivator of the herpes simplex virus DNA polymerase. **The Journal of Biological Chemistry**. 259(15): 9575–9579.

Gaby, A. R. (2006). Natural remedies for herpes simplex. **Alternative Medicine Review**. 11(2): 93–101.

Gebhardt, B. M., Focher, F., Eberle, R., Manikowski, A., and Wright, G. E. (2009). Effect of combinations of antiviral drugs on herpes simplex encephalitis. **Drug Design Development and Therapy**. 3: 289–294.

Gong, Y., Raj, K. M., Luscombe, C. A., Gadawski, I, Tam, T., Chu, J., Gibson, D., Carlson, R., and Sacks, S. L. (2004). The synergistic effects of betulin with acyclovir against herpes simplex viruses. **Antiviral Research**. 64: 127–130.

Gordon, Y. J., Asher, Y., and Becker, Y. (1975). Irreversible inhibition of herpes simplex virus replication in BSC-1 cells by zinc ions. **Antimicrobial Agents and Chemotherapy**. 8: 377–380.

Greco, A., Diaz, J.-J., Thouvenot, D., and Morfin, F. (2007). Novel targets for the development of antiherpes compounds. **Infectious Disorders-Drug Targets**. 7: 11–18.

Greene, T. W. and Wuts, P. G. (1999). **Protective Groups in Organic Synthesis**. Wiley, New York.

Grell, J., Bernstein, J., and Tinhofer, G. 1999. **Graph-set Analysis of Hydrogen Bond Patterns. Some material concepts; Techniques**. Maximilians UniversitÄt MÜnchen, Report TUM M9908.

Gupta, P. and Rapp, F. (1976). Effect of zinc ions on synthesis of herpes simplex virus type 2 induced polypeptides. **Proceedings of the Society for Experimental Biology and Medicine**. 152: 455–458.

Haller, K. J., Johnson, P. L., Feltham, R. D., Enermark, J. H., Ferraro, J. R., and Basile, L. J. (1979). Effects of temperature and pressure on the molecular and electronic structure of N,N'-ethylenebis(salicylideneiminato)nitrosyliron, Fe(NO)(salen). **Inorganica Chimica Acta**. 33: 119–130.

Hayashi, K., Hayashi, T., and Kojima, I. (1996). A natural sulfated polysaccharide, calcium spirulan, isolated from *Spirulina platensis*: *In vitro* and *ex vivo*

evaluation of anti-herpes simplex virus and anti-human immunodeficiency virus activities. **AIDS Research Human Retroviruses**. 12: 1463–1471.

Helliwell, M., Baradarani, M. M., Alyari, M., Afghan, A., and Joule, J. A. (2012). 2-(4-Chloro-3,3,7-trimethyl-2,3-dihydro-1H-indol-2-ylidene)-2-cyanoacetamide. **Acta Crystallographica Section E**. 68: o234.

Ho, H. T., Woods, K. L., Bronson, J. J., De Boeck, H., Martin, J. C., and Hitchcock, M. J. (1992). Intracellular metabolism of the antiherpes agent (S)-1-[3-hydroxy-2-(phosphonylmethoxy)propyl]cytosine. **Molecular Pharmacology**. 41: 197–202.

Hunter, C. A., Singh, J., and Thornton, J. M., (1991). Pi-pi interactions: The geometry and energetics of phenylalanine-phenylalanine interactions in proteins. **Journal of Molecular Biology**. 218: 837–846.

Jeffrey, G. A. and Seanger, W. (1991). **Hydrogen Bonding in Biological Systems**. Springer-Verlag. Berlin. pp. 1–42.

Jeffrey, G. A. (1997). **An Introduction to Hydrogen Bonding**, Oxford University Press. Oxford.

Klenner, F. (1949). The treatment of poliomyelitis and other virus diseases with vitamin C. **South African Journal of Surgery**. 209–214.

Krachodnok, S. and Haller, K. J. (2005). Supramolecular structure analysis: detection of a novel carbonyl-carbonyl interaction in the structure of pyridine-3,5-dicarboxylic Acid. **Proceedings of the 9th Annual National Symposium on Computational Science & Engineering 2005 (ANSCSE 9)**. Mahidol University Press, Bangkok. pp. 464–470.

Krachodnok, S. (2010). **Synthesis and structural studies of organically modified main group vanadates**. Ph.D. Thesis, Suaranaree University of Technology, Thailand.

Kristl, A., Srcic, S., Vrecer, F., Sustar, B., and Vojnovic, D. (1996). Polymorphism and pseudo polymorphism: Influencing the dissolution properties of the guanine derivative acyclovir. **International Journal of Pharmaceutics**. 139: 231–235.

Kutluay, S. B., Doroghazi, J., Roemer, M. E., and Triezenberg, S. J., (2008). Curcumin inhibits herpes simplex virus immediate-early gene expression by a mechanism independent of p300/CBP histone acetyltransferase activity. **Virology**. 373(2): 239.

Larder, B. A. and Darby, G. (1986). Susceptibility to other antiherpes drugs of pathogenic variants of herpes simplex virus selected for resistance to acyclovir. **Antimicrobial Agents and Chemotherapy**. 29: 894–898.

Lee, J. B., Hayashi, K., Hayashi, T., Sankawa, U., and Maeda, M. (1999). Antiviral activities against HSV-1, HCMV, and HIV-1 of rhamnan sulfate from *Monostroma latissimum*. **Journal of Medicinal Plant and Natural Product Research**. 65: 439–441.

Lee, J. B., Srisomporn, P., Hayashi, K., Tanaka, T., Sankawa, U., and Hayashi, T. (2001). Effects of structural modification of calcium spirulan, a sulfated polysaccharide from Spirulina platensis, on antiviral activity. **Chemical & Pharmaceutical Bulletin**. 49: 108–110.

Lehn, J. M. (1993). Supramolecular chemistry. **Science**. 260(5115), 1762–1763.

Lemmerer, A., Bernstein, J., and Kahlenberg, V., (2011). Covalent assistance to supramolecular synthesis: Directing the supramolecular assembly of cocrystals

by *in situ* modification of hydrogen bonding functionality. **CrystEngComm**. 13: 55‒59.

Levitt M. and Park B. H. (1993). Water: now you see it, now you don't. **Structure**. 1(4): 223–226.

Lewis, L. D., Fowle, A. S., Bittiner, S. B., Bye, A., and Isaacs, P. E. (1986). Human gastrointestinal absorption of acyclovir from tablet duodenal infusion and sipped solution. **British Journal of Clinical Pharmacology**. 21(4): 459–62.

Lieb, J. (1981). Immunopotentiation and inhibition of herpes virus activation during therapy with lithium carbonate. **Medical Hypotheses**. 7: 885‒890.

Loregian, A., Gatti, R., Palù, G., and de Palo, E. F. (2001). Review: Separation methods for acyclovir and related antiviral compounds. **Journal of Chromatography B**. 764: 289–311.

Lyu, S. Y., Rhim, J. Y., and Park, W. B. (2005). Antiherpetic activities of flavonoids against herpes simplex virus type 1 (HSV-1) and type 2 (HSV-2) *in vitro*. **Archives of Pharmacal Research**. 28: 1293–1301.

Malathy and Ponnuswamy, 2005. Nature of π-interactions in nitrogen-containing heterocyclic systems: A structural database analysis. **Crystal Growth & Design**. 6(3): 736–742.

McEvoy, G. K., Miller, J., and Litvak, K. (2004). AHFS Drug Information. **United States of American Society of Health-System Pharmacists**. pp 765–775.

Miller, W. H. and Miller, R. L. (1980). Phosphorylation of acyclovir(acyclo-guanosine) monophosphate by GMP kinase. **The Journal of Biological Chemistry**. 255(15): 7204–7207.

Mundinger, T.A. and Efferth, T. (2008). Herpes simplex virus: Drug resistance and new treatment options using natural products (Review). **Molecular Medicine Reports**. 1: 611–616.

Mucsi, I., Molnar, J., and Motohashi, N. (2001). Combination of benzo[a]pheno-thiazines with acyclovir against herpes simplex virus. **International Journal Antimicrobial Agents**. 18: 67–72.

Naesens, L. and de Clercq, E. (2001). Recent developments in herpes virus therapy. **Herpes**. 8: 12–16.

Nangia, A. (2002). Database research in crystal engineering. (Review). **CrystEngComm**. 17: 1–9.

Nawawi, A; Nakamura, N; Meselhy, MR; Hattori, M; Kurokawa, M; Shiraki, K; Kashiwaba, N; Ono, M. (2001). *In vivo* antiviral activity of *Stephania cepharantha* against herpes simplex virus type-1. **Phytotherapy Research**. 15: 497–500.

O'Brien, J. J. and Campoli-Richards, D. M. (1989). Acyclovir. An updated review of its antiviral activity, pharmacokinetic properties and therapeutic efficacy. **Drugs**. 37(3): 233–309.

Olovsson, I., Jonsson, P.-G., Schuster, P., Zundel, G., and Sandorfy C. (1976). Eds; In The Hydrogen Bond. Recent Developments in Theory and Experiments North-Holland: **Amsterdam**, pp 393–455.

Park, N. H., Park, J. B., Min, B. M., and Cherrick, H. M. (1991). Combined synergistic antiherpetic effect of acyclovir and chlorhexidine in vitro. **Oral Surgery Oral Medicine Oral Pathology**. 71(2): 193–196.

Perfect, M. M., Bourne, N., Ebel, C., Rosenthal, S. L. (2005). Use of complementary and alternative medicine for the treatment of genital herpes. **Herpes**. 12(2): 38–41.

Perry, C. M. and Wagstaff, A. J. (1995). Famciclovir. A review of its pharmacological properties and therapeutic efficacy in herpes virus infections. **Drugs**. 50(2): 396–415.

Prichard, M. N., Prichard, L. E., and Shipman, C. (1993). Strategic design and three-dimensional analysis of antiviral drug combinations. **Antimicrobial Agents and Chemotherapy**. 37(3): 540–545.

Pujol, C. A., Scolaro, L. A., Ciancia, M., Matulewicz, M. C., Cerezo, A. S., and Damonte, E. B. (2006). Antiviral activity of a carrageenan from *Gigartina skottsbergii* against intraperitoneal murine herpes simplex virus infection. **Planta Medica**. 72: 121–125.

Ponce, N. M., Pujol, C. A., Damonte, E. B., Flores, M. L., and Stortz, C. A. (2003). Fucoidans from the brown seaweed *Adenocystis utricularis*: Extraction methods, antiviral activity and structural studies. **Carbohydrate Research**. 338: 153–165.

Reddy, D. S., Craig, D. C., and Desiraju, G. R. (1996). Supramolecular synthons in crystal engineering. 4. Structure simplification and synthon interchangeability in some organic diamondoid solids. **Journal of the American Chemical Society**. 118(17): 4090–4093.

Reddy, D. S., Ovchinnikov, Y. E., Shishkin, O. V., Struchkov, Y. T. and Desiraju, G. R. (1996). Supramolecular synthons in crystal engineering. 3. Solid state architecture and synthon robustness in some 2,3-dicyano-5,6-dichloro-1,4-

dialkoxybenzenes. **Journal of the American Chemical Society**. 118(17): 4085–4089.

Ren, Z., Zhang, C-H., Wang, L-J, Cui, Y-X, and Qi, R-B. (2010). *In vitro* antiviral activity of the total alkaloids from *Tripterygium hypoglaucum* against herpes simplex virus type 1. **Virologica Sinica**. 25: 107–114.

Roizman, B. and Sears, A. E. (1990). **Handbook for Herpes simplex virus and their replication**. In: **Virology**, 2nd edition. New York. 2: 1795–1841.

Serkedjieva, J. and Manolova, N. (1992). Plant polyphenolic complex inhibits the reproduction of influenza and herpes simplex viruses. **Basic Life Sciences**. 59: 705–715.

Shlomai, J., Asher, Y., Gordon, Y. J., Olshevsky, U., and Becker, Y. (1975). Effect of zinc ions on the synthesis of herpes simplex virus DNA in infected BSC-1 cells. **Virology**. 66: 330–335.

Skinner, G. R., Hartley, C., Buchan, A., Harper, L., and Gallimore, P. (1980). The effect of lithium chloride on the replication of Herpes simplex virus. **Medical Microbiology Immunology**. 168: 139–148.

Slonczewski, J. and Foster, J. W. (2010). **Handbook for Microbiology: In-text Tools Aid Student Understanding and Stimulate Inquiry**, 2nd edition, New York. 13–14.

Sohn, Y. T. and Kim, S. H. (2008). Polymorphism and pseudopolymorphism of acyclovir. **Archives of Pharmacal Research**. 31(2): 231–234.

Smith, J. S. and Robinson, N. J. (2002). Age-specific prevalence of infection with herpes simplex virus types 2 and 1: A global review. **Journal of Infectious Diseases**. 186: 3–28.

Steed, J. W. and Atwood, J. L. (2000). **Handbook of Supramolecular Chemistry: Nature of Supramolecular Interactions**. pp. 22–28.

Steed, J. W. and Atwood, J. L. (2000). **Handbook of Supramolecular Chemistry: Crystal Engineering**. pp. 392–397.

Steiner, T. (2002). The Hydrogen Bond in the Solid State**. Angewandte Chemie International Edition**. 41: 48–76.

Stella, V. J., Charman, W. N, and Naringrekar, V. H. (1985). Prodrugs. Do they have advantages in clinical practice? **Drugs**. 29(5): 455–473.

Suwińska, K., Golankiewicz, B., and Zielenkiewicz, W. (2001). Water molecules in the crystal structure of tricyclic acyclovir. **Acta Crystallographica Section C**. 57: 767–769.

Suzuki, M., Okuda, T., and Shiraki, K. (2006). Synergistic antiviral activity of acyclovir and vidarabine against herpes simplex virus types 1 and 2 and varicella-zoster virus. **Antiviral Research**. 72: 157–161.

Talarico, L. B., Zibetti, R. G., Faria, P. C., Scolaro, L. A., Duarte, M. E., Noseda, M. D., Pujol, C. A, and Damonte, E. B. (2004). Anti-herpes simplex virus activity of sulfated galactans from the red seaweeds *Gymnogongrus griffithsiae* and *Cryptonemia crenulata*. **International Journal of Biological Macromolecule**. 34: 63–71.

Tanna, S., Wood, C., and Lawrence, M. J. (1992). Mechanism of pyrimidine nucleoside uptake in intestinal brush border membrane vesicles. **Biochemical Society Transactions**. 20(2): 116S.

Thompson, K. D. and Dragar, C. C. (2004). Antiviral activity of *Undaria pinnatifida* against herpes simplex virus. **Phytotherapy Research**. 18: 551–555.

United States Pharmacopeial Convention Inc. (2006). USP 27-NF 22. The United States Pharmacopeia–The National Formulary. Rockville MD: **The United States Pharmacopeial Convention Inc**. 2085.

Whitley, R. J., Tucker, B. C., Kinkel, A. W., Barton, N. H., Pass, R. F., Whelchel, J. D., Cobbs, C. G., Diethelm, A. G., and Buchanan, R. A. (1980). Pharmacology, tolerance, and antiviral activity of vidarabine monophosphate in humans. **Antimicrobial Agents and Chemotherapy**. 18(5): 709–715.

Whitley, R. J., Blum, M. R., Barton, N., and de Miranda, P. (1982). Pharmacokinetics of acyclovir in humans following intravenous administration. A model for the development of parenteral antivirals. **American Journal of Medicine**. 73(1A): 165–171.

Xu, F., Sternberg, M. R., Kottii, B. J., McQuillan, G. M., Lee, F. K., Nahmias, A. J., Berman, S. M., and Markowitz, L. E. (2006). Trends in herpes simplex virus type 1 and type 2 seroprevalence in the United States. **Journal of the American Medical Association**. 296(8): 964–973.

Yang, J.-h., Chen, Y.-x., Wang, S.-h., and Wang, J.-l. (2008). N-(2-Formamido-ethyl)formamide. **Acta Crystallographica Section E**. 64: o2418.

Zandi, K., Zadeh, M. A., Sartavi, K., and Rastian, Z. (2007). Antiviral activity of *Aloe vera* against herpes simplex virus type 2: An *in vitro* study. **African Journal of Biotechnology**. 6(15): 1770–1773.

CHAPTER II

EXPERIMENTAL

2.1 Separation

Separation techniques are physical methods used to separate mixtures. One of the simplest separation techniques depends on the relative solubility of the components of the mixture in solvents of varying polarity. Simple filtration is an easy way to separate an insoluble solid from liquid if the desired product is insoluble in a solvent that dissolves all the other components of the mixture. The solid remains on the filter paper and the liquid goes through the paper into the beaker. In this work filtration was used to separate the drug from the incipients. Impurities from the solution are often trapped as the precipitate forms resulting in impure crystals and/or affecting size and single crystal.

2.2 Recrystallization

Particularly, in the case of similar components or a large number of components, the solid material thus isolated may still require further recrystallization to achieve the highest possible state of purity. The recrystallization of the solid is a valuable technique to master because it is one of the methods used most often for purification of solids. The crystallization process may be quite slow, requiring relatively long periods of time (days to weeks) to ensure that no impurities are trapped in the crystal lattice as the crystal grows. The simplest recrystallization of an impure

solid involves only dissolving the compound in a hot solvent until a saturated solution is obtained, filtering the solution to separate solid impurities from the solution, and then allowing the desired crystals to form in the filtrate while the impurities remain in solution. Various factors and techniques can be modified. Optimum results are generally obtained when the compound is moderately soluble. Too high solubility often results in highly supersaturated metastable solutions and the excess nucleation that results from them, leading to small crystal size, while too low solubility often leads to small crystal size due to rapid excess nucleation and very short growth times. Both cases can be improved by preparing a mixture of solvents such as a 1:1 or 1:2 solvent-water or other suitable solvent mixture to optimize single crystal formation. Several factors affect the size of the crystals during crystal growth, especially choice of a solvent in which the compound is moderately soluble. Many nucleation sites result in a smaller average crystal size which is not desirable. Fewer nucleation sites result in fewer crystals each of larger size. During crystallization ambient dust in the laboratory may provide nucleation sites. It is important to use a clean vessel and to minimize dust or other extraneous particulate matter in the crystal growing vessel. The solvents used in this work are given in Table 2.1.

Table 2.1 Mixtures used in this work.

Solvent	pH of solution	Solvent	pH of solution	Solvent	pH
0.01 mM NaOH	9.22	H_2O:HOAc (1:1)	–	H_2O:DMF (1:1)	–
H_2O	5.66	H_2O:DMSO (1:1)	–	H_2O:THF (1:1)	–
0.5 M HCl	0.58	5% DMF	–	H_2O:iProOH (2:1)	–
0.1 M HCl	1.05	10% DMF	–	H_2O:EtOH (2:1)	–

2.3 Crystal Screening

Crystal screening is a general guideline for discovery of new solid forms of the compound of interest. Efficient screening can be divided into three steps similar to those already proposed (Mirza, Miroshnyk, Heinämäki, and Yliruusi, 2008); (i) crystal screen design, (ii) crystal screening, and (iii) crystal selection. The compounds of interest in this work are the pharmaceutical compounds acyclovir and tricyclic acyclovir. Crystalline forms of these API could include polymorphs, solvates, and cocrystals or salts that may be useful for single crystal X-ray structure determination.

Crystal Screen Design

(1) pH strategies, the different species of acyclovir as a function of pH are given in Chapter I in Figure 1.1. (2) Solvent strategies involve choosing a solvent that has suitable functionality to interact strongly with the API to increase the chance to incorporate solvent molecules into the crystal lattice producing new solid materials (there are various terms, such as synthon, solvate, *etc*. to describe this design strategy). (3) Supramolecular design concepts also apply, especially in modifying the pattern of the supramolecular synthon depending on the pH. If the pH $\leq$ 2.27 the cationic form (ACVH$^+$) shown in Figure 2.1(a) will dominate in solution. Forming the charged species may lead to the energetically more favorable charge stablized hydrogen bonds. Between pH 2.27 and 9.25, the neutral form (ACV) as shown in Figure 2.1(b) dominates in solution. This was the case in the previous acyclovir structure (Birnbaum, Cygler, and Shugar, 1984), and in the 9-(4-hydroxy-butyl)guanine analogue of acyclovir (Birnbaum, Johansson, and Shugar, 1987) shown in Figure 2.1(b). Of course crystal stablization energies play a large role in

determining the species in the actual product and relatively minor components of the solution often are found in the crystalline products.
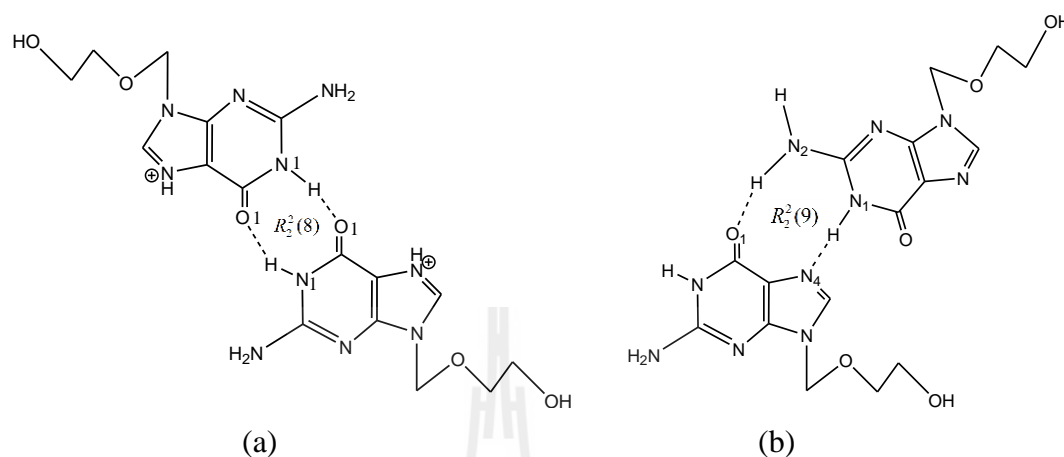
Figure 2.1 Supramolecular synthon patterns of acyclovir structure (a) pKa ≤ 2.27 for N−H···O and N−H···O and (b) pKa ≥ 2.27 and ≤ 9.25 for N−H···N and N−H···O.

Crystal Screening

The crystal screening experimental method used solvent based crystallization methods to optimize size for a crystal suitable for a single crystal X-ray structure determination.

The slow evaporation technique is the simplest way to grow compounds and works well for compounds that are not sensitive to ambient conditions in the laboratory. This is the normal, most successful method to obtain single crystals. A small amount of compound can be dissolved in a single solvent or mixture of solvents and left for slow evaporation. Prepare a solution of the compound in a suitable solvent (saturated or nearly saturated). Filter the solution through a clean glass frit into a clean vessel and cover, but not tightly. Gently put the container in a quiet, out of the way place and allow the solvent to evaporate slowly.

Crystal Selection

The products of the screening experiments were examined under an optical microscope equipped with a polarizing attachment for the first step. When suitable single crystals were found, the product was characterized by additional physical methods to characterize the solid as described in section 2.4.

2.4 Physical Methods for Characterizing Solids

A combination of techniques was used to characterize the solids, including spectroscopic techniques and thermal analysis. Single crystals were characterized by single crystal X-ray diffraction to know about the crystal structure as given in the fractional coordinates of the atoms present in the asymmetric unit that could then be analyzed for supramolecular interactions.

Fourier Transform Infrared Spectroscopy (FTIR)

FTIR is a common technique useful to identify the functional groups in a compound. FTIR spectra of solid products dispersed in KBr pellets were measured on a Spectrum GX (Perkin Elmer, USA) spectrophotometer in the mid-IR range, 4000-400 cm^{-1} with 5 cm^{-1} resolution by summing 50 scans. The spectral peaks correspond to transitions between vibrational energy levels of a molecule, involving the stretching or bending of bonds. Selection rules for IR transitions must be obeyed for IR absorption to occur for a particular vibrational transition of the molecule. The molecule must have a dipole moment and there must be a change in the molecular dipole moment during the vibration, *i.e.* the dipole moment must be different at the extremes of the vibration. Vibrations can be attributed to individual functional groups (characteristic group vibrations). The identification of these groups depends on the

amount of infrared radiation absorbed and the particular frequency at which these groups absorb radiation, characteristics of the specific types of chemical bonds and a quite useful technique to confirm the identity of a particular compound, or as a tool to help determine the structure of a molecule.

Thermogravimetric analysis (TGA)

TGA investigates the properties of a solid as a function of change in temperature. It is useful for investigating loss of water or small molecules from the sample by monitoring sample mass as a function of time as the temperature is increased at a controlled uniform rate. TGA analysis curves were recorded on a TGA/DSC1 instrument (Mettler Toledo, Switzerland) in flowing air with a heating rate of 30°C min^{-1} from room temperature to 500°C. Calibration of the instrument was performed using alumina standards.

X-ray Crystallography

Single crystal X-ray crystallography is a powerful technique, widely used for study of the crystal structure and atomic spacing that determine the arrangement of atoms within a crystal. A beam of X-rays strikes a single crystal which causes the beam to spread into many specific directions, determined by the principles of constructive and destructive interference of collimated monochromatic X-rays from a crystalline sample. The diffracted patterns are detected and counted, consistent with there being intensity above background for the highest scattering angles, and processed. All possible diffraction directions of the lattice should be measured. The directions of the beams in the lattice is the angle between the incident and diffracted rays of the diffraction patterns and are given by Bragg's Law ($n\lambda = 2d\sin\theta$).

Intensity data were collected at 293(2) K for acyclovir dihydrate on an Xcalibur Ruby Gemini (Oxford Diffraction, UK) area detector diffractometer equipped with a highly-oriented pyrolytic graphite crystal incident beam monochromator and an enhanced Mo K_α (λ = 0.71073 Å) X-radiation source. Two dimensional frames were collected by ω-scan rotation of the positioned crystal by a fraction of a degree for each frame. Preliminary determination of the unit cell and space group, the number of frames required to minimize excessive multiple collection of the same reflection while maximizing the coverage of reciprocal space, the collection of the frame data, processing of the frame data after data collection completed to extract the intensities and their standard deviations for all completely measured reflections, and correction of the resulting intensity data for absorption and other systematic effects by the multiscan method using reflections with identical *hkl* indices, and merging to provide a unique (*1* symmetry) reflection data set were carried out under the control of the diffractometer *CrysAlis PRO* operating system (Oxford Diffraction, 2009).

The crystal structure was refined by *SHELXL*-97 (Sheldrick, 1997) based on the intensities of the diffracted beams, the unit cell dimensions, the crystal system, and the space group to produce a 3–D picture of the electron density within the crystallographic lattice, from which atom locations and details of site ordering, and bond lengths and angles can be derived.

2.5 Research Procedure

Crystallized materials of acyclovir were obtained by crystallization screening experiments using solution-based methods (solvents are listed in Table 3.1 of Chapter III). The success or failure of each screening experiment was evaluated by

examination of the product under an optical microscope with and without polarized light to evaluate the suitability of a crystal for single crystal X-ray crystallography. When the preliminary examination indicated success, additional techniques including FTIR and melting point determination, or other techniques that are useful for evaluating if a new phase has been formed were utilized. When the new phase was identified, and an optimum sized crystal was obtained, the 3–D structure of the material was determined by single crystal X-ray diffraction and other properties were characterized as judged appropriate to support the structure analysis. Supramolecular analyses of acyclovir and tricyclic acyclovir were carried out as described in Section 2.6. A short description of the research procedure is given in Figure 2.2.
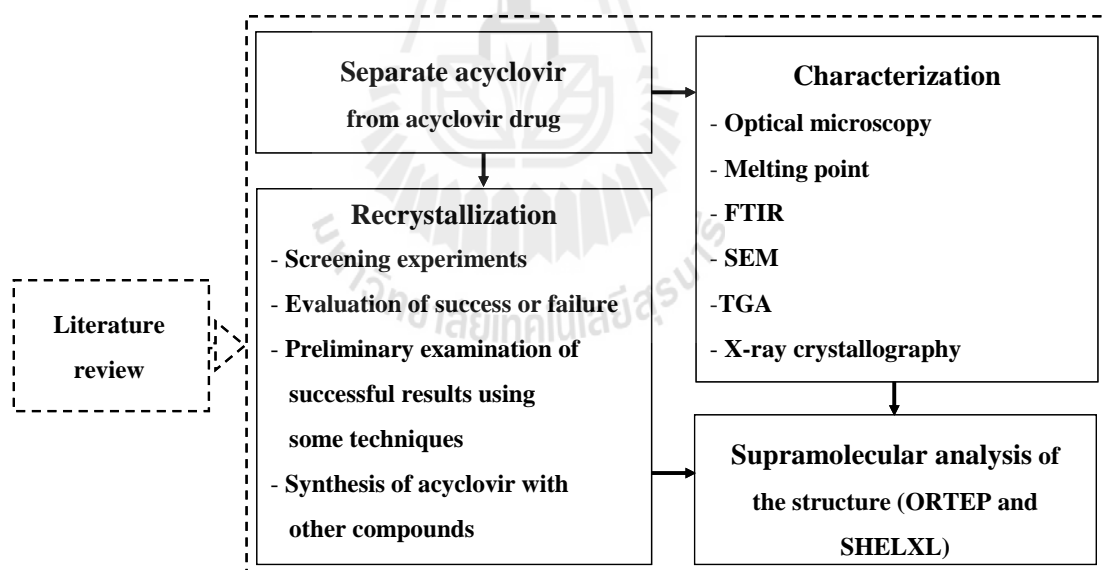
Figure 2.2 Schematic representation of the research procedure.

2.6 Crystallographic Geometry Calculations

Supramolecular Interactiosns

Contact distances and angles were calculated with *ORTEP*-III (Burnett and Johnson, 1996) and are reported for the structures of acyclovir and the acyclovir derivative tricyclic acyclovir. Coordinates for the new acyclovir dihydrate, $C_8H_{11}N_5O_3 \cdot 2H_2O$, structure are given in Table A1 of Appendix A and those of tricyclic acyclovir, $C_{11}H_{13}N_5O_3 \cdot 2H_2O$, obtained from the IUCr electronic archives (Suwińska, Golankiewicz, and Zielenkiewicz, 2001) are given in Table B1 of Appendix B. The computational analysis of supramolecular interactions, including hydrogen bonds, interatomic distances, angles, torsional angles, and graphical analysis of $C_8H_{11}N_5O_3 \cdot 2H_2O$ and $C_{11}H_{13}N_5O_3 \cdot 2H_2O$ were computed by the *ORTEP*-III program (Burnett and Johnson, 1996).

π–π Stacking or Aromatic–Aromatic Interactions

The conventional D−H···A notation or D−H···(A−R) notation, where the acceptor position is nearer the midpoint of the A−R bond contact. The distances between adjacent ring systems were calculated as the perpendicular separation between the given hydrogen atom and the mean plane of the delocalized ring system (calculated with the MPLA instruction of *SHELXL*-97 (Sheldrick, 1997)). Details of the mean plane calculations are given in Appendix A Table A2 for acyclovir and Appendix B Table B2 for tricyclic acyclovir. The ring system consisted of two rings for acyclovir and three rings for the tricyclic acyclovir structure which are parallel to adjacent ring systems. Atoms of the symmetry related planes above and below the mean plane of interest were included in the calculation using the EQIV instruction to define their coordinate transformations and including these positions in the MPLA

instruction, but not in the "Plane Through Atoms" group. When multiple mean planes are specified, the angles between adjacent planes are also displayed in the output files of the program.

Rerefinement of Tricyclic Acyclovir

The crystallographic information file, *cif* file, and the structure factor file, *hkl* file, from the IUCr electronic archives (Suwińska, Golankiewicz, and Zielenkiewicz, 2001) were used for the rerefinement. Preliminary analysis of the hydrogen bonding indicated that the published structure did not completely model the disorder of the hydrogen bonded region. The nonhydrogen atom positions from the published structure were used as the starting point for the rerefinement. The disorder part of atoms O16B and C17B (and associated hydrogen atoms) were assigned as the major component. Hydrogen atoms on the adjacent methylene groups were also divided into major and minor components. The disordered water and hydroxy hydrogen atoms were located from difference electron density Fourier maps and the other hydrogen atoms were placed in calculated idealized geometrical positions using HFIX and AFIX geometrical constraints. Refinement of side chain disorder with the PART instructions in the *ins* file allows *SHELXL*-97 to correctly position hydrogen atoms on the apparently overlapping disordered portions of the side chain divided into two groups, one group containing the major component and the other containing the minor component. For disorder on O19B using PART instructions, the same pattern was written as disorder at the side chain at O16 and C17. The coordinates of all disordered atom positions could be found in the output files of the program. The hydrogen atoms in water molecules were restrained to have similar d[O−H] using SADI instructions in the *ins* file of the *SHELXL*-97 program (Sheldrick, 1997). The hydrogen bonding in

the acyclovir and tricyclic acyclovir structure were analyzed using BOND, CONF, and HTAB instructions of *SHELXL*-97 (see in Chapter V).

2.7 References

Birnbaum, G. I., Cygler, M., and Shugar, D. (1984). Conformational features of acyclonucleosides: Structure of acyclovir. **Canadian Journal of Chemistry**. 62: 2646–2651.

Birnbaum, G. I., Johansson, N. G., and Shugar, D. (1987). Conformation of acyclonucleosides: Crystal structure of 9-(4-hydroxybutyl) guanine, an analogue of acyclovir. **Nucleosides and Nucleotides**. 6(4): 775–783.

Burnett, M. N. and Johnson, C. K. (1996). *ORTEP*-III: Oak Ridge Thermal Ellipsoid Plot Program for Crystal Structure Illustration, Report ORNL-6895, **Oak Ridge National Laboratory**. Tennessee, USA.

Etter, M. C., MacDonald, J. C., and Bernstein, J. (1990). Graph-set analysis of hydrogen-bond patterns in organic crystals. **Acta Crystallographica Section B**. 46: 256–262.

Holden, A. and Singer, P. (1960). Crystals and Crystal Growing. Anchor Books-Doubleday, Garden City, New York. p. 120.

Laudise, R. A. (1970). The Growth of Single Crystals. **Prentice-Hall**: New York. pp. 275–293.

Mirza, S., Miroshnyk, I., Heinämäki, J., and Yliruusi, J. (2008). Co-crystals: An Emerging Approach for Enhancing Properties of Pharmaceutical Solid. **DOSIS**. 24(2): 90–96.

Oxford Diffraction (2009). *CrysAlis PRO CCD* and *CrysAlis PRO RED*. **Oxford Diffraction Ltd**., Yarnton, England.

Sheldrick, G.M. (1997). *SHELXL-97* Program for the Solution and Refinement of Crystal Structures. University of Göttingen, Germany.

Suwińska, K., Golankiewicz, B., and Zielenkiewicz, W. (2001). Water molecules in the crystal structure of tricyclic acyclovir. **Acta Crystallographica Section C**. 57: 767–769.

CHAPTER III

RECRYSTALLIZATION AND SUPRAMOLECULAR

STRUCTURE OF THE DIHYDRATE OF THE ACTIVE

PHARMACEUTICAL INGREDIENT ACYCLOVIR

3.1 Introduction

Acyclovir is the active pharmaceutical ingredient (API) in the most common antiviral drug used for treatment of HSV and VZV infections. Advantages for acyclovir are low cytotoxicity and low HSV resistance as well as the availability of low cost generic forms. Disadvantages are low bioavailability and lower effectiveness than valacyclovir, famciclovir, and fascarnet for HSV infection. As with many viral diseases, after several decades of acyclovir use, resistant strains of the virus are beginning to develop, especially in immunocompromised patients (Greco, Diaz, Thouvenot, and Morfin, 2007).

Pharmaceutical acyclovir is normally present in a hydrated crystalline form consisting of three acyclovir molecules and two water molecules in the crystallographic asymmetric unit (Kristl, Srcic, Vrecer, Sustar, and Vojnovic, 1996) corresponding to a theoretical water content of about 5%. Dose and solubility are normally expressed in units of anhydrous acyclovir. Two anhydrous polymorphs and an unstable hydrate of acyclovir have also been reported. Although only slight and insignificant differences in solubility values exist between anhydrous and hydrated

forms, the anhydrous form of acyclovir possesses poorer dissolution properties than the hydrated form. A stable anhydrous form can be obtained by drying hydrated acyclovir at temperatures above 150°C (Kristl, Srcic, Vrecer, Sustar, and Vojnovic, 1996). Conformation features have been compared with those in other known acyclonucleosides and examined in relation to the behavior of acyclonucleosides in various enzymatic systems, including those related to antiviral activity. The crystal data of the commercial form is in space group $P2_1/n$ with cell parameters, $a =$ 25.459(1) Å, $b =$ 11.282(1) Å, $c =$ 10.768(1) Å, and $\beta =$ 95.16(1)° (Birnbaum, Cygler, and Shugar, 1984).

Previous studies have characterized the crystalline forms by FTIR, solubility, dissolution rate, PXRD (Kristl, Srcic, Vrecer, Sustar, and Vojnovic, 1996; Sohn and Kim, 2008), and by the thermal techniques, DSC and TGA (Sohn and Kim, 2008). both polymorphic and solvate forms have been studied (Kristl, Srcic, Vrecer, Sustar, and Vojnovic, 1996). Some research focused on the compatibility and stability of the drug ingredients; acyclovir API and mixtures of acyclovir with excipients, has been carried out using DSC, PXRD, and FTIR techniques for the purpose of development of acyclovir extended release formulations because potential physical and chemical interaction between drugs and excipients can affect the chemical nature, the stability, and the bioavailability of the drug, and consequently, its therapeutic efficacy and safety. Acyclovir has only exhibited interaction that could influence the stability of the product in the binary mixture of acyclovir with magnesium stearate (Barboza, Vecchia, Tagliari, Silva, and Stulzer, 2009).

More study on acyclovir structure (Lutker, Ones, Xu, Ramamoorthy, and Matzger, 2011) demonstrates the acyclovir structure (ACV) in three forms, form I

(anhydrous), form V (ACV/H_2O; 1:2), and form VI (ACV/H_2O; 3:2) occur in different space groups. All have the planar guanine ring with the side chain extending above the plane of the guanine ring in the gauche conformation, except in residue 1 of from V, where the side chain extends perpendicular to the plane of guanine ring in the trans conformation.

The hydrogen bond pattern in form I (anhydrous) has the amine group of the guanine bonded to the hydroxyl group of another molecule, d[N···O] = 3.05 Å and the carbonyl of still another molecule d[N···O] = 2.92 Å. The nitrogen of the five-membered ring bonds to N−H of the six-membered ring d[N···N] = 2.82 Å. The molecules pack in sheets along the *b*-axis and along the *c*-axis to build columns that alternate the orientation of the guanine ring. In form V ($3C_8H_{11}N_5O_3 \cdot 2H_2O$), one water molecule connects the carbonyl functionality and hydroxyl group of residue 3, and in addition binds to the hydroxyl group of residue 1. The other water molecule is hydrogen bonded to residue 1 through the carbonyl, whereas residue 2 hydrogen bonds through a hydroxyl group and residue 3 hydrogen bonds through the amine. The residues themselves form dimers, with residue 1 forming a homodimer and residue 2 dimerizing with residue 3, creating infinite sheets within the crystal structure. The water molecules in the crystal of form VI ($C_8H_{11}N_5O_3 \cdot 2H_2O$) bind to each other within a channel parallel to the *a*-axis bound to the ACV molecules surrounding them. The ACV molecules stack together to build chains that are orientated toward the water channels with the guanine rings alternating their orientation.

Herein, we report separation of acyclovir from acyclovir drug, and the crystal data of a triclinic form determined by single crystal X-ray diffraction. The selected

thin plates of acyclovir dihydrate, $C_8H_{11}N_5O_3 \cdot 2H_2O$, obtained by recrystallization from water solvent. The water molecules act as interconnectors between the drug molecules in this structure.

3.2 Experimental

Materials, Apparatus, and Crystallization

All chemicals were reagent grade and used without purification. The infrared spectra were measured on a Spectrum GX (Perkin Elmer, USA) over the range 4000-400 cm^{-1} with 5 cm^{-1} resolution by summing 50 scans using KBr pellets. The TGA analysis curve was recorded on a TGA/DSC1 instrument in flowing air with a heating rate 10°C min^{-1} (Mettler Toledo, Switzerland).

Preparation of Material

Acyclovir material was separated from an acyclovir drug, (Vilerm, Siam Pharmaceutical Co., containing 800 mg acyclovir in a 1,032 mg tablet) with 320 mL of deionized H_2O; solubility in water (2.5 mg/mL at 37°C), stirred at 250 rpm and heated at 70–80°C for 30 min and filtered. The filtrate was heated at 70–80°C to reduce the volume until one third remained, cooled to room temperature, and left overnight to precipitate. The precipitate was filtered, washed with distilled H_2O, and dried in air at room temperature (recovery: 33.5% based on acyclovir).

Recrystallization

The recrystallization of acyclovir materials was done by solution-based screening experiments and slow evaporation. The acyclovir material, 10 mg, was mixed with 5 mL solvent, heated at 70–80°C with stirring at 300 rpm for 30 min to obtain a clear solution, and filtered. The filtrate was cooled to room temperature and

stored for several days, the mixture with water as solvent gave colorless crystals with thin plate morphology that were filtered, washed with distilled H_2O, and dried in air at ambient temperature. The dihydrate of $C_8H_{11}N_5O_3$ was the major product (6 mg, yield: ca 60% based on acyclovir material). The crystals were separated by hand under an optical microscope. Similar experiments with other solvents failed to provide suitable crystals, as shown in Table 3.1.

Table 3.1 Screening experiment crystallization by solvent based method.

Acyclovir (mg)	Solvent	Volume (ml)	pH	Products*
10	0.01mM NaOH	5	9.22	X
10a	H_2O	5	5.66	Thin plate crystals, colorless (ca. 60%)
10	0.5 M HCl	5	0.58	X
10	0.1 M HCl	5	1.05	Needle crystals, colorless (ca. 50%)

* % yield based on acyclovir material. X= failed to provide suitable crystal.

Table 3.1 (Continued).

Acyclovir (mg)	Solvent	Volume (ml)	pH	Product colors*
10	H$_2$O:HOAc (1:1)	5	–	X
10	H$_2$O: DMSO (1:1)	5	–	X
10	5% DMF	5	–	Small thin plate crystals, colorless (ca. 45%)
10	10% DMF	5	–	Small needle crystals, colorless (ca. 45%)
10	H$_2$O: DMF (1:1)	5	–	X
10	H$_2$O:THF (1:1)	5	–	X
10	H$_2$O: iPrOH (2:1)	8	–	X
10	H$_2$O: EtOH (2:1)	8	–	X
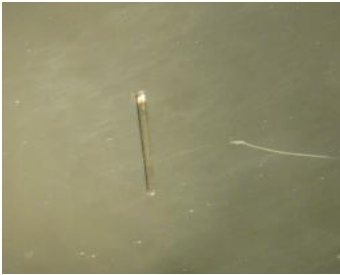
* % yield base on acyclovir material. X= failed to provide suitable crystal.

X-Ray Crystallography

A suitable thin plate of $C_8H_{11}N_5O_3 \cdot 2H_2O$ with size 0.08 mm $\times$ 0.33 mm $\times$ 0.41 mm suitable for single crystal X-ray crystallography was selected and mounted on a thin glass capillary. Intensity data were collected at 293(2) K with an area detector diffractometer equipped with a graphite-monochromated Mo $K\alpha$ X-radiation source (λ= 0.071073). The structure was solved by direct methods and refined by full-matrix least-squares refinement on F^2 using *SHELXL*-97 (Sheldrick, 1997). The hydrogen atoms on C5A, C5B, N1A, N1B, N2A, N2B, 3A and O3B were located from difference electron density Fourier maps and the other hydrogen atoms were placed in calculated, geometrically idealized positions using geometrical constraints [O–H = 0.82 Å, C–H = 0.93 Å (-CH), C–H = 0.97 Å (-CH$_2$), N–H = 0.86 Å (-NH and -NH$_2$) and restrained in idealized geometry using riding model restraits with isotropic atomic displacement parameters set at $U_{iso}(H) = 1.2U_{eq}(O,C,N)$]. The acyclovir distances and angles for the nonhydrogen atoms agree well with the previous report (Birnbaum, Cygler, and Shugar, 1984).

Supramolecular structural interactions were identified by a combination of distance and angle calculations along with examination of graphical images of molecules and fragments of molecules. Inter- and intra-molecular contact distances were calculated by a 102 instruction to the *ORTEP*-III program (Burnett and Johnson, 1996) to a maximum search radius cut-off distance of 3.6 Å, which gives both interatomic distances and interatomic angles about each origin atom. The hydrogen bonding in the acyclovir structure was analyzed using BOND, CONF, and HTAB instructions in the *SHELXL*-97 program, which searched all hydrogen atoms to find

possible bond length, bond angle, torsion angle and, hydrogen bonds or donor atoms and acceptor atoms.

Aromatic–aromatic interactions in and around the guanine ring were evaluated by using the MPLA instruction of *SHELXL*-97 to calculate the best least-squares plane through a given aromatic system (x, y, z in crystal coordinates), deviations from from the plane, equation of the plane, angles to other planes, and the distances between atoms of adjacent guanine rings to the plane.

A comparison of crystal structure data of previously reported acyclovir forms and this work is given in Table 3.2. Fractional triclinic coordinates and equivalent atomic displacement parameters are listed in Table A1 (Appendix A).

Table 3.2 Structure data of previously reported acyclovir forms and this work.

Parameter	Form I (Lutker *et al*, 2011)	Form V (Birnbaum *et al*. 1984; Lutker *et al*. 2011)	Form VI (Lutker *et al*. 2011)	This work
Chemical formula	$C_8H_{11}N_5O_3$	$C_8H_{11}N_5O_3 \cdot 2/3H_2O$	$C_8H_{11}N_5O_3 \cdot 2H_2O$	$C_8H_{11}N_5O_3 \cdot 2H_2O$
Asymmetric unit	$C_8H_{11}N_5O_3$	$3(C_8H_{11}N_5O_3)2(H_2O)$	$2(C_8H_{11}N_5O_3)4(H_2O)$	$2(C_8H_{11}N_5O_3)4(H_2O)$
Molecular weight	225	237.23	261.25	261.25
Temperature (K)	85	293	85	293(2)
Crystal Size (mm)	0.01x0.03x0.11	0.025x0.125x0.55	0.02x0.10x0.22	0.08×0.33×0.41
Crystal system	Monoclinic	Monoclinic	Triclinic	Triclinic
Space group	$P2_1/c$	$P2_1/n$	$P\bar{1}$	$P\bar{1}$
Unit cell				
a (Å)	10.9121(11)	25.459(1)	6.8004(5)	6.8996(6)
b (Å)	11.3111(12)	11.282(1)	11.3317(9)	11.4170(9)
c (Å)	7.8843(8)	10.768(1)	14.9368(12)	15.0806(13)

Table 3.2 (Continued)

Parameters	Form I	Form V	Form VI	This work
α (°)	90	90	82.722(1)	82.595(7)
β (°)	108.262	95.16(1)	82.502(1)	82.395(7)
γ (°)	90	90	89.323(1)	89.368(7)
Volume ($\mathring{A}^3$)	909.42	3080.34	1131.98	1167.65(17)
Z	4	12	4	4
Density (Mg m^{-3})	1.645	1.53	1.533	1.486
Goodness of fit	1.051		1.031	1.017
R_1 [a]; $I_o > 2\sigma(I_o)$	0.0427	0.053	0.0365	0.0397
R_1; all data	0.0652	0.064	0.0523	0.0498
wR; all data	0.0886		0.0857	0.1139

[a]. Discrepency indices: R_1 = conventional; wR = weighted sums based on I.

3.3 Results and Discussion

Single crystal X-ray diffraction data from the thin plate with triclinic space group, $P\bar{1}$, at 293(2) K. shows the asymmetric unit to contain two crystallographically independent molecules of acyclovir and four independent water molecules. The asymmetric unit of $C_8H_{11}N_5O_3 \cdot 2H_2O$, molecules A and B as presented in Figure 3.1.
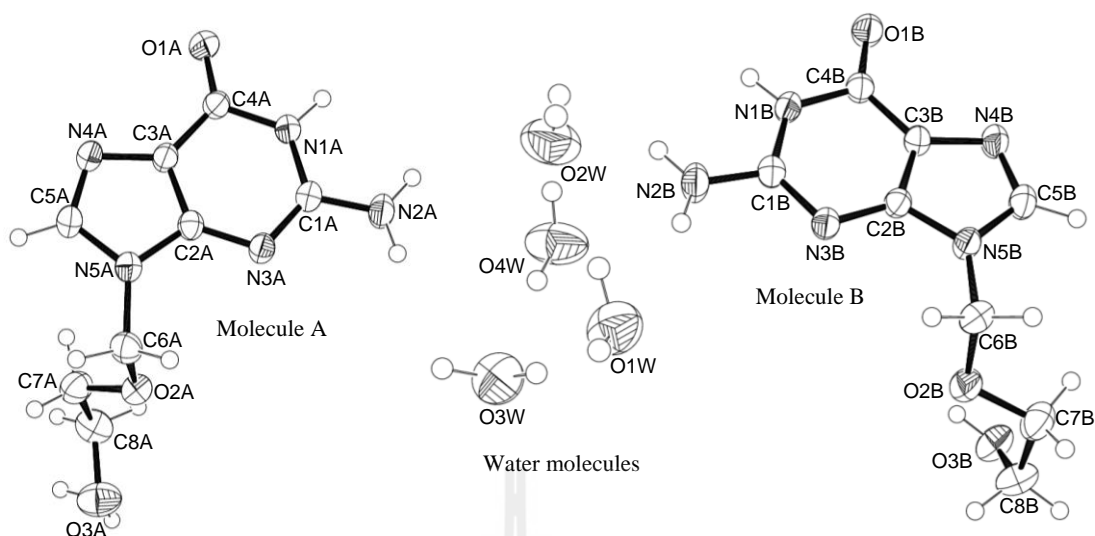
Figure 3.1 The asymmetric unit of $C_8H_{11}N_5O_3 \cdot 2H_2O$. Molecules A and B and the four water molecules are shown. Atomic displacement parameters of the nonhydrogen atoms are represented as 50% probability surfaces, and hydrogen atoms are included as spheres with arbitrary radius for clarity.

The bond lengths and bond angles in the acyclovir structure agree with the previous report (Birnbaum, Cygler, and Shugar, 1984). The bond angle between C5−N5−C6 is slightly larger than C2−N5−C6 about 0−1.3° of molecules A and B which is preference for acyclonucleoside (Birnbaum, Cygler, and Shugar, 1984). The selected interatomic bond distances and bond angles are given in Tables 3.3−3.4.

Table 3.3 Selected interatomic distances[a] (Å) for acyclovir; $C_8H_{11}N_5O_3\cdot2H_2O$.

Atoms	Mole A	Mole B	Atoms	Mole A	Mole B
N1–C1	1.367 (0.001)	1.370 (0.001)	N2–H2	0.860	0.860
N1–C4	1.394 (0.001)	1.385 (0.001)	C5–H5	0.930	0.930
C1–N3	1.324 (0.001)	1.325 (0.001)	C6–H6a(c)	0.970	0.970
C1–N2	1.340 (0.001)	1.336 (0.001)	C6–H6b(d)	0.970	0.970
N3–C2	1.351 (0.001)	1.346 (0.001)	C7–H7a(c)	0.970	0.970
C2–N5	1.372 (0.001)	1.374 (0.001)	C7–H7b(d)	0.970	0.970
C2–C3	1.380 (0.002)	1.381 (0.002)	C8–H8a(c)	0.970	0.970
C3–N4	1.385 (0.001)	1.388 (0.001)	C8–H8b(d)	0.970	0.970
C3–C4	1.419 (0.002)	1.416 (0.002)	O3–H3a(c)	0.820	0.820
C4–O1	1.234 (0.001)	1.245 (0.001)	O3–H3b	0.820	-
N4–C5	1.306 (0.002)	1.307 (0.002)		**Water molecules**	
C5–N5	1.376 (0.001)	1.377 (0.002)	O1W–H1Wa	0.855 (0.017)	
N5–C6	1.458 (0.002)	1.455 (0.002)	O1W–H1Wb	0.873 (0.017)	
C6–O2	1.405 (0.001)	1.402 (0.001)	O2W–H2Wa	0.870 (0.017)	
O2–C7	1.431 (0.002)	1.427 (0.002)	O2W–H2Wb	0.858 (0.017)	
C7–C8	1.494 (0.002)	1.490 (0.002)	O3W–H3Wa	0.862 (0.017)	
C8–O3	1.416 (0.002)	1.423 (0.002)	O3W–H3Wb	0.871 (0.017)	
N1–Ha	0.860	0.860	O4W–H4Wa	0.857 (0.017)	
N2–H2a(c)	0.860	0.860	O4W–H4Wb	0.868 (0.017)	

[a] The standard deviations of the least significant digits are given in parentheses.

Table 3.4 Selected interatomic angles[a] (º) for acyclovir; $C_8H_{11}N_5O_3 \cdot 2H_2O$.

Atoms	Mole A	Mole B	Atoms	Mole A	Mole B
O1–C4–N1	120.1(0.10)	120.13(0.10)	C5–N5–C6	127.3(0.10)	128.6(0.09)
O1–C4–C3	128.3 (0.10)	128.0(0.10)	N4–C5–H5	123.3	123.4
N1–C4–C3	111.6(0.09)	111.8(0.10)	O2–C6–N5	111.9(0.09)	112.17(0.09)
C1–N1–C4	125.1(0.10)	125.13(0.09)	O2–C6–H6a(c)	109.2	109.2
C1–N1–H1	117.5	117.4	N5–C6–H6a(c)	109.2	109.2
C4–N1–H1	117.5	117.4	O2–C6–H6c(d)	109.2	109.2
N3–C1–N2	119.6(0.10)	119.7(0.11)	N5–C6–H6c(d)	109.2	109.2
N3–C1–N1	123.9(0.10)	123.8(0.10)	H6a(c)–C6–H6b(d)	107.9	107.9
N2–C1–N1	116.5(0.10)	116.5(0.10)	C6–O2–C7	113.2(0.09)	113.8(0.10)
C1–N2–H2a(c)	120.0	120.0	O2–C7–C8	109.6(0.11)	108.0(0.11)
C1–N2–H2b(d)	120.0	120.0	O2–C7–H7a(c)	109.7	110.1
H2–N2–H2(b)(d)	120.0	120.0	C8–C7–H7a(c)	109.7	110.1
C1–N3–C2	112.3(0.09)	111.9(0.10)	O2–C7–H7b(d)	109.7	110.1
N3–C2–N5	126.0(0.10)	125.6(0.10)	C8–C7–H7b(d)	109.7	110.1
N3–C2–C3	128.2(0.10)	128.6(0.10)	H7a(c)–C7–H7b(d)	108.2	108.4
N5–C2–C3	105.8(0.09)	105.7(0.09)	O3–C8–C7	109.7(0.11)	112.9(0.11)
C2–C3–N4	110.6(0.10)	110.5(0.09)	O3–C8–H8a(c)	109.7	109.9
C2–C3–C4	118.9(0.09)	118.6(0.10)	C7–C8–H8a(c)	109.7	109.9
N4–C3–C4	130.4(0.10)	130.8(0.10)	O3–C8–H8b(d)	109.7	109.9
C5–N4–C3	104.3(0.09)	104.5(0.09)	C7–C8–H8b(d)	109.7	109.9
N4–C5–N5	113.4(0.10)	113.2(0.10)	H8a(c)–C8–H8b(d)	108.2	107.8
N5–C5–H5	123.3	123.4	C8–O3–H3	109.5	109.5
C2–N5–C5	105.9(0.09)	106.04(0.09)	C8–O3–H3	109.4	–
C2–N5–C6	126.3(0.09)	125.4(0.09)	H3a(c)–O3–H3b(d)	87.6	–

[a] The standard deviations of the least significant digits are given in parentheses.

Table 3.4 (Continued).

Atoms	Angle	Atoms	Angle
Water molecules			
H1WA–O1W–H1WB	106.7(2.11)	H3WA–O3W–H3WB	106.7 (2.06)
H2WA–O2W–H2WB	105.7(2.09)	H4WA–O4W–H4WB	110.5 (2.10)

[a] The standard deviations of the least significant digits are given in parentheses.

The torsion angles at the guanine ring are close to 0º at C3–C4–N1–C1, C4–N1–C1–N3, N1–C1–N3–C2, C1–N3–C2–C3, N5–C2–C3–N4, N3–C2–C3–C4, N1–C4–C3–C2, O1–C4–C3–N4, C2–C3–N4–C5, C3–N4–C5–N5, C3–C2–N5–C5, N3–C2–N5–C6 and N4–C5–N5–C2 meaning that the fourth atom nearly eclipses the first atom. However, the torsion angles at O1–C4–N1–C1, C4–N1–C1–N2, N2–C1–N3–C2,   C1–N3–C2–N5,   N3–C2–C3–N4,   N5–C2A–C3–C4, O1–C4–C3–C2, N1–C4–C3–N4, C4–C3–N4–C5, N3–C2–N5–C5, C3–C2–N5–C6 and N4–C5–N5–C6 in the acyclovir structure are nearer 180º, indicating the trans configuration. Selected torsion angles at the guanine ring are given in Table 3.5.

Table 3.5 Selected torsion angles (º)[a] at the guanine ring for acyclovir; $C_8H_{11}N_5O_3 \cdot 2H_2O$.

Torsion angle (º)	Mole A	Mole B	Torsion angle (º)	Mole A	Mole B
O1–C4–N1–C1	−178.8 (0.11)	−179.2 (0.10)	N1–C4–C3–C2	−1.8 (0.14)	−2.1 (0.14)
C3–C4–N1–C1	0.4 (0.15)	0.5 (0.15)	O1–C4–C3–N4	0.8 (0.20)	1.2 (0.20)
C4–N1–C1–N3	0.8 (0.17)	0.7 (0.17)	N1–C4–C3–N4	−178.3 (0.11)	−178.4 (0.11)
C4–N1–C1–N2	178.8 (0.11)	−179.2 (0.11)	C2–C3–N4–C5	0.02 (0.13)	−0.3 (0.12)
N2–C1–N3–C2	−178.4 (0.10)	179.6 (0.11)	C4–C3–N4–C5	176.7 (0.11)	176.3 (0.11)
N1–C1–N3–C2	−0.4 (0.15)	−0.2 (0.15)	C3–N4–C5–N5	0.1 (0.13)	−0.2 (0.13)
C1–N3–C2–N5	178.4 (0.10)	177.6 (0.10)	N3–C2–N5–C5	−179.6 (0.10)	179.9 (0.10)
C1–N3–C2–C3	−1.2 (0.16)	−1.6 (0.16)	C3–C2–N5–C5	0.12 (0.11)	−0.7 (0.11)
N3–C2–C3–N4	179.6 (0.10)	180.0 (0.10)	N3–C2–N5–C6	−7.1 (0.17)	1.0 (0.17)
N5–C2–C3–N4	−0.1 (0.12)	0.6 (0.12)	C3–C2–N5–C6	172.6 (0.10)	178.4 (0.10)
N3–C2–C3–C4	2.5 (0.17)	3.0 (0.17)	N4–C5–N5–C2	−0.1 (0.13)	0.6 (0.13)
N5–C2–C3–C4	−177.2 (0.09)	−176.4 (0.09)	N4–C5–N5–C6	−172.5 (0.10)	−178.5 (0.10)
O1–C4–C3–C2	177.3 (0.11)	177.6 (0.11)			

[a] The standard deviations of the least significant digits are given in parentheses.

The torsion angle of C2−N5−C6−O2 is −77.6º for molecule A in this work, which is similar to molecule A and the 90.9º for molecule B is similar to molecule C but the torsion angle in molecule B are opposite direction in molecule C in the previous report (Birnbaum, Cygler, and Shugar, 1984). The C5−N5−C6−O2 is 93.3º for molecule A and −90.2º for molecule B are nearly the same values in molecule C from previous report, only molecule B of this work present opposite direction. The torsion angle of N5−C6−O2−C7 is −73.1º of molecule A which is similar to molecule

molecule A from the previous report, only 3º different, while this torsion angle of molecule B is 101.6º which is different from previous report. The similar values and same direction of torsion angle, C6–O2–C7–C8 in molecule B from this work to molecule C from previous report and molecule A in this work present similar value to molecule A from previous report, but in the opposite direction. The O2–C7–C8–O3 of molecules A and B are quite similar to molecule B of previous work (Birnbaum, Cygler, and Shugar, 1984). Moreover, the side chain at O2–C7–C8–O3 presents eclipsed conformations in both molecules A and B in which the dihedral angle is between 69.3º and 72.4º. The C7–C8–O3–H is −175.9º for molecule A, and this torsion angle value is close to those of molecules B and C, while it is only 3.4º different and in the opposite sense compared to molecule B from previous work. The torsion angle of molecule B in this work is different from molecule A in the previous report by about 14.5º. The selected torsion angles at the guanine ring and side chain of the acyclovir compound are given in Table 3.6 and the two eclipsed conformations of molecules A and B at the O2–C7–C8–O3 bond in the side chain are shown in Figure 3.2.

Table 3.6 Selected interatomic torsion angles (°)[a] of the side chain for acyclovir; $C_8H_{11}N_5O_3 \cdot 2H_2O$.

Torsion angle (°)	ACV [Birnbaum et al, 1984]			ACV [This work]	
	Mole A	Mole B	Mole C	Mole A	Mole B
C2–N5–C6–O2	-76.5	-74.4	-90.5	-77.6 (0.13)	90.9 (0.12)
C5–N5–C6–O2	97.3	104.3	91.4	93.3 (0.13)	-90.2 (0.14)
N5–C6–O2–C7	-76.9	-66.3	-173.3	-73.1 (0.12)	101.6 (0.12)
C6–O2–C7–C8	173.2	-176.2	-171.9	177.1 (0.11)	-171.8 (0.11)
O2–C7–C8–O3	60.6	73.5	-174.4	69.2 (0.16)	72.4 (0.16)
C7–C8–O3–H3	-82.6	172.5	-172.6	-175.9	-68.1

[a] The standard deviations of the least significant digits are given in parentheses.

Mol A
(+)-sc

Mol B
(+)-sc
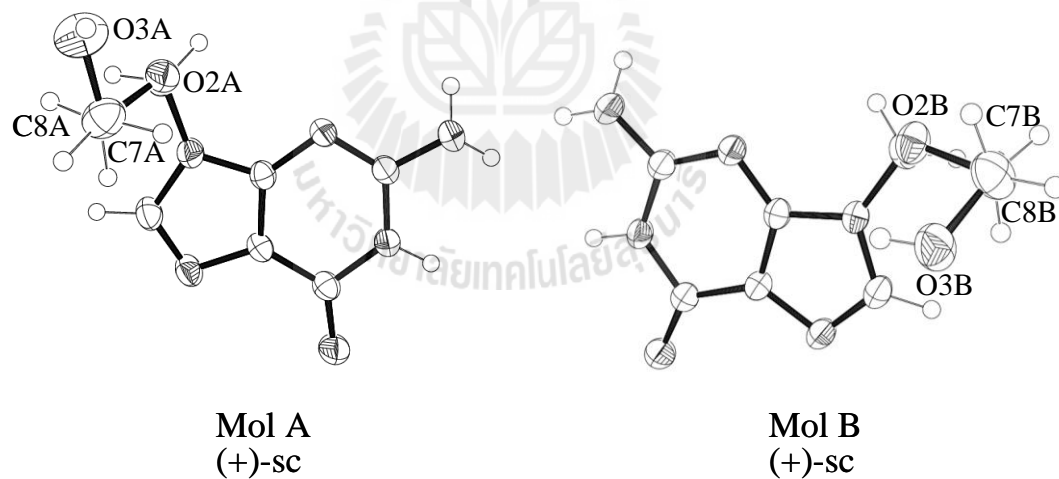
Figure 3.2 The two eclipsed conformations of molecules A and B at the O2–C7–C8–O3 bond in side chain (sc) of acyclovir structures.

The 12 atoms involved in the formation of the two guanine rings are planar. The r.m.s. deviations of the fit are 0.0167 Å for molecule A and 0.0194 Å for molecule B. Additionally, the ring systems of molecule A and molecule B are nearly parallel with a dihedral angle of 2.17(2) Å. The substituted atoms directly below the guanine plane are displaced from the mean plane of molecule A by −0.1896(16) Å for C6A, −0.0292(15) Å for; N2A, and −0.0484(14) Å for O1A, and from below the mean plane of molecule B by −0.0104(15) Å for N2B and above the mean plane by 0.0831(15) Å for C6B and 0.0495(14) Å for O1B (Table A2).

Supramolecular Structure of $C_8H_{11}N_5O_3 \cdot 2H_2O$

The supramolecular structure of $C_8H_{11}N_5O_3 \cdot 2H_2O$ consists of the guanine bases of the two crystallographically unique molecules joined together into infinite chains of alternating A and B molecules. Hydrogen bond interactions between adjacent molecules form concerted $R_2^2(7)$ and $R_2^2(9)$ motifs that translate perpendicular to the a axis direction with d[H5a···O1B] = 2.96 Å, d[H1a···N4B] = 2.00 Å, d[H2c···O1A] = 2.05 Å, d[H5b···O1A] = 2.98 Å, d[H1b···N4A] = 1.98Å, and d[H2b···O1B] = 1.99 Å, in a pattern similar to that in the previous report (Birnbaum, Cygler, and Shugar, 1984). The difference of this structure to the previous report is the conformation of their chains, which in this work created a 1−D wave-like chain related inversion center, while in the previous report all guanine bases joined together into infinite ribbons; one formed by 2_1 screw axis relates A molecules and the other by alternating B and C molecules. The hydrogen packing of acyclovir of this work and previous report as illustrated in Figure 3.3.

(a)

(b)
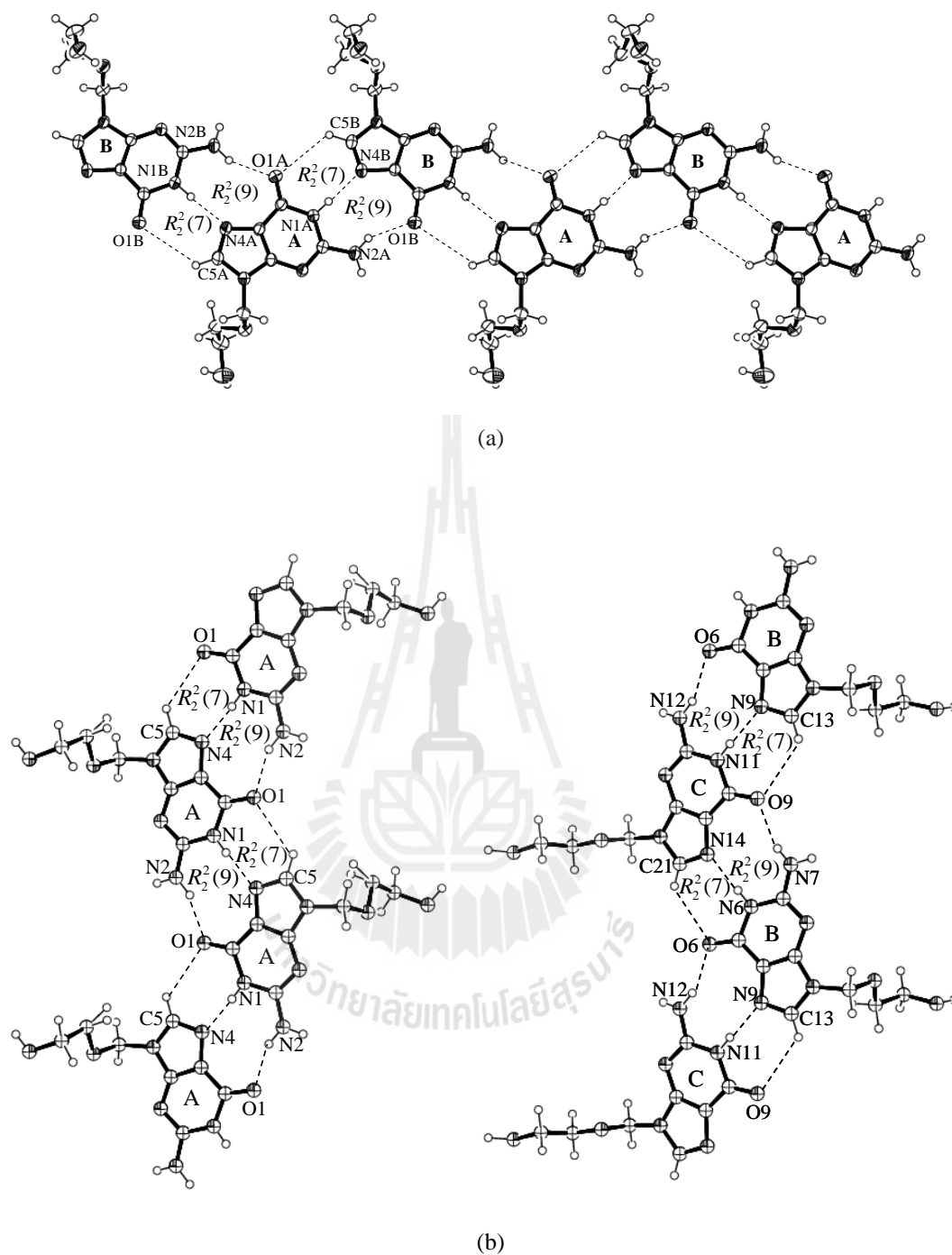
Figure 3.3 Packing of acyclovir as result of a 1–D wave-like infinite chain (a) this work along *a* axis (b) the infinite ribbon formed by 2_1 screw axis relates A molecules in left and the others by alternating B and C molecules in right, view along the *c* axis (Birnbaum, Cygler, and Shugar, 1984).

The side chain of each wave-like infinite chain of one of the independent acyclovir molecules involves hydrogen bonds to other independent acyclovir molecules to create 2–D sheet networks via bifurcated hydrogen bonds at d[H8c⋯O2A] = 2.067 Å and d[H8c⋯O3A] = 3.019 Å perpendicular to the *a* axis direction (Figure 3.4). The adjacent 2–D sheet networks connect together to create 3–D networks parallel through guanine stacking with the average distance of 3.295(13) Å for A/B and 3.392(18) Å for B/A interactions (Figure 3.5(a)).

The water molecules form infinite serpentine chains through the crystal, and participate in alternating pentagonal rings, each made up of four water molecules and one carbonyl oxygen atom (O1B) or one hydroxyl group (O3A) of the side chain. Presumably the water interactions further stabilize the crystal structure packing shown in Figure 3.5(b) and 3.5(c). Comparison of Figures 3.5(a) and 3.5(b) reveals the water channels occupied by the serpentine chains described on pages 87. The hydrogen bond interactions are given in Table 3.7.
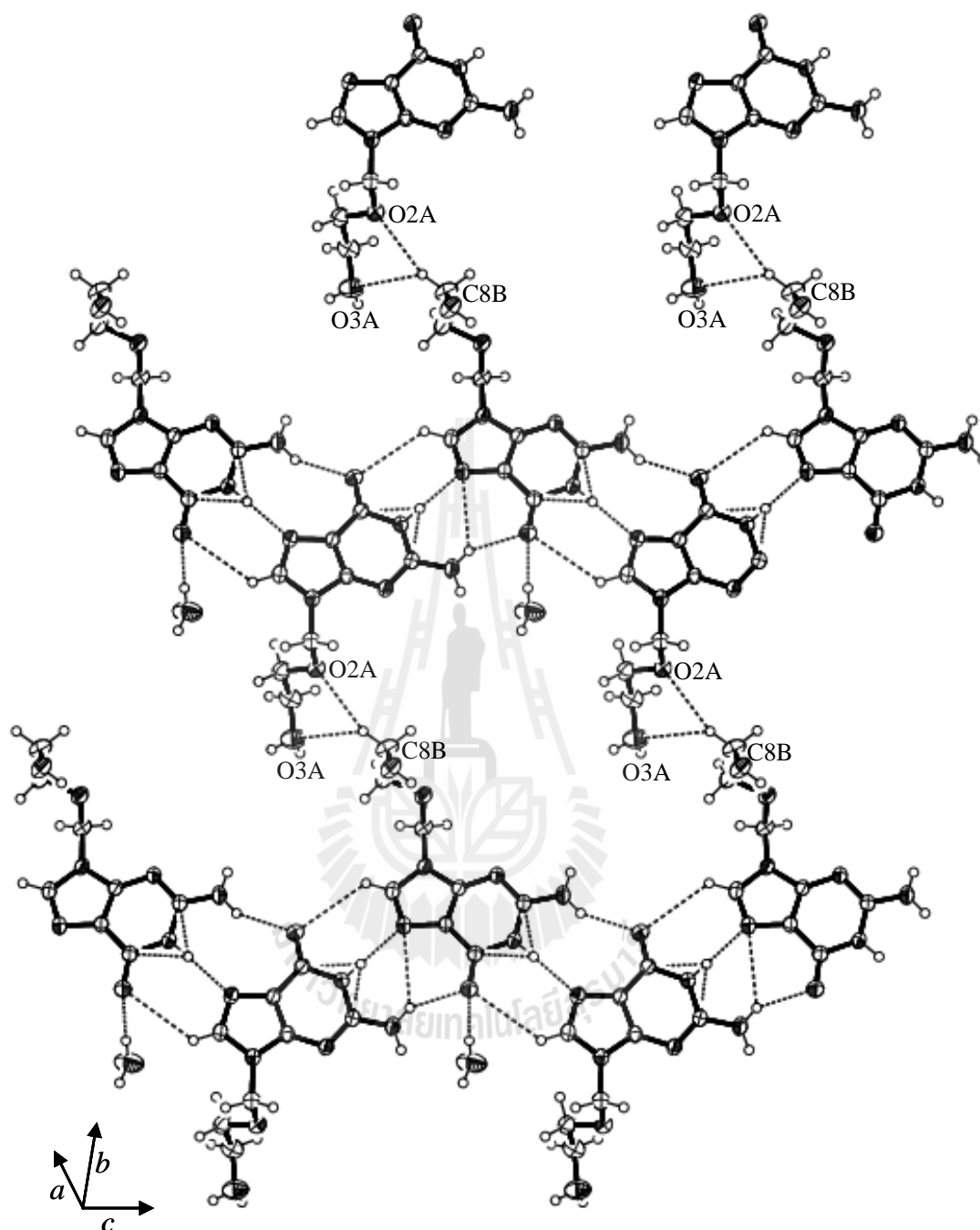
Figure 3.4 View of the 2–D hydrogen bonded network showing the 1–D wave-like infinite chains connect to adjacent chain by side chain connections. This is view along the *a* axis.
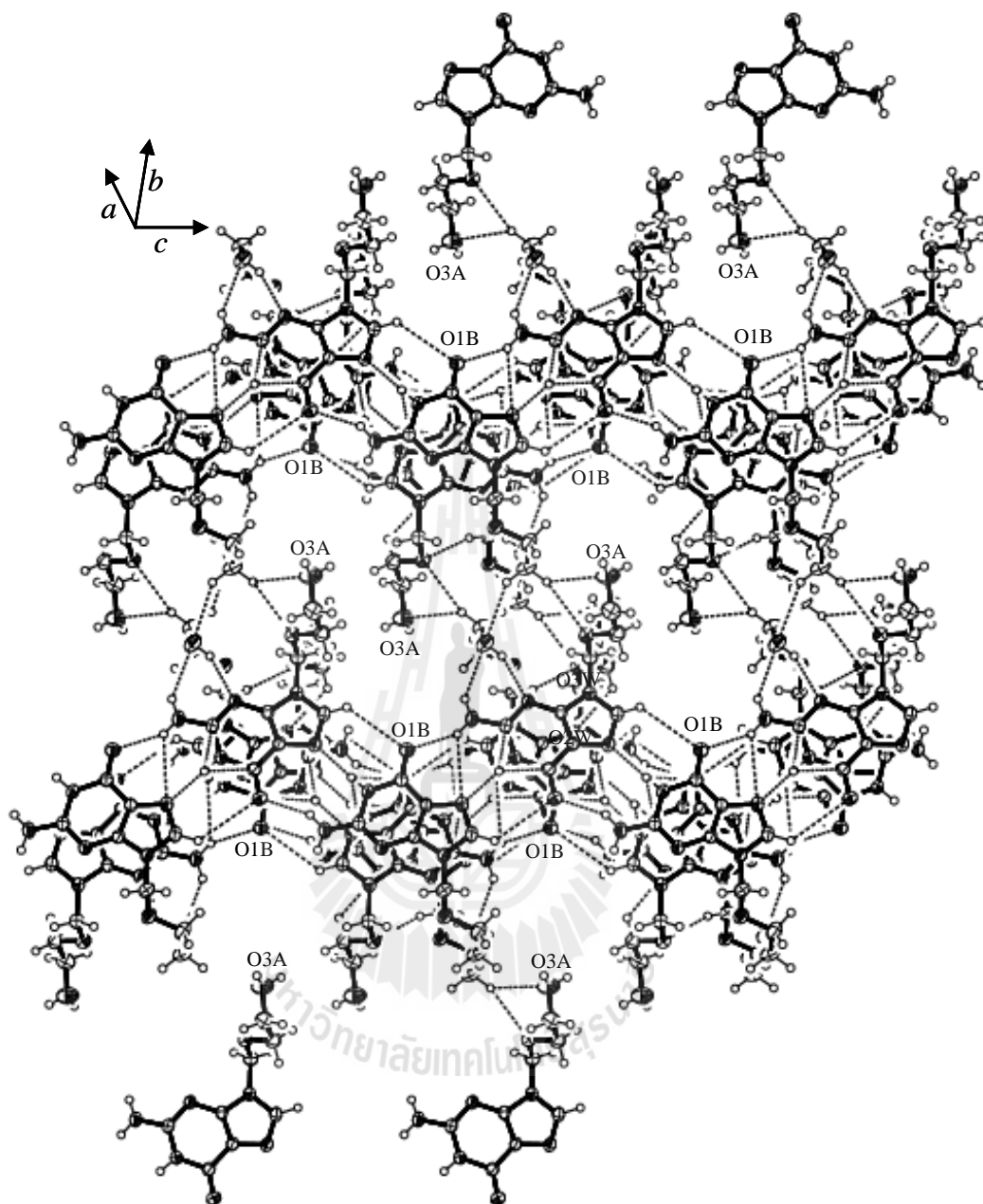
(a)

Figure 3.5 View of 3–D hydrogen bonded network of acyclovir. The view is perpendicular to (a) the *a* axis without water molecules, (b) the *a* axis, and (c) the *b* axis.
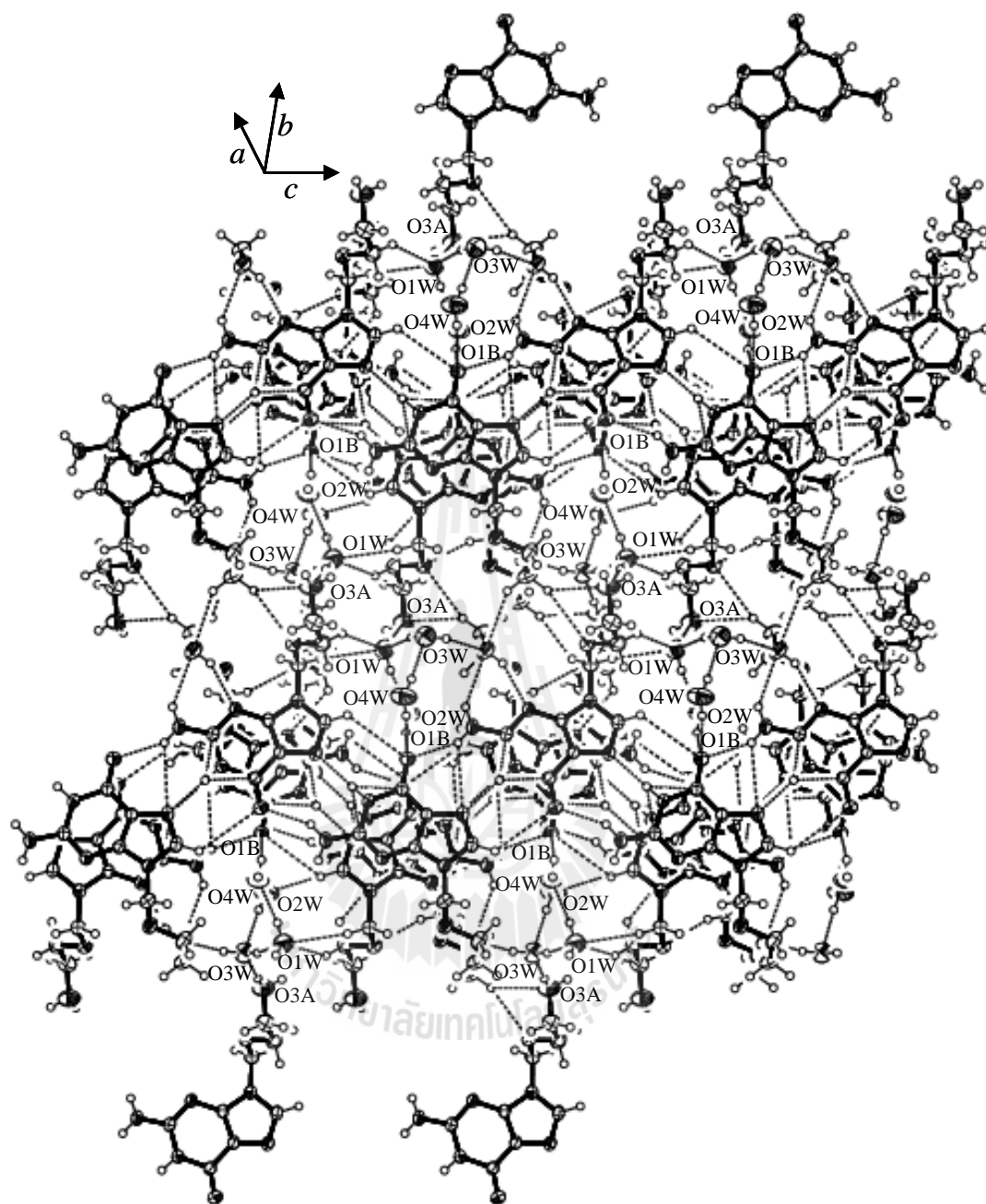
(b)

Figure 3.5 (Continued).
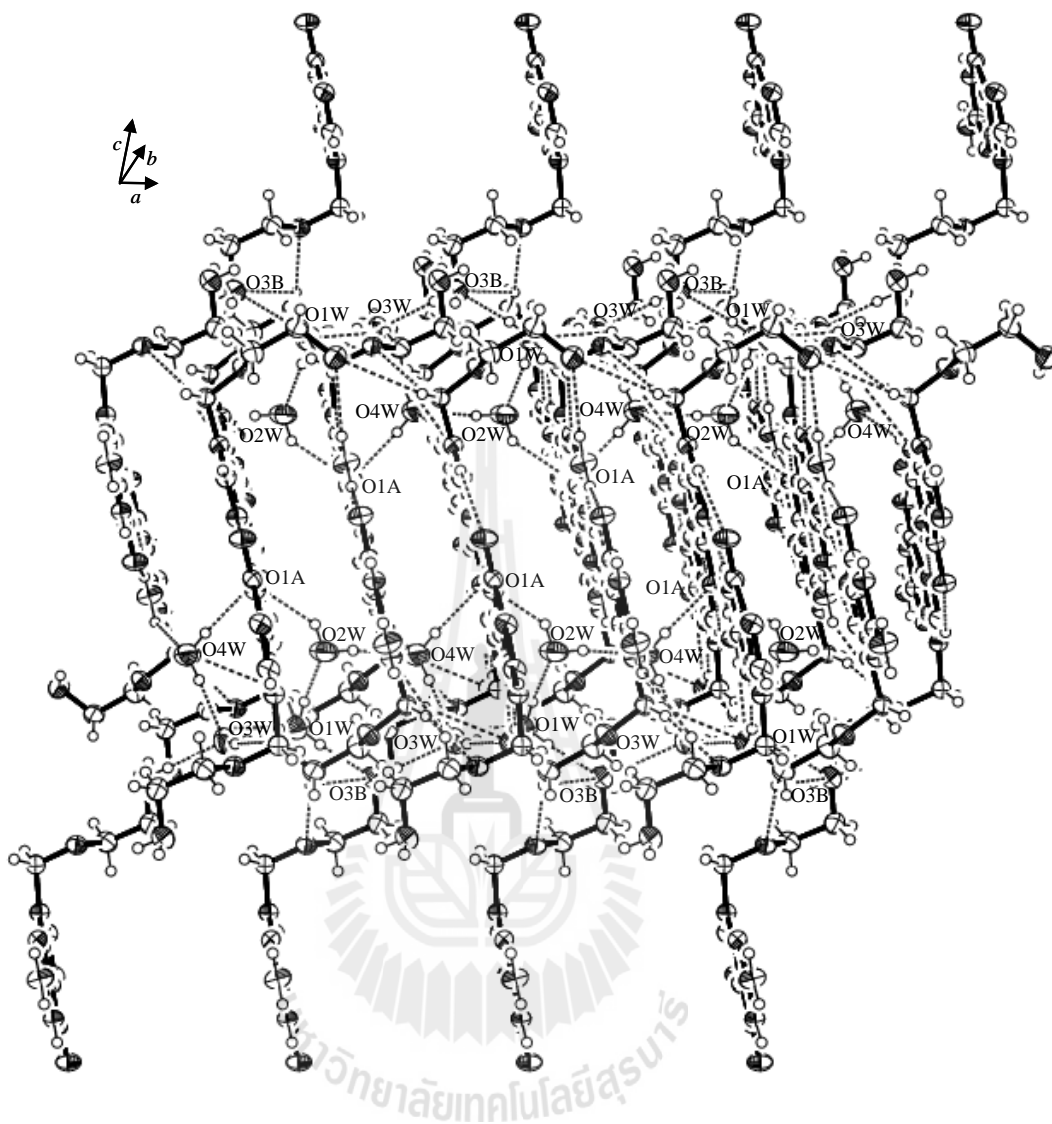
(c)

Figure 3.5 (Continued).

Table 3.7 Hydrogen bond interactions for acyclovir; $C_8H_{11}N_5O_3 \cdot 2H_2O$.

D–H···A	d[D–H] (Å)	d[H···A] (Å)	d[D···A] (Å)	∠[D–H···A] (º)
Guanine base				
N1A–H1a···N4B[i]	0.86	2.01	2.871	177.0
N1B–H1b···N4A[ii]	0.86	2.01	2.872	175.6
N2A–H2b···O1B[iv]	0.86	2.08	2.865	150.8
N2B–H2d···O1A[v]	0.86	2.07	2.861	151.7
C5A–H5a···O1B[xii]	0.93	2.96	3.572	124.3
C5B–H5b···O1A[xiii]	0.93	2.98	3.593	124.5
N2A–H2a···O3B[iii]	0.86	2.37	3.092	141.6
N2B–H2c···O4W	0.86	2.41	3.028	129.4
Side chain (mol A)				
C6A–H6b···O1W	1.00	2.53	3.496	162.81
C6B–H6d···O2A	1.01	2.58	3.533	158.33
C8B[vi]–H8c[vi]···O2A	0.96	2.61	3.515	158.31
C7A–H7a···N3B	0.98	2.94	3.635	128.47
C7A–H7b···O1W	0.98	2.85	3.654	140.47
C8B[vii]–H8c[vii]···O3A	0.96	3.02	3.638	123.58

Symmetry transformations used to generate equivalent atoms:

(i) =-x, -y+2, -z+1; (ii) = -x, -y+1, -z+1; (iii) = x+1, y, z; (iv) = -x, -y+2, -z+1; (v) = -x, -y+1, -z+1; (vi) = -x, -y-1, -z; (vii) = x+1, y-1, z; (viii) = -x, -y+1, -z; (ix) = x, y-1, z; (x) = x-1, y, z; (xi) = -x+1, -y+1, -z; (xii) = -x+1, y, z. (xiii) = x, y+2, z+1.

Table 3.7 (Continued).

D–H⋯A	d[D–H] (Å)	d[H⋯A] (Å)	d[D⋯A] (Å)	∠[D–H⋯A] (º)
Side chain (mol B)				
O1W[vi]–H1w[vi]⋯O3A	0.88	1.92	2.789	173.2
O3A–H3a⋯O3W[viii]	0.82	1.99	2.807	177.7
C6B–H6c⋯O3B[vii]	0.99	2.81	3.593	136.6
C6B–H6d⋯O1A	1.01	2.58	3.533	158.3
C8B–H8c⋯O2A[vii]	0.96	2.61	3.515	158.3
C8B–H8c⋯O3A[vii]	0.96	3.02	3.637	123.5
C6B[vi]–H6c[vi]⋯O3B	0.99	2.81	3.593	136.6
C8B[vii]–H8d[vii]⋯O3B	0.98	2.70	3.448	134.0
O3W[ix]–H3wa[ix]⋯O3B	0.87	2.00	2.832	161.4
O3B–H3c⋯N3A[x]	0.82	2.11	2.860	152.2
Water interactions				
O1W–H1Wa⋯O2W	0.86	1.87	2.720	169.8
O1W–H1Wb⋯O3A[xi]	0.87	1.92	2.788	174.1
O1W–H1Wb⋯O3A[xi]	0.87	1.92	2.788	174.1

Symmetry transformations used to generate equivalent atoms:

(i) =-x, -y+2, -z+1; (ii) = -x, -y+1, -z+1; (iii) = x+1, y, z; (iv) = -x, -y+2, -z+1; (v) = -x, -y+1, -z+1; (vi) = -x, -y-1, -z; (vii) = x+1, y-1, z; (viii) = -x, -y+1, -z; (ix) = x, y-1, z; (x) = x-1, y, z; (xi) = -x+1, -y+1, -z.

Table 3.7 (Continued).

D–H···A	d[D–H] (Å)	d[H···A] (Å)	d[D···A] (Å)	∠[D–H···A] (º)
Water interactions				
O2W–H2Wa···O4W[iii]	0.87	1.96	2.818	170.0
O2W–H2Wb···O1B[v]	0.86	2.23	2.948	141.1
O2W–H2Wb···O1A[xii]	0.86	2.41	2.967	122.7
O3W–H3Wa···O3B[vii]	0.86	2.00	2.831	162.8
O3W–H3Wb···O1W	0.87	1.87	2.729	167.7
O4W–H4Wa···O3W	0.86	2.00	2.855	174.6
O4W–H4Wb···O1B[ii]	0.87	2.08	2.944	173.3

Symmetry transformations used to generate equivalent atoms:

(i) =-x, -y+2, -z+1; (ii) = -x, -y+1, -z+1; (iii) = x+1, y, z; (iv) = -x, -y+2, -z+1; (v) = -x, -y+1, -z+1; (vi) = -x, -y-1, -z; (vii) = x+1, y-1, z; (viii) = -x, -y+1, -z; (ix) = x, y-1, z; (x) = x-1, y, z; (xi) = -x+1, -y+1, -z.

π−π Stacking Interactions

Adjacent chains are connected together across inversion centers perpendicular to the *b* axis direction to form a 3−D network dominated by guanine ring motifs (one offset *ff* interaction), π···π, C–H···π, N–H···π, and carbonyl–carbonyl dipole–dipole interactions to stabilize the acyclovir structure. This arrangement is maintained despite the fact that the orientation of molecule A is different from that of molecule B. There is considerable overlapping of guanine rings between the A/B and B/A pairs. The π···π stacking separation between the successive guanine rings are 3.295 Å for A/B

(πR1$\cdots$$\pi$R4) and 3.392 Å for B/A (πR2$\cdots$$\pi$R3) [molecule A; R1 is N1/C1/N3/C2/C3/C4/N2, R2 is C2/C3/N4/C5/N5 and molecule B; R3 is N1/C1/N3/C2/C3/C4/N2, R4 is C2/C3/N4/C5/N5], which are shorter that normal interaction contacts see in Figure 3.6. These distances are essentially the same as those found between adjacent base pairs in DNA (Birnbaum, Johansson, and Shugar, 1987) and indeed between adjacent π-clouds in general (Haller, Johnson, Feltham, Enermark, Ferraro, and Basile, 1979). There are several C–H$\cdots$$\pi$ and N–H$\cdots$$\pi$ interactions in this structure; C–H$\cdots$$\pi$ interactions C5A–H5a$\cdots$$\pi$R3 (3.289 Å), C5B–H5b$\cdots$$\pi$R1 (3.246 Å), and four N–H$\cdots$$\pi$ interactions; N1A–H1a$\cdots$$\pi$R4 (3.441 Å, 73.0º), N2A–H2b$\cdots$$\pi$R4 (3.141 Å), N1B–H1b$\cdots$$\pi$R2 (3.420 Å), N2B–H2c$\cdots$$\pi$R2 (3.372 Å). Ring–ring interaction are shown in Figure 3.6 and Table 3.8.
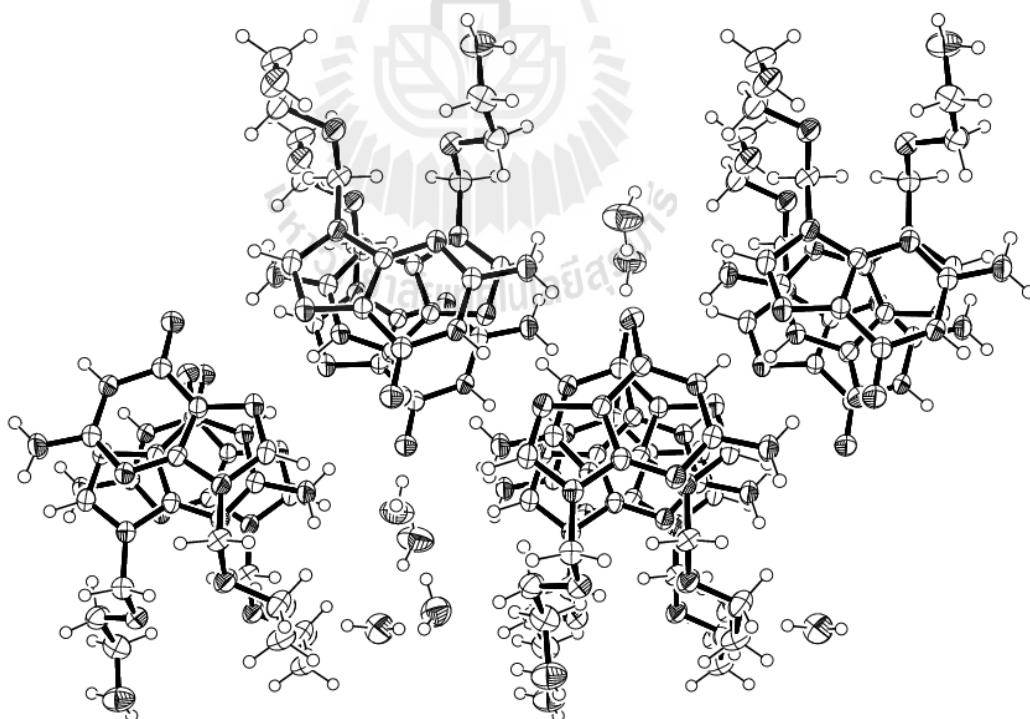
Figure 3.6 Ring–ring interactions forming stacks of molecules in the acyclovir structure.

Table 3.8 Carbonyl−carbonyl, C–H⋯π, N–H⋯π interactions, and π⋯π contacts for acyclovir; $C_8H_{11}N_5O_3 \cdot 2H_2O$.

D–H⋯A	d[D⋯A] (Å)
Carbonyl−carbonyl interactions	
C4A⋯O1B	3.341
C4B[i]⋯O1A	3.590
C–H⋯π hydrogen bonds	
C5A–H5a⋯πR3	3.289(17)
C5B–H5b⋯πR1	3.246(15)
N–H⋯π hydrogen bonds	
N1A–H1b⋯πR4	3.441(20)
N1B–H1b⋯πR2	3.420(18)
π⋯π contacts	
πR1⋯πR4	3.295(13)
πR2⋯πR3	3.392(18)

Notation: guanine ring

Mol A; R1=N1/C1/N3/C2/C3/C4/N2, R2= C2/C3/N4/C5/N5, mol B; R3=N1/C1/N3/C2/C3/C4/N2, R4= C2/C3/N4/C5/N5.

Symmetry codes: (i) = 1+x,-y,-z.

The analysis of the crystallographic data for carbonyl−carbonyl interactions $(C(\delta^+)\cdots O(\delta^-))$ found the slipped parallel motif type (Figure 3.7) involving a pair of C⋯O interactions, with d[C⋯O] of 3.590 Å for A/B with angles A1 = 71.8º and A2 = 72.3º, and the torsion angle of −159.1º, and 3.342 Å for B/A with angles A1 = 94.5º

and A2 = 91.5º, and the torsion angle of −160.3º (I= C4=O1···C4′=O′, A1= C4−O1−C4′, A2 = O1−C4′−O1′). The C···O distances in this structure are shorter than the sum of van der Waals radii in both of B/A and A/B in which the C···O distance less than 3.6 Å (Allen, 1998). The carbonyl oxygen atom on molecule A is well positioned to form the parallel carbonyl−carbonyl motif, while the carbonyl group on molecule B acts as a bifurcated acceptor from two water molecules in one $R_5^5(10)$ motif, making O3B less available to participate in a carbonyl−carbonyl interaction with molecule A. The different patterns for these two carbonyl−carbonyl interactions is easily seen in Figure 3.7.
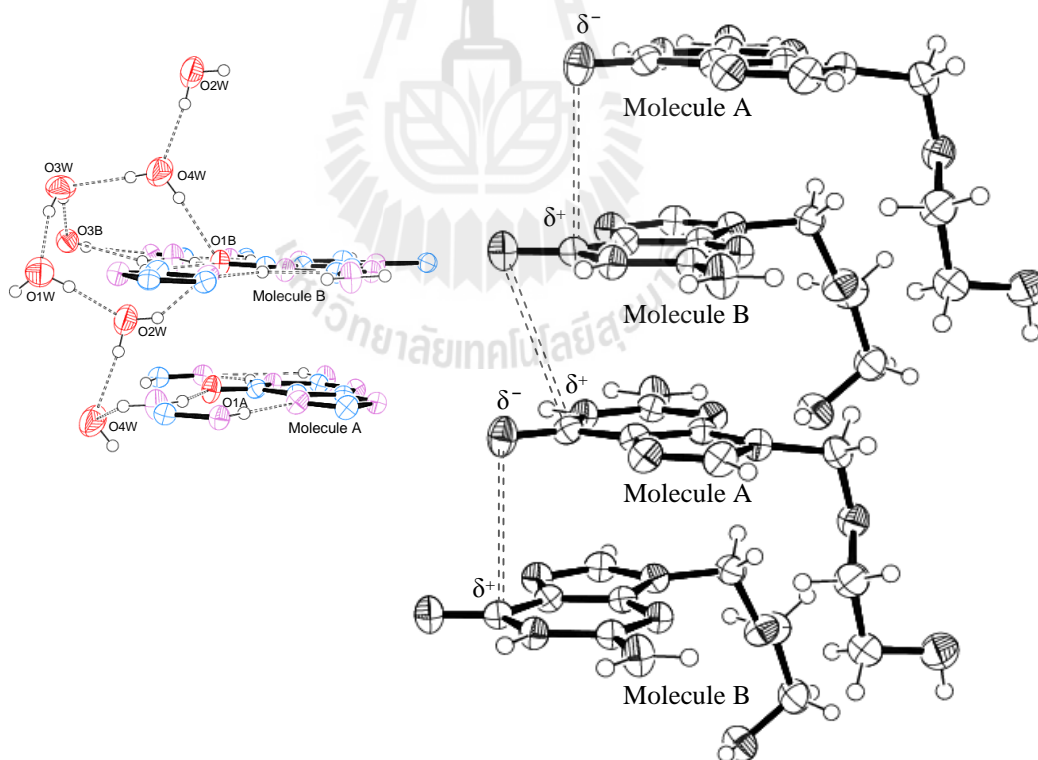
Figure 3.7 Carbonyl−carbonyl dipole interaction in acyclovir structure. View normal to [100].

Water Regions

The water structure in the acyclovir has a ribbon of water-drug interactions including an infinite serpentine chain of water molecules, $\cdot[\cdot O2-H\cdots O1-H\cdots O3-H\cdots O4-H\cdot]_\infty$ that propagates as two alternating $R_5^5(10)$ motifs completed by inclusion of drug functional groups, one by one oxygen atom of a carbonyl group, and other by one hydroxyl group, to make stable pentagonal forms with an average angle nearly the ideal pentagonal value of 108° linking the entire structure into an extensive supramolecular network as shown in Figure 3.8 and Table 3.8.
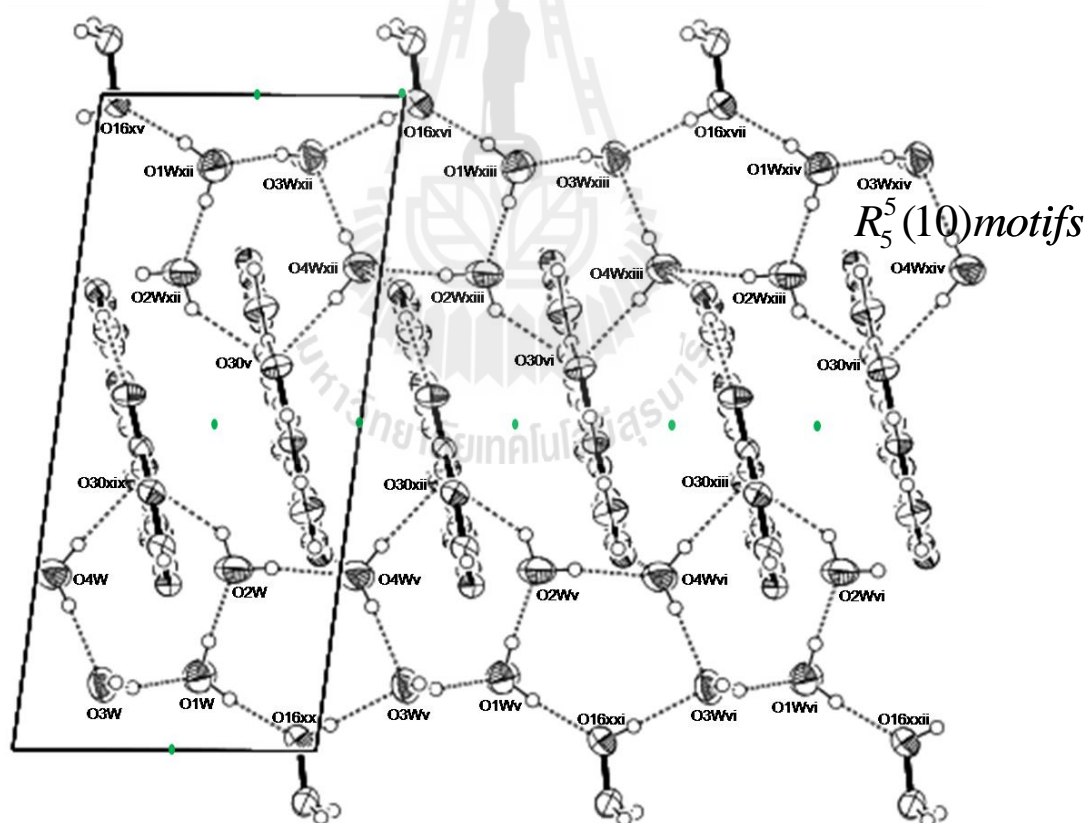
Figure 3.8 Structure of the water molecules in infinite chain of the acyclovir structure with hydrogen bond interactions via $R_5^5(10)$ motifs, view along *b* axis.

Difference Surface Waters

The ordered water in acyclovir dihydrate assembles into pentagonal motifs which have average angles near the ideal pentagonal value of 108º. The electron density maps (F_o-F_c) at 1.5 Å resolution, present the bound water molecules at that point in the acyclovir structure has a local minimum; *i.e.* the free energy of a water at nearby neighboring regions is relatively high, forming an energy, high electron density would be found since, on average, waters would be located relatively uniformly in that region (Levitt and Park, 1993). The (F_o-F_c) maps of water systems without hydrogen atoms show in Figure 3.9.
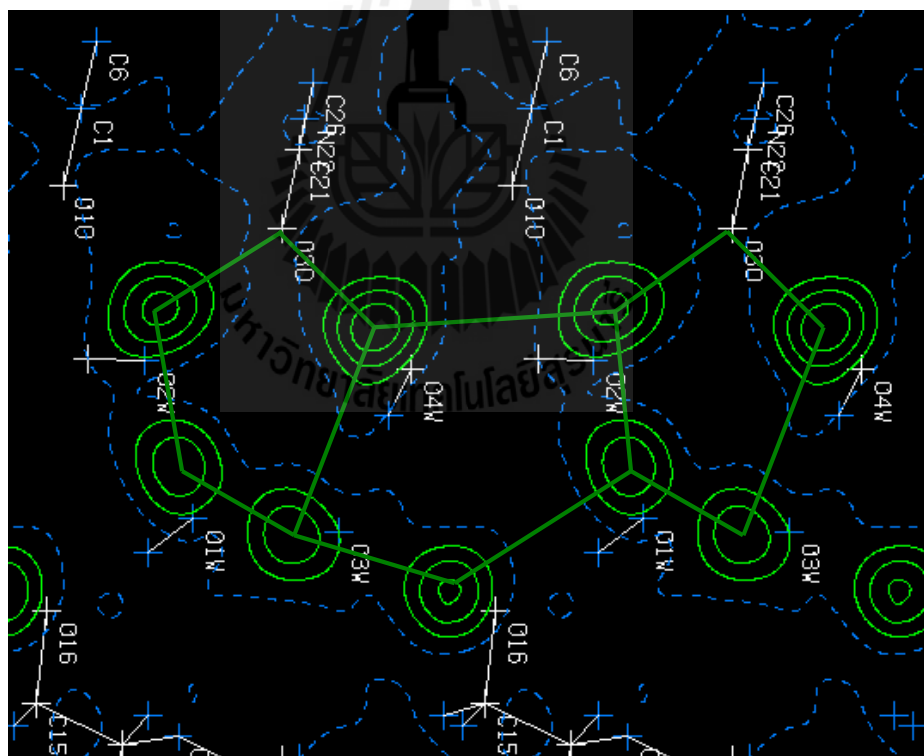
Figure 3.9 The $(F_o\text{-}F_c)$ maps of water systems without hydrogen atoms at 1.5 Å, 2.5 σ, used *ins* file, view is perpendicular to water region axis. The $(F_o\text{-}F_c)$ map was generated with *PLATON*.

Infrared Spectra

The FTIR spectrum of acyclovir dihydrate is similar to previous spectra reported in the literature and databases (Barboza, Vecchia, Tagliari, Silva, and Stulzer, 2009; SDBS). The bands at 3376 and >3376 cm^{-1} correspond to υ(O–H) stretching vibrations of two water molecules which can be related to the TGA result indicating that two pairs of water molecules are lost at significantly different temperatures. The region of 3312 and 3124 cm^{-1} corresponds to υ(N–H) stretching bands of the primary amine and secondary amide from asymmetric stretching, and weaker bands about at 3100 and 2954 cm^{-1}, and a medium band at 2793 cm^{-1} correspond to υ(C–H) asymmetric stretching. The very strong peaks at 1693 and 1664 cm^{-1} were assigned to the υ_{as}(C=O) stretching vibration (carbonyl absorption in amide). There is a band at 1613 cm^{-1} due to δ(H–O–H) bending vibration and a band at 1585 cm^{-1} due to δ(H–N–H) bending vibration in aromatic primary amine.
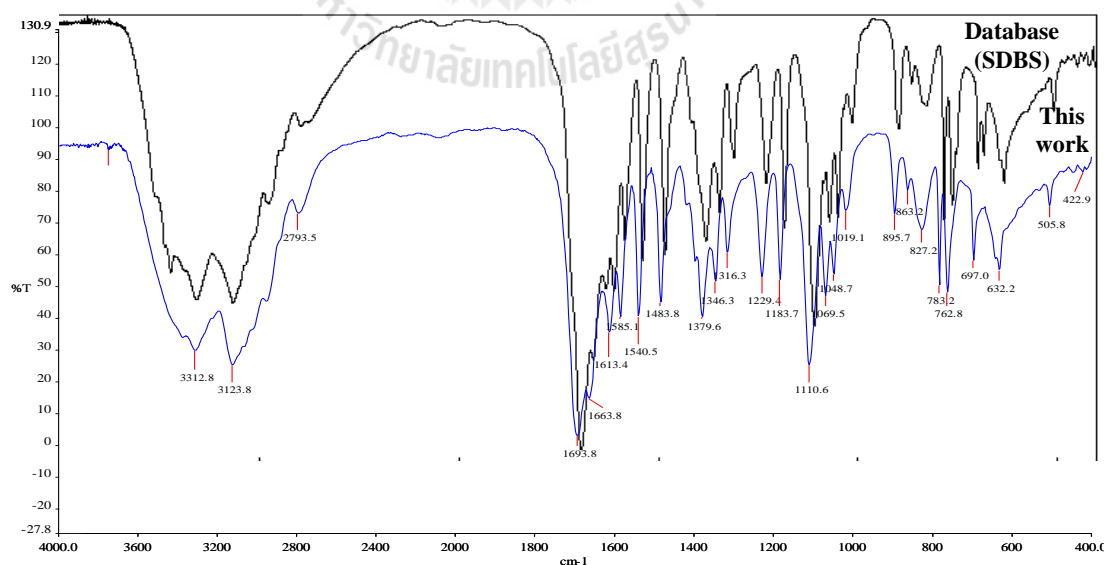
Figure 3.10 Infrared spectra of acyclovir separated from drug (Pressed KBr pellets).

The bands at 1540, 1483 and 1379 cm^{-1} were assigned to υ(C–H) assymetric streaching. The υ(C–N) stretching absorption at 1346 and 1316 cm^{-1} can be assigned to the aromatic amines. The strong peak at 1111 cm^{-1} and peaks at 1070, 1049, and 1019 cm^{-1} were assigned to υ(C–O) stretching vibrations as presented in the Table 3.10 and infrared spectra of acyclovir is shown in Figure 3.10.

Table 3.9 IR Spectral data for acyclovir; $C_8H_{11}N_5O_3 \cdot 2H_2O$ extracted from drug.

[a]Assignment	Acyclovir (separated from drug)	[a]Assignment	Acyclovir (separated from drug)
υ_{as}(O−H)	>3376 sh	δ_{as}(C−H)	1540 m
υ_{as}(O−H)	3376 w		1483 m
υ_{as}(N−H) 1° amine	3312 m		1379 m
υ_{s}(N−H) 2° amide	3124 m	υ_{as}(C−N)	1346 m
υ_{s}(C−H)	3100 w		1316 m
	2954 w		1229
	2793 m		1184
υ_{as}(C=O)	1693 vs	υ_{as}(C−O) s	1111
	1664 s		1070
δ(H−O−H) + δ(H−N−H)	1613 m		1049
	1585 m		1019 w

a Relative intensities and shape of peak are indicated by vs = very strong, s = strong,

m = medium, w = weak, sh = shoulder, respectively.

Thermal Analysis

Thermal study was performed using TGA. The TGA curve (Figure 3.11) shows the expected 2:4 acyclovir:hydrate when the first two overlapping waves are considered together. The weight loss starts at 63−155°C with two approximately equal overlapping steps comprising 7.28% (calc. 6.90% for loss of $4H_2O$) due to loss of two different types of solvate water. The third wave shows weight loss of 28.22% (calc. 28.74% corresponding to loss of two methoxy-methanol side chains) at temperatures between 252−277°C. The previously reported melting point is 256°C (USP 27-NF 22, 2006) which is apparently a melting/decomposition temperature. The fourth wave at temperatures between 447.8−486.7°C corresponds to a weight loss of 21.68%. Removal of two $NHCH_2N=CH_2$ would require 24.14% weight loss. The residual 42.82% could correspond to 2-amino-3*H*-pyrimidin-4-one (calc 42.53% for $C_4N_3OH_5$). The rate of heating was rather rapid. Slower heating should enable better separation of the two solvent water loss waves. Still, it is clear that the stoichiometry found in the single crystal structural characterization matches the TGA curve, *i.e.* there are four solvent water molecules per two acyclovir molecules. Furthermore, the four water solvent molecules occur as two distinct types of water. The water molecules binding to the carbonyl group of molecule B appear more tightly bound to the acyclovir framework and are likely lost at the higher temperature.

The TGA curve is still trending downward at 500°C, the temperature at which the experiment was terminated. Heating should be carried to a higher temperature to more completely characterize the material. Thermogravimetric analysis showed that acyclovir compound be changed to the hydrate by exposure to atmospheric water vapor, and in the first stage from TGA curve shows a weight loss of 2.41%, which is

similar to Form IV for dihydrate acyclovir (Lutker, Quinones, Xu, Ramamoorthy, and Matzger, 2011) which reports two water molecules in asymmetric unit from single crystal X- ray but reports only one water molecule from TGA. The TGA result is presented in Table 3.11.
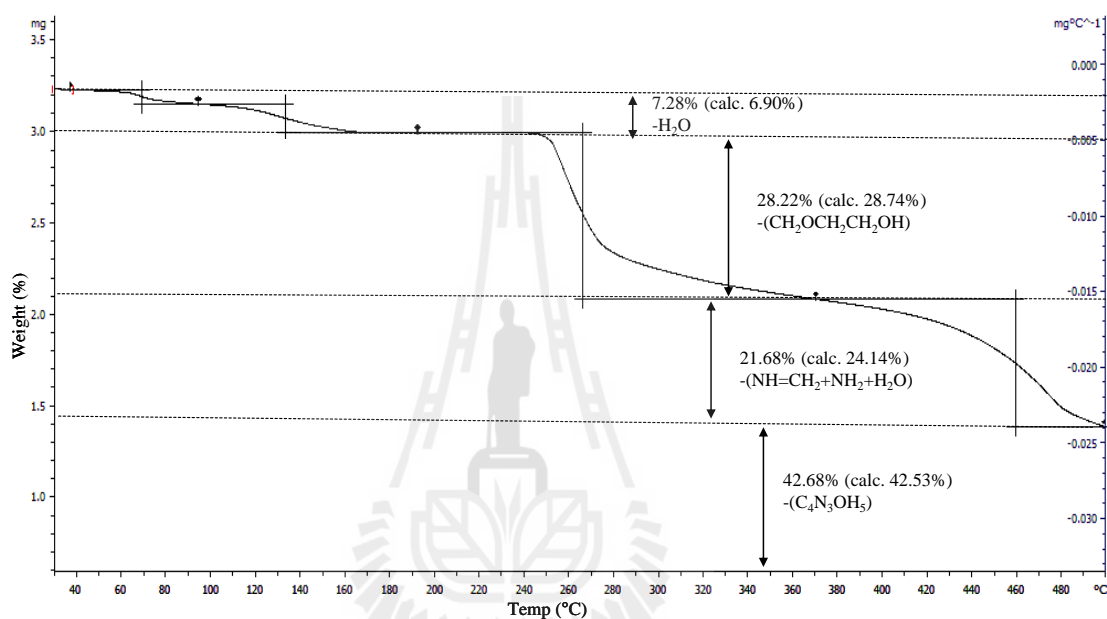
Figure 3.11 TGA curve of acyclovir dihydrate.

Table 3.10 Thermal analysis data for acyclovir dihydrate.

Compound	Items	% Weight loss = (fragment/ 261) x 100			Temperature (°C)	Composition (Mw)
		Calc.	Measure	Error		
$C_8H_{11}N_5O_3 \cdot 2H_2O$	Decomposition	-		-	63.8-74.6,	
		6.90	7.28	0.38	117.8-155.2	H_2O
			(2.41+4.87)			
		28.74	28.22	1.53	252.3-277.7	
						$CH_2OCH_2CH_2OH$
		24.14	21.68	2.46	447.8-486.7	(2-methoxy-ethanol)
	Residual					
		42.53	42.68	0.15	>486.7	
						$NH=CH_2+NH_2+H_2O$
						(Methyleneamine)
						$C_4N_3OH_5$
						(6-Amino-5,6-
						dihydro-3H-
						pyrimidin-4-one)

* Step 1 and step 2 are one water decomposition

3.4 Conclusions

Acyclovir was separated from acyclovir drug then crystallized from water solution as thin plates of the dihydrate, $C_8H_{11}N_5O_3 \cdot 2H_2O$, as shown by single crystal structural analysis (triclinic space group $P\bar{1}$, with cell dimensions of a = 6.8996(6) Å, b = 11.4170(9) Å, c = 15.0806(13) Å, α = 82.595(7)º, β = 82.395(7)º, γ = 89.368(7)º at 293(2) K). The crystal lattice contains two crystallographically independent acyclovir molecules and four independent water molecules in the asymmetric unit. TGA results confirm the crystal structure stoichiometry for the bulk sample, and further indicate that there are two types of solvent water molecules (two of each type) with dissociation waves at about 60°C and 100°C.

The bond lengths and bond angles agree well with previous reports for acyclovir, except for the bond angle of C5−N5−C6 of molecule A, which was slightly larger (0−3.1°) than C2−N5−C6 in molecule B. The two side chain conformations are quite similar with the exception of the relative position of atom H3c for molecule B. The side chains at O2−C7−C8−O3 present eclipsed conformations in both molecules A and B. The ring systems of molecules A and B are closely parallel with dihedral angle about 1.600(1) Å. The glycosidic side chain was partially folded in molecules A and B and almost perpendicular to the guanine ring.

The supramolecular interaction of the acyclovir structure contains extensive strong hydrogen bond interactions among the acyclovir and water molecules extending in all directions from the acyclovir molecules. The guanine ring systems connect together with C−H⋯O, N−H⋯N, and N−H⋯O hydrogen bonds to create 1−D chains. The side chains connect to adjacent chains by weak C−H⋯O hydrogen bonds to contribute to a 2−D sheet, while the adjacent 2−D sheets are parallel and connected together across inversion centers perpendicular to the b axial direction to form a 3−D network via hydrogen bonds of the water region. It is stabilized by guanine moieties that stack with concerted C−H⋯π, N−H⋯π, and carbonyl-carbonyl dipole-dipole interactions in a slipped parallel motif type. The glycosidic side chain was partially folded and almost perpendicular to the guanine ring and present in an eclipsed conformation at O2−C7−C8−O3 in both independent molecules.

The supramolecular pattern of the water region in acyclovir has a ribbon of water-drug interactions including an infinite serpentine chain of water molecules, $\cdot[\cdot O2−H\cdots O1−H\cdots O3−H\cdots O4−H\cdot]_\infty$, that propagates as two alternating $R_5^5(10)$

motifs completed by inclusion of drug functional groups, one by an oxygen atom of a carbonyl group, and an other by a hydroxyl group, to make stable pentagonal forms with an average angle nearly the ideal pentagonal value of 108°. The water regions integrate with the drug molecules to form an extensive strongly hydrogen bonded 3-D supramolecular network that may play an important role in their properties. The F_o maps at 1.5 Å resolution with water hydrogen atoms removed shows rational positions for ordered water molecules in the acyclovir structure.

3.5 References

Balzarini, J. and McGuigan, C. (2002). Bicyclic pyrimidine nucleoside analogues (BCNAs) as highly selective and potent inhibitors of varicella-zoster virus replication. **Journal of Antimicrobial Chemotherapy**. 50: 5–9.

Birnbaum, G. I., Cygler, M., and Shugar, D. (1984). Conformational features of acyclonucleosides: Structure of acyclovir. **Canadian Journal of Chemistry**. 62: 2646–2651.

Boryski, J., Golankiewicz, B., and de Clerk, E. (1988). Synthesis and antiviral activity of novel N-substituted derivatives of acyclovir. **Journal of Medicinal Chemistry**. 31(7): 1351–1355.

Boryski, J., Golankiewicz, B., and de Clerk, E. (1991). Synthesis and antiviral activity of 3-substituted derivatives of 3,9-dihydro-9-oxo-5H-imidazo[1,2-a]purines, tricyclic analogs of acyclovir and ganciclovir. **Journal of Medicinal Chemistry**. 34(8): 2380–2383.

Bryn, S. R. (1982). Solid State Chemistry of Drugs. **Academic Press**. New York, 6–9.

Burnett, M. N. and Johnson, C. K. (1996). *ORTEP*-III*:* Oak Ridge Thermal Ellipsoid Plot Program for Crystal Structure Illustration, Report ORNL-6895, **Oak Ridge National Laboraty**, Tennessee, USA.

Chatkon, A. (2001). Structural Studies of Supramolecular Microporous Materials**. M.Sc. Thesis**, Suaranaree University of Technology, Thailand.

Etter, M. C., MacDonald, J. C., and Bernstein, J. (1990). Graph-set analysis of hydrogen-bond patterns in organic crystals. **Acta Crystallographica Section B**. 46: 256–262.

Fung, H.-L. and Nealon, T. (1974). Solvent effect on comparative dissolution of pharmaceutical solvates. **Chemical and Pharmaceutical Bulletin**. 22, 454–458.

Greene, T. W. and Wuts, P. G. (1999). Protective Groups in Organic Synthesis, 3rd ed. **Wiley**. New York.

Grell, J., Bernstein, J., and Tinhofer, G. 1999. Graph-set Analysis of Hydrogen Bond Patterns. **Some material concepts; Techniques**. Maximilians UniversitÄt MÜnchen, Report TUM M9908.

Haller, K. J., Johnson, P. L., Feltham, R. D., Enermark, J. H., Ferraro, J. R., and Basile, L. J. (1979). Effects of temperature and pressure on the molecular and electronic structure of N,N'-ethylenebis(salicylideneiminato)nitrosyliron, Fe(NO)(salen). **Inorganica Chimica Acta**. 33: 119–130.

Lutker, K. M., Ones R. Q., Xu, J., Ramamoorthy, A., and Matzger, A. (2011). Polymorphs and hydrates of acyclovir, **Jouranl of Pharmaceutical Science**. 100(3): 949–963.

Levitt, M. and Park, B. H. (1993). Water: Now you see it, now you don't. **Structure** 1(4): 223–226.

Puntharod, R. and Haller, K. J. (2005). Preparation and characterization of NiCl(NO)(PPh$_3$)$_2$. **Acta Crystallographica Section A**. 61: C306.

Sheldrick, G.M. (1997). *SHELXL*-97 Program for the Solution and Refinement of Crystal Structures. **University of Göttingen**. Germany.

Steiner, T. (2002). The Hydrogen Bond in the Solid State. **Angewandte Chemie International Edition**. 41: 48–76.

Suwińska, K., Golankiewicz, B., and Zielenkiewicz, W. (2001). Water molecules in the crystal structure of tricyclic acyclovir. **Acta Crystallographica Section C**. 57: 767–769.

Werner, M. (2000). Crystal Structure Determination, **Marburg University**. Germany, 142–147.

Wenger, M. and Bernstein (2006). Designing a cocrystal of γ-amino butyric acid. **Angewandte Chemie International Edition**. 45: 7966–7769.

CHAPTER IV

REREFINEMENT OF TRICYCLIC ACYCLOVIR

DIHYDRATE: $C_{11}H_{13}N_5O_3 \cdot 2H_2O$

4.1 Introduction

Many crystal structures exhibit rational disorder. Often the origin of the disorder can be attributed to a simple cause; the two components have similar steric bulk and X-ray scattering density in the solid state structure, as in chloro and nitrosyl disorder in coordination compounds (Haller and Enemark, 1978; Puntharod and Haller, 2005). This type of disorder, sometimes called site occupancy disorder, is characterized by one (and only one) or none of the components occupying the site in any given asymmetric unit of structure. Because the diffraction pattern arises from the total scattering of the crystal, the model necessarily contains the structure averaged over all the scattering units in the crystal. Thus, the sum of the site occupancy factors for a given position must always be equal to or less than one (Massa, 2000). Another common type of disorder is positional or split atom disorder. This type of disorder is characterized by alternative positions for an atom or group of atoms when one looks at different unit cells. Positional disorder often results from, or causes less than optimal lattice packing, *i.e.* there is empty space within the crystal lattice. Positional disorder can be subdivided into two types. In one type the source of disorder is competing supramolecular interactions, such as those for the disordered water molecule in the

$MV_2O_6 \cdot 2H_2O$ system (Chatkon and Haller, 2002), where the framework presents multiple acceptor interaction sites and the disordered moiety alternately selects among them in the different units of structure. It is also possible that multiple donors or acceptors occur on the group that is disordered or even on both the ordered and disordered components.

Tricyclic acyclovir, 3-[(2-hydroxyethoxy)-methyl]-6-methyl-3*H*-imidazo-lo[1,2-*a*]purin-9(5*H*)-one has been reported (Suwińska, Golankiewicz, and Zielenkiewicz, 2001) as the water disolvate, $C_{11}H_{13}N_5O_3 \cdot 2H_2O$, with a crystallographic unit cell consisting of two independent molecules of tricyclic acyclovir and four molecules of water. The original report included two disordered regions in the structure. First, one hydrogen atom of one water molecule in an $(H_2O)_8$ cluster, located near an inversion center is statistically disordered, and second, the ether oxygen atom in concert with the adjacent methylene carbon atom of molecule B occupies two positions (in a 75:25 ratio).

Preliminary rerefinement of this structure has been reported (Meepripruk and Haller, 2011) using intensity data from the original report (Suwińska, Golankiewicz, and Zielenkiewicz, 2001). The refinement of the structure is presented in the current chapter and the complex concerted hydrogen bond network of water and tricyclic acyclovir molecules is reanalyzed in the following chapter. An intriguing feature of the solvent region (clusters of eight water molecules) is statistical disorder, apparent only in the hydrogen atom positions, between the centermost two water molecules.

4.2 Experimental

The crystallographic information file, *cif* file, for the crystal structure was retrieved from the IUCr electronic archives (Suwińska, Golankiewicz, and Zielenkiewicz, 2001) and the 6873 reflections from the original report were used for the rerefinement, based on F^2 using *SHELXL*-97 program (Sheldrick, 1997), is reported in this chapter.

The hydrogen atoms on C1, C6, C13, C15, C17, C18, N3 and O19 were placed in calculated, geometrically idealized positions for molecules A and B using geometrical constraints [O–H = 0.82 Å, C–H = 0.93 Å (-CH, -CH$_2$ and -CH$_3$), N–H = 0.86 Å (-NH) and restrained in idealized geometry using riding model restraints with isotropic atomic displacement parameters set at $U_{iso}(H) = 1.2U_{eq}(C,N)$]. The distances, angles, and torsional angles were compared with those originally reported (Suwińska, Golankiewicz, and Zielenkiewicz, 2001) as a check on the veracity of the crystallographic parameters. The published structure includes minor component hydrogen atoms only on C17B. Minor component hydrogen atoms on C15B and C18B were not included in the published model and major component hydrogen atoms on these positions were assigned full occupancy factors. Refinement of side chain disorder by adding PART instructions in the *ins* file to divide the atoms into two groups containing major and minor components each with its own occupancy factor, PART1 with occupancy α and PART2 with occupancy $1-\alpha$, respectively. The coordinates of all disordered atoms are found in the output files of the program. Details of the PART instructions for refinement of the side chain disorder as two groups containing major and minor components are given in Figure 4.1.

```
Part 1
O19B   4   211.000000   221.000000   231.000000    10.50000
241.00000   251.00000 =
       261.00000   271.00000   281.00000   291.00000
rem AFIX 147  0.8200
AFIX 147
H19B  2     0.056733    0.500582    0.968915    10.50000    -
1.50000
AFIX   0
Part 2
O19C   4   211.000000   221.000000   231.000000    10.50000
241.00000   251.00000 =
       261.00000   271.00000   281.00000   291.00000
rem AFIX 147  0.8200
AFIX 147
H19C  2     0.226030    0.464777    0.989456    10.50000    -
1.50000
AFIX   0
Part 0
```

Figure 4.1 PART instructions for refinement of side chain disorder as two groups containing major and minor components, respectively.

The bond distances between pairs of atom were restrained to be equal with standard deviation about 0.005 Å, with pairs of O16B C17B and O16C C17C for major and minor components, and for oxygen and hydrogen atoms in water molecules; O1W H1Wa, O1W H1Wb, O1W H1Wc, O2W H2Wa, O2W H2Wb, O3W H3Wa, O3W H3Wb, O4W H4Wa, O4W H4Wb, and H1Wa, H1Wb, H1Wa, H1Wc, H2Wa, H2Wb, H3Wa, H3Wb, H4Wa, H4Wb, using the SADI and DANG instructions of the *SHELXL*-97 program (Sheldrick, 1997). These instructions were included in the *ins* file for the analysis reported herein. The hydrogen bonding in the tricyclic acyclovir structure was analyzed using the BOND, CONF, and HTAB instructions of the *SHELXL*-97 program which search all hydrogen atoms to find possible bond lengths, bond angles, torsion angles, and hydrogen bonds or donor atoms and acceptor atoms, and include results in the output files of the program. The

SADI and DANG instructions and the BOND, CONF, and HTAB instructions for analysis of hydrogen bonding in the tricyclic acyclovir structure as shown in Figures 4.2 and 4.3, respectively.

```
SADI  0.005  O16b  C17b  O16c  C17c
DFIX 0.82 0.005  O19b H19b  O19b H19c
SADI  0.005  O1W  H1Wa  O1W  H1Wb  O1W  H1Wc  O2W  H2Wa  O2W
H2Wb
SADI  0.005  O3W  H3Wa  O3W  H3Wb  O4W  H4Wa  O4W  H4Wb
DANG 1.374  0.005   H1Wa H1Wb  H1Wa H1Wc  H2Wa H2Wb  H3Wa H3Wb
H4Wa H4Wb
```

Figure 4.2 SADI and DANG instructions for similar distances between pairs of atoms restrained to be equal with standard deviation about 0.005 Å.

```
BOND   $H
HTAB
```

Figure 4.3 The BOND $H and HTAB instructions for analysis of hydrogen bonding in the tricyclic acyclovir structure.

The *SHELXL*-97 program (Sheldrick, 1997) was used for refinement and *ORTEP*-III (Burnett and Johnson, 1996) for structure illustrations. Details of data collection and refinement of tricyclic acyclovir are given in Table 4.1. Fractional triclinic coordinates and equivalent isotropic atomic displacement parameters for the nonhydrogen atoms are given in Table 4.2, fractional coordinates and isotropic

thermal parameters for the hydrogen atoms are given in Table 4.3 and atom displacement parameters for the anisotropically modeled atoms are given in Table 4.4.

Table 4.1 Data collection and structure refinement details for tricyclic acyclovir.

Refinement	Suwińska *et al.*, 2001	This Work
Chemical formula	$C_{11}H_{13}N_5O_3 \cdot 2H_2O$	$C_{11}H_{13}N_5O_3 \cdot 2H_2O$
θ range $(2\theta_{max})$ (°)	2.02–29.97 (59.93)	2.02–28.28 (56.56)
Index ranges	$-11 =< h =< 11$	$-10 =< h =< 11$
	$-15 =< k =< 16$	$-14 =< k =< 15$
	$0 =< l =< 20$	$0 =< l =< 19$
Refinement on	F^2	F^2
$R_1 [F^2 > 2\sigma(F^2)], wR(F^2)$	0.062, 0.155	0.056, 0.142
S	1.02	1.04
Measure reflections	8414	6873
Independent reflections	8047	6873
Reflections with $I > 2\sigma(I)$	4182	3924
Parameters	389	420
R_{int}	0.023	0.000
H-atoms treatment	Mixture of independent and constrained refinement	Geometrically idealized
Weighting scheme where $P = (F_0^2 + 2F_c^2)/3$	$w = 1/[\sigma2(F_0^2) + 0.0709P)^2]$	$w = 1/[\sigma2(F_0^2) + (0.065P)^2 + 0.081P]$
$(\Delta/\sigma)_{max}$	0.016	0.001

R_1 = conventional discrepancy index, wR = the weighted R-factor, S = The goodness of fit.

Table 4.2 Fractional triclinic coordinates and equivalent isotropic atomic displacement parameters[a] ($Å^2$) for the nonhydrogen atoms of tricyclic acyclovir.

Atoms	X	Y	Z	U_{iso}
C1A	-0.5279(3)	0.1796(2)	0.3237(17)	0.0517(6)
C2A	-0.5202(2)	0.2108(18)	0.4129(15)	0.0393(5)
N3A	-0.5959(2)	0.1409(15)	0.4500(12)	0.0405(4)
C4A	-0.5711(2)	0.1841(17)	0.5706(15)	0.0344(5)
N5A	-0.4756(19)	0.2841(14)	0.5283(12)	0.0350(4)
C6A	-0.4466(2)	0.2996(19)	0.4297(15)	0.0405(5)
N7A	-0.6285(2)	0.1418(15)	0.6621(12)	0.0382(4)
C8A	-0.5783(2)	0.2090(17)	0.7106(15)	0.0363(5)
C9A	-0.4781(2)	0.3084(18)	0.6773(16)	0.0382(5)
C10A	-0.4177(2)	0.3532(18)	0.5789(15)	0.0380(5)
O11A	-0.3273(19)	0.4379(13)	0.5351(11)	0.0505(4)
N12A	-0.4558(2)	0.3498(17)	0.7528(14)	0.0483(5)
C13A	-0.5402(3)	0.2784(2)	0.8274(17)	0.0506(6)
N14A	-0.6180(2)	0.1910(16)	0.8080(13)	0.0437(4)
C15A	-0.7247(3)	0.0979(2)	0.8723(17)	0.0561(6)
O16A	-0.8903(2)	0.1258(17)	0.8748(12)	0.0619(5)
C17A	-0.9597(4)	0.1914(3)	0.9415(2)	0.0795(9)
C18A	-1.1255(4)	0.2321(3)	0.9293(2)	0.0777(9)
O19A	-1.2377(2)	0.1396(18)	0.9534(14)	0.0735(6)
C1B	-0.1151(3)	0.5772(2)	0.3299(16)	0.0467(6)
C2B	-0.0636(2)	0.6499(18)	0.3865(15)	0.0372(5)
N3B	-0.1187(2)	0.6265(14)	0.4846(12)	0.0360(4)
C4B	-0.0535(2)	0.7042(16)	0.5193(14)	0.0319(4)
N5B	0.0437(19)	0.7778(14)	0.4416(11)	0.0336(4)
C6B	0.0353(3)	0.7430(19)	0.3603(15)	0.0400(5)
N7B	-0.0774(2)	0.7095(14)	0.6083(12)	0.0343(4)
C8B	0.0081(2)	0.8002(17)	0.6152(14)	0.0324(4)
C9B	0.1092(2)	0.8794(17)	0.5422(14)	0.0338(5)
C10B	0.1349(2)	0.8729(17)	0.4469(15)	0.0348(5)
O11B	0.2197(18)	0.9341(13)	0.3751(10)	0.0481(4)
N12B	0.1736(2)	0.9595(15)	0.5786(13)	0.0399(4)
C13B	0.1130(3)	0.9296(18)	0.6693(16)	0.0403(5)
N14B	0.0114(2)	0.8329(15)	0.6969(12)	0.0372(4)
C15B	-0.0670(3)	0.7761(2)	0.7941(15)	0.0433(5)
O16B	0.0437(3)	0.7162(19)	0.8466(14)	0.0431(7)
C17B	0.1089(5)	0.6152(3)	0.8139(2)	0.0497(9)
C18B	0.2285(3)	0.5539(3)	0.8688(2)	0.0647(7)
C15C	-0.0670(3)	0.7761(2)	0.7941(15)	0.0433(5)
O16C	0.0027(7)	0.6597(6)	0.8219(4)	0.044(2)
C17C	0.1667(9)	0.6696(10)	0.8271(8)	0.055(3)
C18C	0.2285(3)	0.5539(3)	0.8688(2)	0.0647(7)

[a]The standard deviations of the least significant digits are given in parentheses.

Table 4.2 (Continued).

Atoms	X	Y	Z	U_{iso}
O19B	0.1556(3)	0.4911(3)	0.9600(15)	0.0958(8)
O19C	0.1556(3)	0.4911(3)	0.9600(15)	0.0958(8)
O1W	0.3884(2)	0.4139(17)	0.0594(12)	0.0578(5)
O2W	0.2875(3)	0.4602(2)	0.2313(13)	0.0802(7)
O3W	0.2823(3)	-0.0208(2)	0.1753(15)	0.0839(6)
O4W	0.4739(3)	0.1711(2)	0.0731(2)	0.0983(8)

[a]The standard deviations of the least significant digits are given in parentheses.

Table 4.3 Fractional triclinic coordinates and isotropic atomic displacement parameters [a] ($Å^2$) for the hydrogen atoms of tricyclic acyclovir.

Atoms	X	Y	Z	U_{iso}
H1A1	-0.4862	0.2415	0.2722	0.0770
H1A2	-0.6354	0.1662	0.3241	0.0770
H1A3	-0.4667	0.1114	0.3188	0.0770
H3A	-0.6532	0.0762	0.5079	0.0490
H6A	-0.3871	0.3605	0.3840	0.0490
H13A	-0.5473	0.2858	0.8887	0.0610
H15A	-0.7000	0.0277	0.8531	0.0670
H15B	-0.7064	0.0859	0.9330	0.0670
H17A	-0.8947	0.2565	0.9330	0.0950
H17B	-0.9657	0.1447	1.0026	0.0950
H18A	-1.1634	0.2851	0.9668	0.0930
H18B	-1.1192	0.2725	0.8664	0.0930
H19A	-1.2320	0.1119	0.9074	0.1100
H1B1	-0.0762	0.6110	0.2656	0.0700
H1B2	-0.2280	0.5741	0.3433	0.0700
H1B3	-0.0733	0.5010	0.3453	0.0700
H3B	-0.1870	0.5687	0.5195	0.0430
H6B	0.0892	0.7783	0.2985	0.0480
H13B	0.1358	0.9694	0.7115	0.0480
H15C	-0.1238	0.8356	0.8249	0.0520
H15D	-0.1471	0.7203	0.7936	0.0520
H17C	0.1616	0.6393	0.7471	0.0600
H17D	0.0216	0.5612	0.8208	0.0600
H18C	0.2928	0.4998	0.8350	0.0780
H18D	0.3017	0.6122	0.8732	0.0780

[a]The standard deviations of the least significant digits are given in parentheses.

Table 4.3 (Continued).

Atoms	X	Y	Z	U_{iso}
H15E	-0.0524	0.8239	0.8361	0.0520
H15F	-0.1827	0.7691	0.7993	0.0520
H17E	0.1734	0.7243	0.8654	0.0660
H17F	0.2326	0.7005	0.7639	0.0660
H18E	0.2263	0.5035	0.8264	0.0780
H18F	0.3419	0.5641	0.8680	0.0780
H19B	0.0567	0.5006	0.9689	0.1440
H19C	0.2260	0.4648	0.9895	0.1440
H1WA	0.3590(5)	0.4300(4)	0.1112(15)	0.1440
H1WB	0.3120(5)	0.4010(8)	0.0370(4)	0.1440
H1WC	0.4500(10)	0.4630(6)	0.0200(3)	0.1440
H2WA	0.3340(5)	0.5140(3)	0.2410(3)	0.1440
H2WB	0.2350(4)	0.4160(3)	0.2800(2)	0.1440
H3WA	0.3480(4)	0.0360(3)	0.1530(2)	0.1440
H3WB	0.2700(5)	-0.0400(4)	0.2350(9)	0.1440
H4WA	0.4550(5)	0.2419(19)	0.0770(3)	0.1440
H4WB	0.5670(3)	0.1670(3)	0.0380(3)	0.1440

[a]The standard deviations of the least significant digits are given in parentheses.

Table 4.4 Anisotropic atomic displacement parameters[a] (Å^2) of tricyclic acyclovir.

Atoms	U^{11}	U^{22}	U^{33}	U^{23}	U^{13}	U^{12}
C1A	0.0548(14)	0.0530(14)	0.0493(14)	-0.0167(11)	-0.0101(11)	-0.0050(12)
C2A	0.0352(11)	0.0362(11)	0.0444(12)	-0.0069(9)	-0.0066(9)	-0.0042(9)
N3A	0.0402(10)	0.0327(9)	0.0486(11)	-0.0094(8)	-0.0073(8)	-0.0111(8)
C4A	0.0285(10)	0.0285(10)	0.0449(12)	-0.0076(9)	-0.0054(9)	-0.0070(8)
N5A	0.0325(9)	0.0294(8)	0.0405(10)	-0.0054(7)	-0.0042(7)	-0.0095(7)
C6A	0.0369(11)	0.0397(12)	0.0404(12)	-0.0061(10)	-0.0012(9)	-0.0094(9)
N7A	0.0385(9)	0.0315(9)	0.0415(10)	-0.0054(8)	-0.0040(8)	-0.0103(7)
C8A	0.0330(10)	0.0323(11)	0.0402(12)	-0.0057(9)	-0.0042(9)	-0.0027(9)
C9A	0.0344(11)	0.0337(11)	0.0476(13)	-0.0127(9)	-0.0071(9)	-0.0054(9)
C10A	0.0322(10)	0.0318(10)	0.0501(13)	-0.0113(9)	-0.0067(9)	-0.0060(9)
O11A	0.0524(9)	0.0408(9)	0.0552(10)	-0.0059(7)	-0.0051(8)	-0.0262(8)
N12A	0.0495(11)	0.0488(11)	0.0483(11)	-0.0132(9)	-0.0097(9)	-0.0131(9)
C13A	0.0548(14)	0.0539(14)	0.0449(14)	-0.0144(11)	-0.0101(11)	-0.0085(12)
N14A	0.0448(10)	0.0412(10)	0.0422(11)	-0.0057(8)	-0.0071(8)	-0.0075(8)
C15A	0.0614(16)	0.0518(14)	0.0455(14)	-0.0004(11)	-0.0017(12)	-0.0146(12)
O16A	0.0556(11)	0.0783(12)	0.0497(10)	-0.0212(9)	0.0033(8)	-0.0192(9)
C17A	0.0720(2)	0.0950(2)	0.076(2)	-0.0425(18)	0.0047(16)	-0.0234(18)
C18A	0.0730(2)	0.0684(19)	0.081(2)	-0.0202(16)	0.0104(16)	-0.0151(16)
O19A	0.0647(12)	0.0774(14)	0.0719(13)	-0.0205(11)	0.0052(10)	-0.0184(10)

[a]The standard deviations of the least significant digits are given in parentheses.

Table 4.4 (Continued).

Atoms	U^{11}	U^{22}	U^{33}	U^{23}	U^{13}	U^{12}
C1B	0.0528(14)	0.0450(13)	0.0457(13)	-0.0152(10)	-0.0116(11)	-0.0056(11)
C2B	0.0364(11)	0.0353(11)	0.0390(12)	-0.0081(9)	-0.0074(9)	-0.0013(9)
N3B	0.0369(9)	0.0292(9)	0.0399(10)	-0.0060(7)	-0.0039(7)	-0.0116(7)
C4B	0.0282(10)	0.0248(10)	0.0386(11)	-0.0026(8)	-0.0040(8)	-0.0045(8)
N5B	0.0341(9)	0.0284(8)	0.0349(9)	-0.0038(7)	-0.0033(7)	-0.0070(7)
C6B	0.0421(12)	0.0402(12)	0.0352(11)	-0.0079(9)	-0.0034(9)	-0.0069(10)
N7B	0.0353(9)	0.0307(9)	0.0343(9)	-0.0032(7)	-0.0049(7)	-0.0097(7)
C8B	0.0302(10)	0.0293(10)	0.0373(11)	-0.0057(8)	-0.0091(8)	-0.0006(8)
C9B	0.0305(10)	0.0270(10)	0.0423(12)	-0.0025(9)	-0.0096(9)	-0.0063(8)
C10B	0.0290(10)	0.0287(10)	0.0432(12)	-0.0034(9)	-0.0053(9)	-0.0052(8)
O11B	0.0487(9)	0.0444(9)	0.0425(9)	-0.0023(7)	0.0033(7)	-0.0213(7)
N12B	0.0411(10)	0.0339(9)	0.0466(11)	-0.0063(8)	-0.0148(8)	-0.0097(8)
C13B	0.0434(12)	0.0354(11)	0.0451(13)	-0.0082(10)	-0.0161(10)	-0.0066(9)
N14B	0.0391(9)	0.0353(9)	0.0366(10)	-0.0045(8)	-0.0099(8)	-0.0068(8)
O16B	0.0564(14)	0.0432(13)	0.0340(11)	-0.0140(9)	-0.0145(9)	0.0037(10)
C17B	0.0690(2)	0.0463(19)	0.0341(17)	-0.0119(14)	-0.0138(16)	0.0102(18)
O19B	0.0803(15)	0.1176(19)	0.0634(13)	0.0309(12)	-0.0223(12)	0.0008(16)
O19C	0.0803(15)	0.1176(19)	0.0634(13)	0.0309(12)	-0.0223(12)	0.0008(16)
O1W	0.0574(11)	0.0645(12)	0.0467(10)	-0.0070(9)	-0.0061(8)	-0.0114(9)
O2W	0.1113(17)	0.0790(14)	0.0484(11)	-0.0206(10)	0.0057(11)	-0.0552(12)
O3W	0.1056(18)	0.0777(15)	0.0615(13)	-0.0167(11)	-0.0022(13)	-0.0115(12)
O4W	0.0961(18)	0.0742(15)	0.1008(18)	-0.0214(14)	0.0269(14)	-0.0040(13)

[a]The standard deviations of the least significant digits are given in parentheses.

4.3 Results and Discussion

The new refinement produced an improved model as implied by the decrease from previous $R[F^2 > 2\sigma\ (F^2)] = 0.062$ to 0.056 and wR (all of F^2 data) = 0.155 to 0.142 and seen in the improved model geometry. The geometric parameters from the new refinement of tricyclic acyclovir are compared to those of the previous report. The bond distance of X−H for X=C, N, and O of the new refinement agree with idealized geometrical positions. The C−H distances are the same values with previous report at C6, C13 about 0.930 Å in both of molecule A and B, and about 0.970 Å at C15, C17, and C18 in molecule B and C except in C17−H17a and C17−H17b of molecule C are shorter that previous report about 0.970 Å of this work and 1.331 Å and 1.502 Å from

the previous report with the same bond distance values at C15 and C18 of molecule C. Moreover, the O−H distance in this work show shorter than previous report about 0.820 Å for present work and 1.031 Å from previous report in molecule A. The more rational values in the present report are the result of the refinement restraints described above. Selected interatomic bond distances are given in Table 4.5.

Table 4.5 Selected interatomic bond distances[a] (Å) for tricyclic acyclovir.

Atoms	Mole A	Mole B	Mole C	Atoms	Mole A	Mole B	Mole C
C1− H1A1	0.930 (0.960)	0.930 (0.960)	-	C15−H15b	0.930 (0.971)	0.970 (0.970)	0.970 (0.970)
C1−H1A2	0.930 (0.961)	0.930 (0.960)	-	C17−H17a	0.930 (0.971)	0.970 (0.970)	0.970 (1.331)
C1−H1A3	0.930 (0.960)	0.930 (0.960)	-	C17−H17b	0.930 (0.969)	0.970 (0.970)	0.970 (1.502)
N3−H3a	0.860 (0.978)	0.860 (0.865)	-	C18−H18a	0.930 (0.969)	0.970 (0.970)	0.970 (0.970)
C6−H6a	0.930 (0.930)	0.930 (0.930)	-	C18−H18b	0.930 (0.971)	0.970 (0.970)	0.970 (0.970)
C13−H13a	0.930 (0.930)	0.930 (0.930)	-	O19−H19a	0.820 (1.031)	0.820 (0.819)	0.820 (0.819)
C15−H15a	0.930 (0.970)	0.970 (0.970)	0.970 (0.970)	O19−H19c		0.82 (-)	0.82(-)

[a] The distance values of the original report are given in parentheses.

The bond angles are also quite similar when comparing this work and the previously published structure (Suwińska, Golankiewicz, and Zielenkiewicz, 2001). Only three bond angles, all involving hydrogen atoms, presented significantly different values in C2−N3−H3a and C18−O19−H19a which narrow the angle 3.8−10.7° and for C4−N3−H3a which widens the angle 3.9−6.1° from previous report

in both of molecules A and B, except, C18–O19–H19a of molecule B shows equivalent bond angle. For the minor occupancy molecule C bond angles involving hydrogen atoms change considerably, consistent with including properly modeled hydrogen atoms in the current refinement (the bond angles are larger in O16–C15–H15f, O16–C17–H17f, and C17–C18–H18e between 8.9–35.6º and narrower in O16–C15–H15e and C17–C18–H18f between 19.1–27.9º. Selected interatomic bond angles are given in Table 4.6.

Table 4.6 Selected interatomic bond angles[a] (º) for tricyclic acyclovir.

Atoms[*]	Mole A	Mole B	Mole C	Atoms	Mole A	Mole B	Mole C
C2–C1–H1a	109.5 (109.5)	109.5 (109.5)	-	N14–C15–H15a	109.2 (109.2)	109.1 (109.1)	109.7
C2–C1–H1b	109.5 (109.5)	109.5 (109.4)	-	N14–C15–H15b	109.2 (109.1)	109.1 (109.1)	109.7 (109.1)
C2–C1–H1c	109.5 (109.5)	109.5 (109.4)	-	H15a–C15–H15b	107.9 (107.9)	107.8 (-)	108.2 (-)
H1a–C1–H1b	109.5 (109.4)	109.5 (109.5)	-	O16–C17–H17a	109.7 (109.8)	109.6 (109.5)	109.7 (109.8)
H1a–C1–H1c	109.5 (109.5)	109.5 (109.5)	-	C18–C17–H17a	109.7 (109.8)	109.6 (109.5)	109.7 (109.7)
H1b–C1–H1c	109.5 (109.4)	109.5 (109.5)	-	O16–C17–H17b	109.7 (109.8)	109.6 (109.5)	109.7 (90.8)
C2–N3–H3a	124.7 (130.3)	124.9 (128.7)	-	C18–C17–H17b	109.7 (109.7)	109.6 (109.6)	109.7 (109.7)
C4–N3–H3a	124.7 (118.6)	124.9 (121.0)	-	H17a–C17–H17b	108.2 (108.3)	108.1 (108.1)	108.2 (108.2)
C2–C6–H6a	126.1 (126.0)	126.1 (126.1)	-	O19–C18–H18a	108.9 (108.9)	109.0 (108.9)	107.1 (-)
N5–C6–H6a	126.1 (126.1)	126.1 (126.1)	-	C17–C18–H18a	108.9 (108.9)	109.0 (108.9)	107.1 (73.4)
N12–C13–H13a	122.9 (122.8)	123.3 (123.4)	-	O19–C18–H18b	108.9 (108.8)	109.0 (108.9)	107.1 (-)
N14–C13–H13a	122.9 (122.9)	123.3 (123.4)	-	C17–C18–H18b	108.9 (108.9)	109.0 (109.0)	107.1 (126.2)

[a] The distance values of the original report are given in parentheses.

Table 4.6 (Continued).

Atoms[*]	Mole A	Mole B	Mole C	Atoms[*]	Mole A	Mole B	Mole C
O16–C15–H15a	109.2 (109.2)	109.1 (109.1)	109.7 (137.6)	H18a–C18–H18b	107.7 (107.6)	107.8 (107.7)	106.8 (-)
O16–C15–H15b	109.2 (109.2)	109.1 (109.1)	109.7 (74.1)	C18–O19–H19a	109.5 (120.2)	109.5 (109.5)	109.5 (-)

[a] The distance values of the original report are given in parentheses.

The torsional angles of the side chains are approximately the same as in the previous report. Only molecules B and C at C17–C18–O19–H19 show significantly different values in the new refinement, −1.97º for this work and −44.0º for the previous report for molecule B and an opposite signed value in molecule C at 37.6º for this work compared to −4.4º for the previous report. Both are present in eclipsed conformations. The torsional angles of the 2-hydroxyethoxy-methyl side chain are given in Table 4.7

Table 4.7 Torsional angles (º) of the 2-hydroxyethoxy-methyl side chain.

Torsion angle(º)	Molecule A	Molecule B	Molecule C
C8–N14–C15–O16	-78.3(-78.4)	107.1(106.7)	65.4(65.0)
C13–N14–C15–O16	100.2(100.2)	-69.4(-70.0)	-111.1(-111.7)
N14–C15–O16–C17	-87.3(-87.2)	-69.0(-68.5)	67.2(67.1)
C15–O16–C17–C18	171.6(171.4)	178.9(178.8)	171.4(171.2)
O16–C17–C18–O19	67.5(67.5)	74.6(74.7)	-59.9(-59.4)
C17–C18–O19–H19	-85.9(-88.2)	-1.97(-44.0)	37.6(-4.4)
C17–C18–O19–H19c	-	-173.9	-134.4

[a] The distance values of the original report are given in parentheses.

The bond distances in the water molecules (0.820–0.847 Å) of the new refinement are much closer to ideal values than those obtained from the previous work (0.771–1.002 Å), as are the H–O–H bond angles (108.4–113.9º compared to 98.6–117.7º in the original report, closer to tetrahedral values) due to the restraints employed during the refinement. X–H distances are determined too short by X-ray analysis due to the electrons being localized between the atoms reducing the apparent bonding distances for hydrogen atoms (Müller, Herbst-Irmer, Spek, Schneider, and Sawaya, 2006). Selected interatomic bond distances and angles for the water molecules are given in Table 4.8.

Table 4.8 Selected interatomic bond distances[a] (Å) and bond angles (º) in the water molecules of tricyclic acyclovir.

Bonds	d[D–H] (Å)	Bonds	d[D–H] (Å)
O1W–H1Wa	0.823(1.002)	O3W–H3Wa	0.846(0.838)
O1W–H1Wb	0.821(0.886)	O3W–H3Wb	0.847(0.974)
O1W–H1WC	0.821(0.818)	O4W–H4Wa	0.845(0.771)
O2W–H2Wa	0.820(0.842)	O4W–H4Wb	0.845(0.819)
O2W–H2Wb	0.820(0.780)		
Bond angles	**∠[H–D–H] (º)**	**Bond angles**	**∠[H–D–H] (º)**
H1Wa–O1W–H1Wb	113.5(104.7)	H2Wa–O2W–H2Wb	113.9(117.7)
H1Wa–O1W– H1Wc	113.3(108.5)	H3Wa–O3W–H3Wb	108.4(104.6)
H1Wb–O1W–H1Wc	110.1(104.0)	H4Wa–O4W–H4Wb	108.9(98.6)

[a] The distance values of the original report are given in parentheses.

Moreover, make sure again for new refinement present better model and more accurate bond distances and bond angles than previous structure with check the intermolecular nonbonded contact of the guanine ring and side chain disorder from this work shows similar interaction with the previous report. The hydrogen bonding geometry of the guanine ring system and side chain disorder are shown in Tables 4.9-4.10.

Table 4.9 Hydrogen bonding geometry[a](Å, º) for tricyclic acyclovir.

D–H···A	d[D–H] (Å)	d[H···A] (Å)	d[D···A] (Å)	∠[D–H···A] (º)
N3a–H3a···N12b[i]	0.89(0.98)	1.98(1.85)	2.803(2.800)	153.2(163.4)
N3b–H3b···O11a	0.89(0.86)	1.92(1.98)	2.748(2.747)	153.0(148)
O19b[v]–H19b[v]···O19b[xi]	0.82(0.82)	1.87(2.02)	2.644(2.671)	156.4(135)
O19a–H19a···O3W[iv]	0.82(1.02)	1.95(1.71)	2.738(2.731)	161.4(177)
O1W–H1Wb···O19b[v]	0.82(0.89)	2.03(1.84)	2.709(2.706)	140.2(164)
O2W–H2Wa···N12a[ii]	0.82(0.84)	1.98(1.96)	2.793(2.797)	172.8(177)
O2W–H2Wb···N7b[iii]	0.82(0.78)	2.17(2.21)	2.982(2.982)	170.3(173)
O3W–H3Wb···O11b[iii]	0.847(0.97)	1.98(1.85)	2.82(2.8219)	171.8(176)
O4W–H4Wb···O19a[vi]	0.845(0.82)	1.90(2.00)	2.73(2.738)	171.1(149)
O1W–H1Wa···O2W	0.823(1.00)	1.87(1.69)	2.689(2.679)	177.0(170)
O1W–H1Wc···O1W[viii]	0.82(0.82)	1.99(1.99)	2.806(2.808)	171.5(175)
O3W–H3Wa···O4W	0.84(0.84)	1.92(1.94)	2.748(2.751)	165.2(163)
O4W–H4Wa···O1W	0.845(0.77)	2.019(2.11)	2.848(2.852)	166.8(163)
O19b[xi]–H19c[xi]···O1W[xii]	0.82	1.89	2.709	176.2(-)

Symmetry codes: (i) = 1+x, 1+y, z; (ii) = -x, 1-y, 2-z; (iii) = -x, 1-y, 1-z; (iv) = -x, 2-y, 1-z; (v) = -x, 1-y, 2-z; (vi) = -1-x, 1-y, 1-z; (viii) = 1-x, 1-y, -z; (ix) = -x, 1-y, 1-z; (xi) = -1+x, y, z; (xii) = -x, 1-y, -z.

[a] The distance values of the original report are given in parentheses.

Table 4.10 Hydrogen bonding geometry[a] (Å, º) for the side chain disorder.

D–H⋯A	d[D–H] (Å)	d[H⋯A] (Å)	d[D⋯A] (Å)	∠[D–H⋯A] (º)
Major component				
C15b–H15c⋯O3W[ii]	0.97	2.47	3.360	152.6
C15b–H15c⋯O4W[ii]	0.97	2.99	3.652	126.2
C15b–H15d⋯O2W[ii]	0.97	2.62	3.565	163.2
C15b–H15d⋯O1W[ii]	0.97	2.83	3.555	131.9
C17a[ii]–H17b[ii]⋯O16b	0.93	3.03	3.501	113.4
C18a[ii]–H18a[ii]⋯O16b	0.93	3.17	3.765	123.4
C17b–H17d⋯O2W[ii]	0.97	2.93	3.763	144.0
C17b–H17d⋯O19b[iv]	0.97	3.19	3.562	104.7
C18b–H18c⋯N12a[vi]	0.97	2.91	3.864	166.9
C18b–H18d⋯O1W[i]	0.97	2.99	3.705	131.6
Minor component				
C15c–H15e⋯O3W[ii]	0.97	2.91	3.360	109.4
C15c–H15f⋯O4W[iii]	0.97	2.919	3.652	134.2
C15c–H15f⋯O1W[iii]	0.97	2.92	3.555	124.0
C15c–H15f⋯O2W[iii]	0.97	3.04	3.565	115.3
C15c–H15f⋯O3W[iii]	0.97	3.10	3.360	97.4
O1W[ii]–H1Wa[ii]⋯O16c	0.82	3.15	3.418	102.4
O1W[ii]–H1Wb[ii]⋯O16c	0.83	2.98	3.418	114.9
O2W[ii]–H2Wb[ii]⋯O16c	0.83	3.07	3.238	94.2
O19b[iii]–H19b[iii]⋯O16c	0.82	3.16	3.300	92.8
O19b[iii]–H19c[iii]⋯O16c	0.82	3.09	3.300	97.5
C18b–H18f⋯O1W[ii]	0.97	2.79	3.705	157.4
C18b–H18f⋯O1W[v]	0.97	3.05	3.429	104.8
C18b–H18f⋯O2W[ii]	0.97	3.17	4.026	148.2

Symmetry codes: (i) = 1-x, 2-y, 2-z; (ii) = 1+x, 1+y, 1+z; (iii) = 1+x, y, 1+z; (iv) = x, 1+y, 1+z;

(v) = -x, 2-y, 2-z; (vi) = -x, 1-y, 2-z. [a] The distance values of original report are given in parentheses.

4.4 Conclusion

The rerefinement of tricyclic acyclovir dihydrate, $C_{11}H_{13}N_5O_3 \cdot 2H_2O$, used the 6873 reflections with θ_{max} less than 28.28° from the original refinement. All hydrogen atoms were generated geometrically with O–H (0.82 Å), C–H (0.93 Å), and N–H (0.86 Å) with riding model with $1.2[U_{eq}(C,N)]$.

The new refinement was successful with decreased discrepency indices relative to the original report with $R[F^2 > 2\sigma (F^2)] = 0.056$ and wR (all of F^2 data) = 0.142 for 6873 reflections and more complete and more reasonable modeling of the hydrogen atom disorder. Refinement of the site occupancy factor of the side chain disorder at O16 and C17 led to an occupancy of 0.738(5) for the major component, insignificantly different from the previous report. Inclusion of a disordered hydrogen atom at O19B with site occupancy factors of 0.5 clearly improves the structure analysis. In the water molecules the O–H bond distances range 0.820–0.847 Å, closer to the ideal than those in the original report [range 0.771–1.002 Å] and H–O–H angles range 108.4–113.9° more nearly tetrahedral (109.5°) than the previous report.
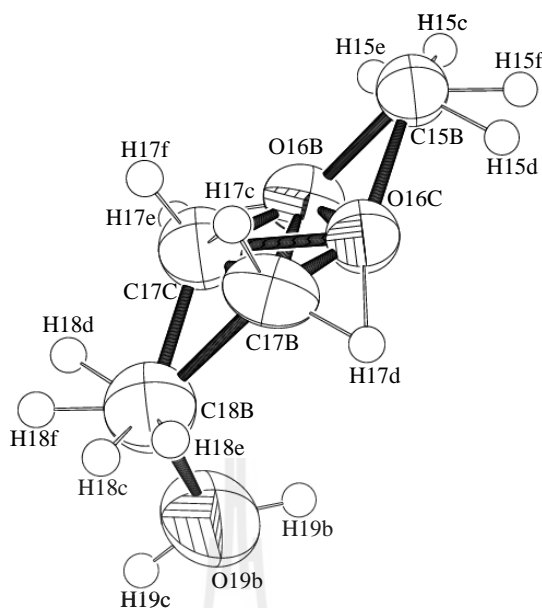
Figure 4.4 The (2-hydroxyethoxy)-methyl side chain disordered of major component indicated in O16B and C17B and minor component in O16C and C17C and disordered hydrogen atoms in H19b: H19c are included half: half occupancy.

Supplementary Material

The PART instruction is the following :

PART 1 component which set the coordinates (positions) for each atoms and occupancies (ratios) and for the site occupancy factor (*sof*) for each atom in the sixth column of the .ins file add 21.0000 for atom in PART 1 (the mean that *sof* set to 1.0000 times) and add −21.0000 in PART 2. Directly before all atoms of the minor component write PART 2 and after all disordered atoms write PART 0 to end of the instruction (Müller, Herbst-Irmer, Spek, Schneider, and Sawaya, 2006). For disorder on O19B and O19C using PART instruction write the same pattern as described above in the disorder at side chain with add 10.5000 for *sof* in PART 1 and −10.5000 in PART 2.

4.5 References

Burnett, M. N. and Johnson, C. K. (1996). *ORTEP*-III: Oak Ridge Thermal Ellipsoid Plot Program for Crystal Structure Illustration, Report ORNL-6895, **Oak Ridge National Laboratory**. Tennessee, USA.

Chatkon, A. and Haller, K. J. (2002). **3rd National Graduate Student Symposium**. Suranaree University of Technology, Nakhon Ratchasima.

Haller, K. J. and Enemark, J. H. (1978). Structure Chemistry of the {CoNO}[8] Group. The structure of N,N′-ethylenebis(salicylideneiminato)nitrosylcobalt(II), Co(NO)(salen). **Inorganica Chimica Acta**. 17(12): 3552–3558.

Meepripruek, M. and Haller, K. J. (2010). Solvation in 3-[(2-Hydroxyethoxy)-methyl]-6-methyl-3H-imidazolo[1,2-a]Purin-9(5H)-one Dihydrate; $C_{11}H_{13}N_5O_3 \cdot 2H_2O$. **Proceedings of ANSCSE14**. Mae Fah Luang University, Chiang Rai, Thailand, p. 315.

Meepripruek, M. and Haller, K. J. (2011). Rerefinement of Tricyclic Acyclovir: $C_{11}H_{13}N_5O_3 \cdot 2H_2O$. **Acta Crystallographica Section A**. 67: C761–762.

Müller, P., Herbst-Irmer, R., Spek, A. L., Schneider, T. R., and Sawaya, M. R. (2006). Crystal Structure Refinement: A Crystallographer's Guide to SHELXL. **IUCr, Oxford University**. England.

Prasad, S. M. and Rani, A. (2001). Rerefinement of sodium thiosulfate pentahydrate. **Acta Crystallographica Section E**. 57: i67–i69.

Puntharod, R. and Haller, K. J. (2005). Preparation and characterization of NiCl(NO)(PPh$_3$)$_2$. **Acta Crystallographica Section A**. 61: C306.

Sheldrick, G. M. (1997). *SHELXL*-97 Program for the Solution and Refinement of Crystal Structures. **University of Göttingen**. Germany.

Suwińska, K., Golankiewicz, B., and Zielenkiewicz, W. (2001). Water molecules in
the crystal structure of tricyclic acyclovir. **Acta Crystallographica Section C**.
57: 767–769.

Wenger, M. and Bernstein (2006). Designing a cocrystal of γ-amino butyric acid.
Angewandte Chemie International Edition. 45: 7966–7769.

CHAPTER V

SUPRAMOLECULAR STRUCTURE AND DISORDER

OF AN ACYCLOVIR DERIVATIVE:

TRICYCLIC ACYCLOVIR, $C_{11}H_{13}N_5O_3 \cdot 2H_2O$

5.1 Introduction

Tricyclic acyclovir was expected to be inactive since the NH_2 group at C2 of acyclovir was blocked by the closure of the third ring (Boryski, Golankiewicz and de Clercq, 1988). However, tricyclic acyclovir exhibits a marked antiherpetic activity with potent and selective activity against HSV-1 and HSV-2, VZV, and cytomegalovirus, and at the same time lower cytotoxicity which results in a higher selectivity index than that of acyclovir (Boryski, Golankiewicz, and de Clercq, 1991; Balzarini, Ostrowski, Goslinski, de Clercq, and Golankiewicz, 2002). Many studies focused on the potent and selective antiherpetic activity and it was also noted that the new compound had higher dissolution rate than that of acyclovir (Boryski, Golankiewicz, and de Clercq, 1991).

The structure of tricyclic acyclovir has also been reported (Suwińska, Golankiewicz, and Zielenkiewicz, 2001). One feature of the structure is a large water solvent region with eight molecules of water, hydrogen bonded together, leading to the suggestion that the large solvent content may relate to the solvation behavior of the molecules in solution. The original publication reported disorder of two water

molecules but did not report the related inversion center and related disorder of a side chain hydroxyl groups (Meepripruk and Haller, 2010) that contributes to a highly concerted hydrogen bond chain as in Figure 5.1, exhibiting an intriguing statistical disorder apparent only in the hydrogen atom positions.
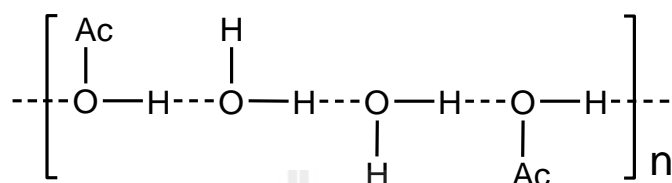
Figure 5.1 Concerted hydrogen bond chain.

The structure exhibits a second disorder region in the (2-hydroxyethoxy)-methyl side chain of one of the two crystallographically independent tricyclc acyclovir molecules. Relevant to their therapeutic use, pharmaceutical water solvates generally have higher dissolution rates than nonsolvated compounds (Fung and Nealon, 1974) and confirmed as is the case for this hydrous form as compared to the anhydrous form of tricyclic acyclovir (Kristl, Srcic, Vrecer, Sustar, and Vojnovic, 1996).

Solvates and polymorphs of active pharmaceutical ingredients (API) have long been interested (Bryn, 1982), not only because of patent law, but also the modification of physical properties, relevant to the therapeutic value and the processability of the API, they provide. More recently the emphasis has shifted to cocrystals for the same benefits, but with a much larger range of possibilities through the groups of compounds already approved as additives, or classified as generally regarded as safe (GRAS) by the Food and Drug Administration (Wenger and Bernstein, 2006). Cocrystals can be conveniently defined as crystalline molecular complexes containing two or more species with essentially molecular properties that can, at least in

principle, be separated into the pure components with similar chemical natures to those they possess in the cocrystal. In this sense cocrystals and solvates are closely related.

5.2 Experimental

The crystallographic information file, *cif* file, for the rerefined crystal structure reported in chapter IV was used for the analysis presented in this chapter. The crystal lattice contains two complete tricyclic acyclovir molecules and four water molecules in each asymmetric unit. The minor component of molecule B is identical to the major component except that O16B and C17B are replaced by O16C and C17C, and the six hydrogen positions on C15B, C17C, and C18B represented by labels ending in c and d for the major component and e and f for the minor component. Molecule B has a 74(5):26(5) disorder of atoms O16B and C17B (and associated hydrogen atoms) as the major component, and atoms O16C and C17C (and associated hydrogen atoms) as the minor component. The hydrogen atom at O19B was modeled as a statistical disorder (0.5:0.5 ratio) of atoms H19b and H19c.

The computational analysis of supramolecular interactions, including hydrogen bonds, interatomic distances, angles, and torsional angles, were computed and molecular graphic was illustrated by the *ORTEP*-III program (Burnett and Johnson, 1996). Inter- and intra-molecular contact distances were calculated by a 102 instruction to the *ORTEP*-III program (Burnett and Johnson, 1996) to a maximum search radius cut-off distance of 3.6 Å. The 102 instruction gives both interatomic distances and angles about each origin atom. The hydrogen bonding in the acyclovir structure was analyzed using BOND, CONF, and HTAB instructions in the *SHELXL-*

97 program, searching around all hydrogen atoms to find possible bond lengths, bond angles, torsion angles, and hydrogen bonds or donor atoms and acceptor atoms. The results of this search can be found in the output files of the program.

Aromatic–aromatic interactions in and around the ring system were evaluated by calculating distances from atoms to the plane using the MPLA instruction (number of atoms to create plane by the *SHELXL*-97 as result of least-squares planes (x,y,z in crystal coordinates) and deviations, equation of plane for molecules and angle to previous plane (with approximate esd), and the distance between atoms of adjacent guanine ring to plane that the atoms add in MPLA instruction.

Analysis of electron density. The characteristic disorder positions was produce electron density map (F_o) with the relevant hydrogen atoms and different electron density map (F_o–F_c) with the relevant hydrogen atoms by used *ins* file to with data resolution 1.5 Å at 2.5σ and view is perpendicular to water region axis with view at the four plane level; Plane = 0.0, –0.1, = –0.2, and –0.3. The (F_o) and (F_o–F_c) maps were generated via *PLATON*. The two water (O1W⋯O1W′), each water molecule bound to hydroxyl group of the (2-hydroxyethoxy)methyl side chain of one tricyclic acyclovir molecule and the hydrogen position between bound point was expected.

5.3 Results and Discussions

The crystal lattice contains two complete tricyclic acyclovir molecules and four water molecules in the asymmetric unit. Molecule B has a 74(5):26(5) disorder of atoms O16B and C17B as the major component, and atoms O16C and C17C as the minor component. The published structure includes minor component hydrogen atoms only on C17B. Minor component hydrogen atoms on C15B and C18B were not

included and major component hydrogen atoms on these were assigned full occupancy factors. The minor component of molecule B is modeled as identical to the major component except that O16B and C17B are replaced by O16C and C17C, and the six hydrogen positions on C15B, C17C, and C18B represented by labels ending in e and f. Asymmetric unit in crystal structure of the tricyclic acyclovir molecules and four water molecules which molecule B has a 74(5):26(5) disorder of O16B and C17B as major component and the hydrogen atom labeling a to f of C15, C17 and C18 used indicated in asymmetric unit of structure as illustrated in Figures 5.1 and 5.2, respectively.
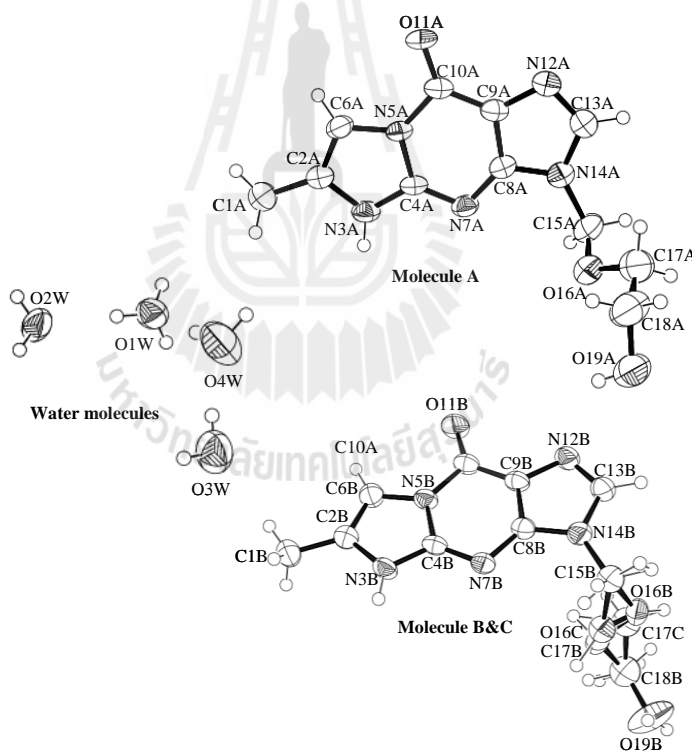
(a)

Figure 5.2 Asymmetric unit in crystal structure of the tricyclic acyclovir molecules and four water molecules which molecule B has a 74:26 disorder of O16B and C17B as major component (a) best view side, (b) view along *c* axis with 50% probability displacement ellipsoids for nonhydrogen atoms.

Molecule B&C

Molecule A

Water molecules

(b)
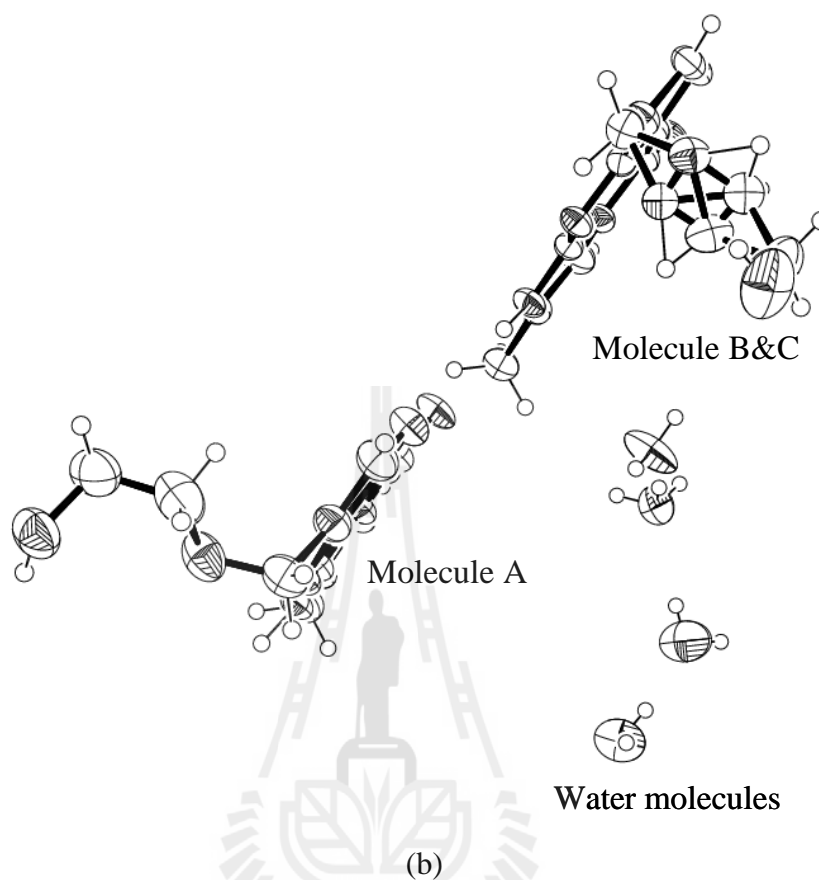
Figure 5.2 (Continued).

The fully ordered molecule A conformation and the disorder in molecule B allows three crystallographically independent conformers of the 2-hydroxyethoxy-methyl side chain. In the figures the tricyclic ring systems are placed in the same relative orientation in all three conformers to aid comparison. The 2-hydroxyethoxy-methyl side chain are perpendicular to the tricyclic ring system, but than of molecule A has opposite sense to molecules B and C. The three conformations in the crystal structure of tricyclic acyclovir are illustrated in Figure 5.3.

(a)

(b)

(c)
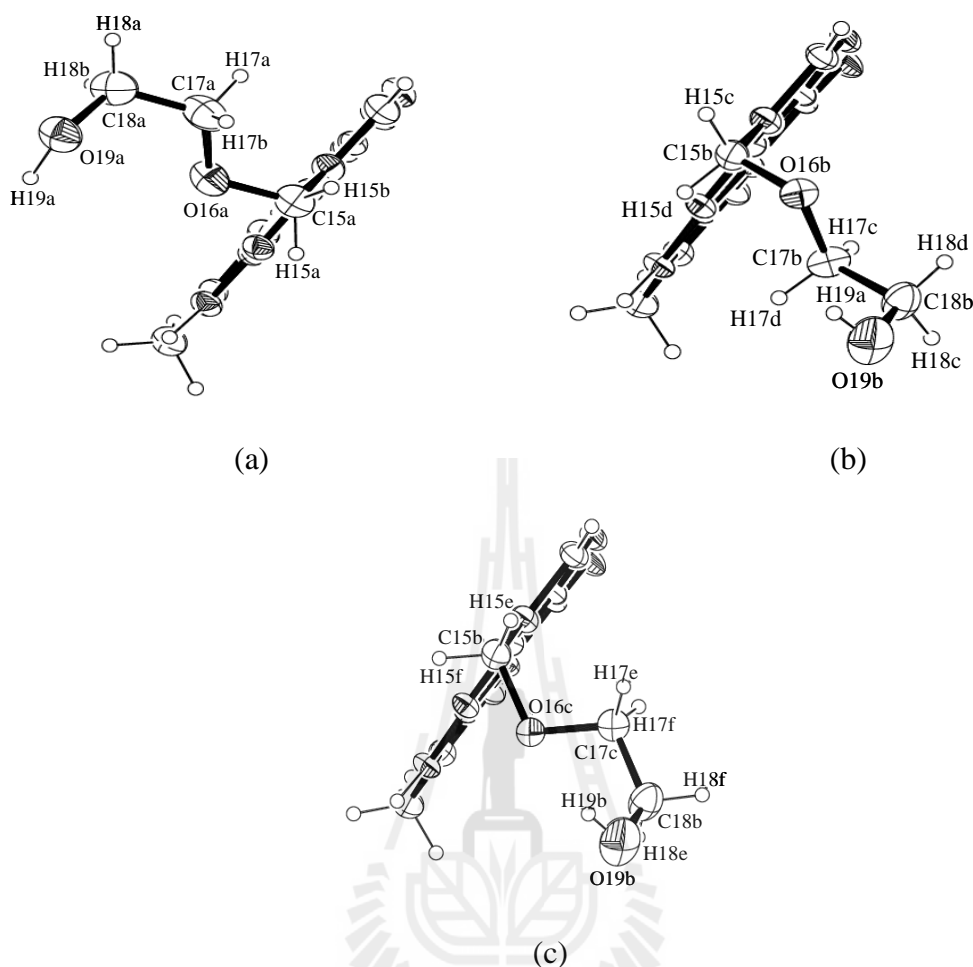
Figure 5.3 The three conformations in the crystal structure of tricyclic ring systems are in the same relative orientation in all three conformers to aid comparison, (a) molecule A, (b) molecule B, and (c) molecule C.

Torsional angles as are generally used for conformational analysis of organic compounds for the three side chain conformations consider the torsional angles, N14–C15–O16–C17, C15–O16–C17–C18, and O16–C17–C18–O19 of molecules A and B are quite similar, while those of molecule C have the opposite sense but are otherwise also similar to those of molecules A and B. Only the torsional angle involving the hydroxyl hydrogen, C17–C18–O19–H19, shows significant difference

with -85.9º and 37.6º for molecule A, and C, respectively, that present synclinal conformations while only -1.97º from the eclipsed conformation position (highest energy position) in molecule B (Moss, 1996). The three conformations are quite similar with the exception of the relative position of atom H19b for molecule C. However, Steiner (Steiner, 2002) has noted that while the preferred placement of H in X–C–O–H in free molecules is trans to X, in crystal structures an H···X hydrogen bond always overrides the preference and there is essentially no preferred torsional angle for the grouping. The bond lengths for the minor occupancy atoms in molecule C are different from those in molecules A and B (but not statistically different due to the relatively high estimated standard deviations in molecule C) which the d[O19–H19] of those molecule appears approximately the same about 0.82 Å, this may be an illusion created by refining and fixing the H19b position. The torsional angles and bond distances of the 2-hydroxyethoxy-methyl side chain as given in Table 5.1.

Table 5.1 Selected a torsional angle (º) and bond distances (Å) [a] of the 2-hydroxy-ethoxy-methyl side chain.

Torsion angle (º)	Molecule A	Molecule B	Molecule C
C8–N14–C15–O16	-78.3(0.28)	107.1(0.24)	65.4(0.37)
C13–N14–C15–O16	100.2(0.28)	-69.4(0.27)	-111.1(0.35)
N14–C15–O16–C17	-87.3(0.27)	-69.0(0.29)	67.1(0.70)
C15–O16–C17–C18	171.6(0.22)	178.9(0.24)	171.4(0.56)
O16–C17–C18–O19	67.5(0.34)	74.6(0.37)	-59.9(0.96)
C17–C18–O19–H19	-85.9	-1.97	37.6

[a] The standard deviation of the least significant digits are given in parentheses.

Table 5.1 (Continued).

Torsion angle (º)	Molecule A	Molecule B	Molecule C
C17–C18–O19–H19c	-	-173.9	-134.4
Bond distance (Å)			
N14–C15	1.454(3)	1.454(3)	1.454(3)
C15–O16	1.411(3)	1.400(3)	1.446(7)
O16–C17	1.407(3)	1.419(3)	1.419(5)
C17–C18	1.488(4)	1.484(4)	1.457(11)
C18–O19	1.403(3)	1.391(3)	1.391(3)
O19–H19	0.82	0.82	-
O19–H19c	-	0.82	-

[a] The standard deviations of the least significant digits are given in parentheses.

The supramolecular structure of tricyclic acyclovir is held together by strong hydrogen bond interactions between two tricyclic acyclovir molecules using one water molecule via N3b–H3b···O11a, d[H···O] = 2.75 Å are involve donating a proton in hydrogen bond (molecule B) with adjacent (molecules A) and the water molecule involve in bridging the molecule A with molecule B by donating a proton in hydrogen bond; O–H···N (d[H···N] = 2.80 – 2.98 Å), formation of $R_2^3(11)$ motif view along *a* axis. The hydrogen bonds play an important role in the crystal structure and may potentially affect the stability of the supramolecular structure. The hydrogen bonds network of tricyclic acyclovir structure as shown in Figure 5.4 and Table 5.2.
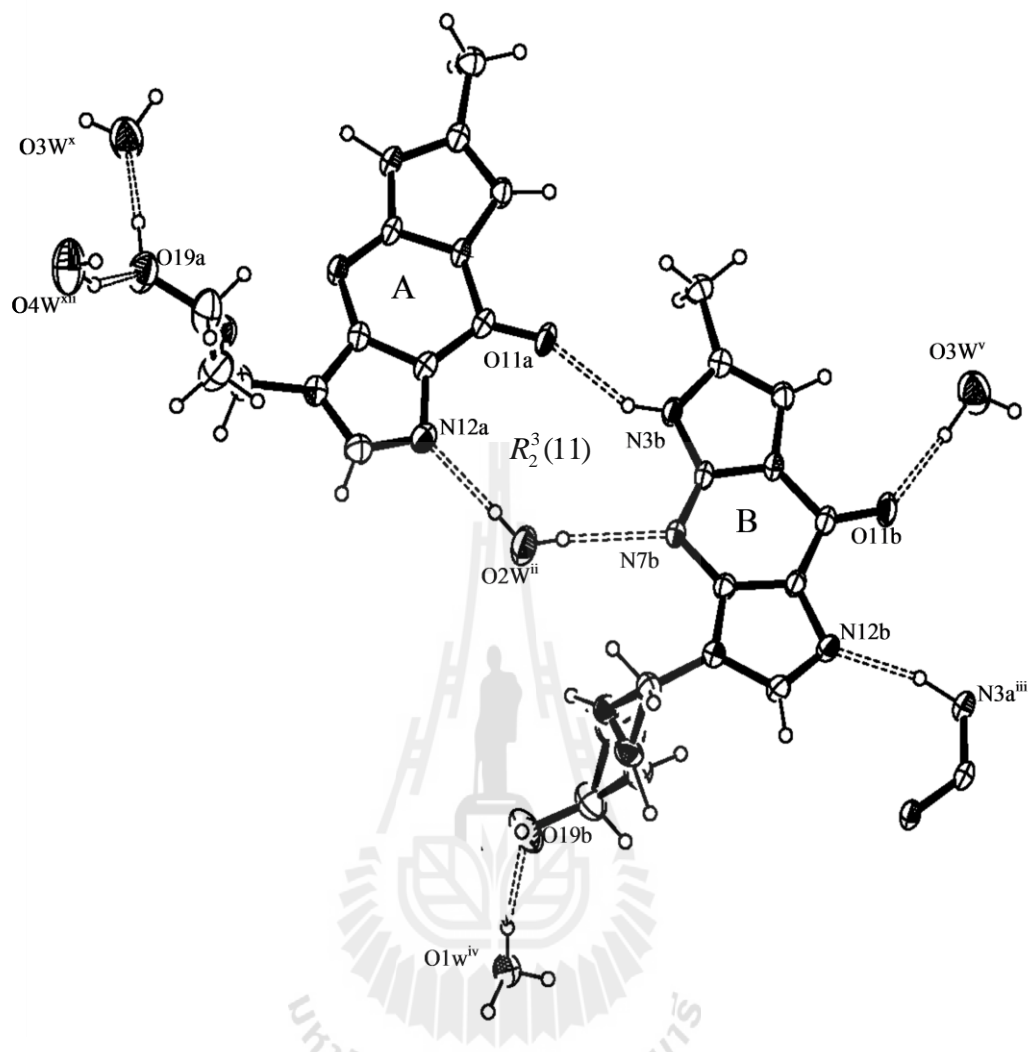
Figure 5.4 The hydrogen bond network of tricyclic acyclovir viewed along the *a* axis.

Table 5.2 Hydrogen bonding geometry (Å, °) [a] of tricyclic acyclovir.

D–H···A	d[D–H] (Å)	d[H···A] (Å)	d[D···A] (Å)	∠[D–H···A] (°)
N3a–H3a···N12b[i]	0.89(0.98)	1.98(1.85)	2.803(2.800)	153.2(163.4)
N3b–H3b···O11a	0.89(0.86)	1.92(1.98)	2.748(2.747)	153.0(148)
O19b[v]–H19b[v]···O19b[xi]	0.82(0.82)	1.87(2.02)	2.644(2.671)	156.4(135)

Symmetry codes: (i) = 1+x, 1+y, z; (ii) = -1-x, 1-y, 2-z; (iii) = -x, 1-y, 1-z; (iv) = -x, 2-y, 1-z; (v) = -x, 1-y, 2-z; (vi) = -1-x, 1-y, 1-z; (viii) = 1-x, 1-y, -z; (ix) = -x, 1-y, 1-z; (xi) = -1+x, y, z; (xii) = -x, 1-y, -z.

[a] The distance values of original report are given in parentheses.

Table 5.2 (Continued).

D–H···A	d[D–H] (Å)	d[H···A] (Å)	d[D···A] (Å)	∠[D–H···A] (°)
O19a–H19a···O3W[iv]	0.82(1.02)	1.95(1.71)	2.738(2.731)	161.4(177)
O1W–H1Wb···O19b[v]	0.82(0.89)	2.03(1.84)	2.709(2.706)	140.2(164)
O2W–H2Wa···N12a[ii]	0.82(0.84)	1.98(1.96)	2.793(2.797)	172.8(177)
O2W–H2Wb···N7b[iii]	0.82(0.78)	2.17(2.21)	2.982(2.982)	170.3(173)
O3W–H3Wb···O11b[iii]	0.847(0.97)	1.98(1.85)	2.82(2.8219)	171.8(176)
O4W–H4Wb···O19a[vi]	0.845(0.82)	1.90(2.00)	2.73(2.738)	171.1(149)
O1W–H1Wa···O2W	0.823(1.00)	1.87(1.69)	2.689(2.679)	177.0(170)
O1W–H1Wc···O1W[viii]	0.82(0.82)	1.99(1.99)	2.806(2.808)	171.5(175)
O3W–H3Wa···O4W	0.84(0.84)	1.92(1.94)	2.748(2.751)	165.2(163)
O4W–H4Wa···O1W	0.845(0.77)	2.019(2.11)	2.848(2.852)	166.8(163)
O19b[xi]–H19c[xi]···O1W[xii]	0.820	1.892	2.709	176.2

Symmetry codes: (i) = 1+x, 1+y, z; (ii) = -1-x, 1-y, 2-z; (iii) = -x, 1-y, 1-z; (iv) = -x, 2-y, 1-z; (v) = -x, 1-y, 2-z; (vi) = -1-x, 1-y, 1-z; (viii) = 1-x, 1-y, -z; (ix) = -x, 1-y, 1-z; (xi) = -1+x, y, z; (xii) = -x, 1-y, -z.

[a] The distance values of original report are given in parentheses.

One asymmetric unit of the tricyclic acyclovir structure contains two tricyclic acyclovir molecules and four water molecules. One hydrogen atom of one water molecule is disordered. The ordered OH of this water molecule is connected with the three independent ordered water molecules. These four water molecules, one asymmetric unit of water, connect to another four water molecules across an inversion center through one of the disordered hydrogen atoms (d[O···O] = 2.81 Å]) forming an $(H_2O)_8$ cluster. The water cluster, consisting of four independent solvent water molecules forming an $(H_2O)_8$ cluster through a strong hydrogen bond (d[O··· O] =

2.81 Å) between two water molecules across an inversion center, and their relationship to previously unreported disorder. The water molecules form an $(H_2O)_8$ cluster across the inversion center, the disordered hydrogen atom violates the local inversion symmetry, and the disordered hydrogen atom on the hydrogen bond acceptor water must be in the alternate position as shown in Figure 5.5.

(a)

(b)

Figure 5.5 Positions of hydrogen atoms in (a) the concerted O···O bonded chain (two unit cells of structure) and (b) alternate disorder positions of hydrogen atoms.

Three of the four potential hydrogen bonds for the disordered water molecules are to other water molecules, and the mutually exclusive hydrogen atom positions give rise to the concerted supramolecular structure across the inversion center (pseudo inversion center in an order chain). The fourth potential hydrogen bond position of O1w is used to interact with two equivalent molecules of tricyclic acyclovir, but the location of the hydroxyl hydrogen atoms of their side chains are determined by the positions of the disordered water hydrogen atoms and are therefore also not inversion related. The four hydrogen bonds, as well as the local relationship among these two water molecules and two tricyclic acyclovir hydroxyl groups are shown in the left half of Figure 5.5(a). The alternative positions for the disordered hydrogen atoms are shown in Figure 5.5(b). The hydroxyl groups in turn relate to equivalent groups on the next molecules through a strong hydrogen bond ($d[O \cdots O] = 2.67$ Å) across another (pseudo) inversion center, requiring a previously unreported statistical disordering of the hydroxyl hydrogen atom as shown in the center of Figure 5.5. This chain includes only water and one of the two crystallographically independent tricyclic acyclovir molecules.

Both tricyclic acyclovir molecules participate via strong $O-H \cdots O$ water-water and water-drug and $O-H \cdots N$ water-drug interactions in a sheet structure for which the hydrogen disorder is irrelevant. The sheet is best viewed in the context of the $(H_2O)_8$ cluster as indicated in Figure 5.6 with solid and dot bonds. The sheets and chains intersect through the water clusters to create a 3D hydrogen bonded network.

The relatively large number of water molecules form localized $(H_2O)_8$ clusters about inversion centers. The supramolecular structure exhibits an infinite 1–D hydrogen-bonded chain displaying an unusual disorder of an elaborate concerted unit

containing pair-wise alternating tricyclic acyclovir molecules and water molecules across the inversion center (pseudo inversion center in an order chain). The previously unreported statistical disordering of the hydroxyl hydrogen atoms of one of the two crystallographically independent tricyclic acyclovir molecules lies about the second (pseudo) inversion center. The third notable feature is a 2–D sheet structure utilizing all four independent water molecules and both independent tricyclic acyclovir molecules. The sheets and chains intersect through the water clusters to create the 3–D hydrogen-bonded network.
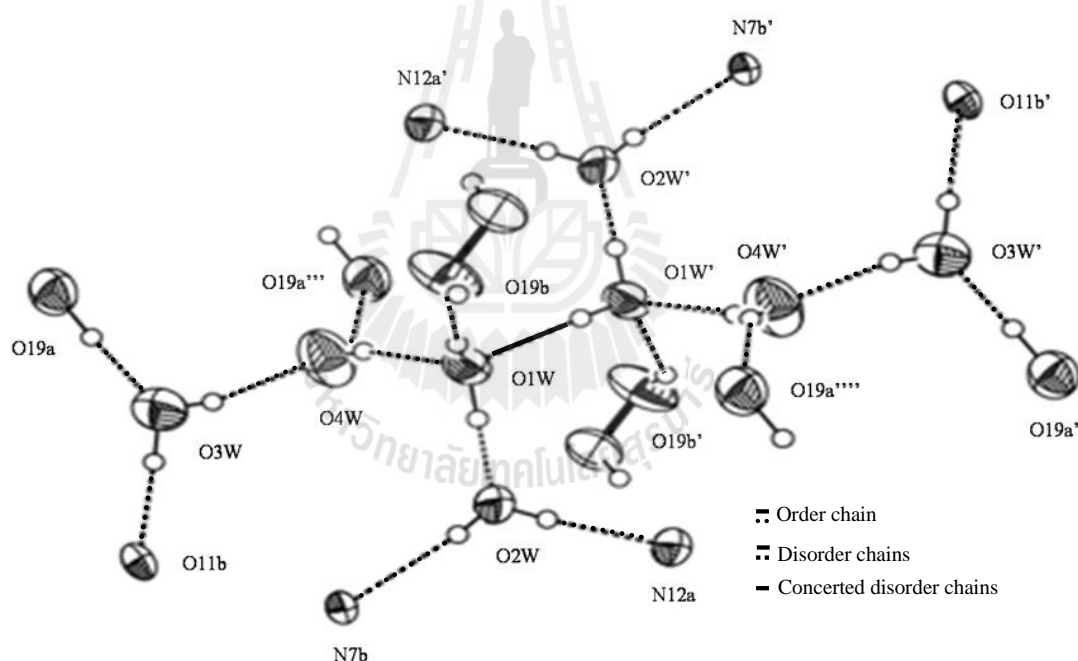
Figure 5.6 Environment about the water cluster. The solid lines indicate the concerted (disorder) O···O bonded chain direction and the solid and dot lines indicate the sheet made up of O···O and N···O hydrogen bonds.

Electron Density Map

The F_o map of the two bound waters (O1W$\cdots$O1W$'$) at each water molecule bound to hydroxyl group of the (2-hydroxyethoxy)methyl side chain of one tricyclic acyclovir molecule at 1.5 Å, view plane = 0.0 are shown the two hydrogen positions between bound site which expected to see and more clearly at 1.5 Å, view plane = 0.0,−0.1, −0.2 and −0.3 as shown three hydrogen at each water position that reported by previously (Suwińska, Golankiewicz, and Zielenkiewicz, 2001), and two hydrogen atoms at hydroxyl positions with unreported. The characteristic disorder positions by using F_o−F_c maps with the relevant hydrogen atoms removed. Surprising herein, the F_o−F_c maps showed continuous chain consist of $\cdot\cdot$[OW−OW$'$−O19B−O19B$'$]$\cdot\cdot$ which obtain one hydrogen position between bound area of water−water and water−tricyclic acyclovir while got two hydrogen positions between bound hydroxyl−hydroxyl area. The illustrate that the bound water molecules in the tricyclic acyclovir structure are disordered while tricyclic acyclovir structure has a local maximum, the fact that the water region closely neighboring regions to make continuous chain which the side chain may bind the water tightly but itself be moving enough to make the hydrogen atoms of water molecule (O1W) and hydroxyl group (O19B) appear disordered (Saenger, Betzel, Zabel, Brown, Hingerty, Lesyng, and Mason, 1985). The F_o and F_o−F_c maps of water system with hydrogen atoms at 1.5 Å, 2.5 σ as illustrated in Figures 5.7 and 5.8.
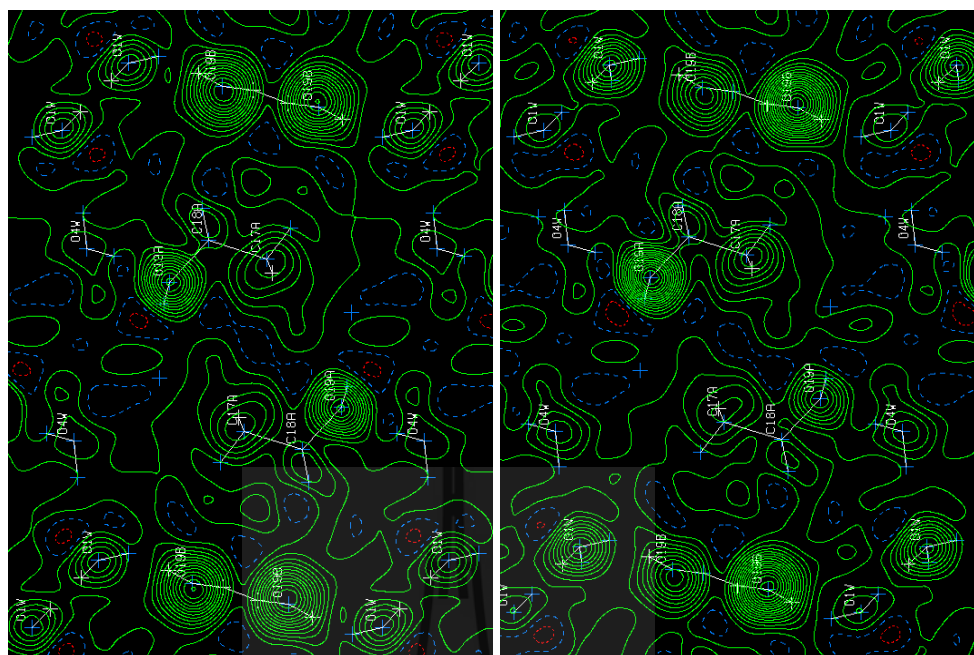
(a)   (b)
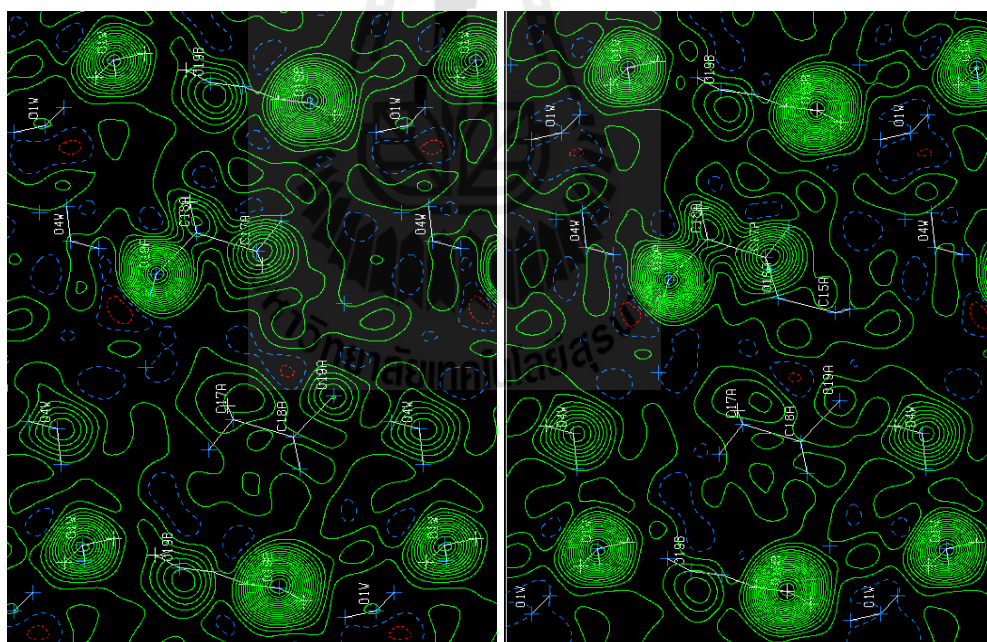
(c)   (d)

Figure 5.7 The F_o maps of water system with hydrogen atoms at 1.5 Å, 2.5 σ, used *ins* file, view is perpendicular to water region axis. (a) Plane = 0.0, (b) Plane = −0.1, (c) Plane = −0.2, (d) Plane = −0.3. The F_o maps were generated with *PLATON*.
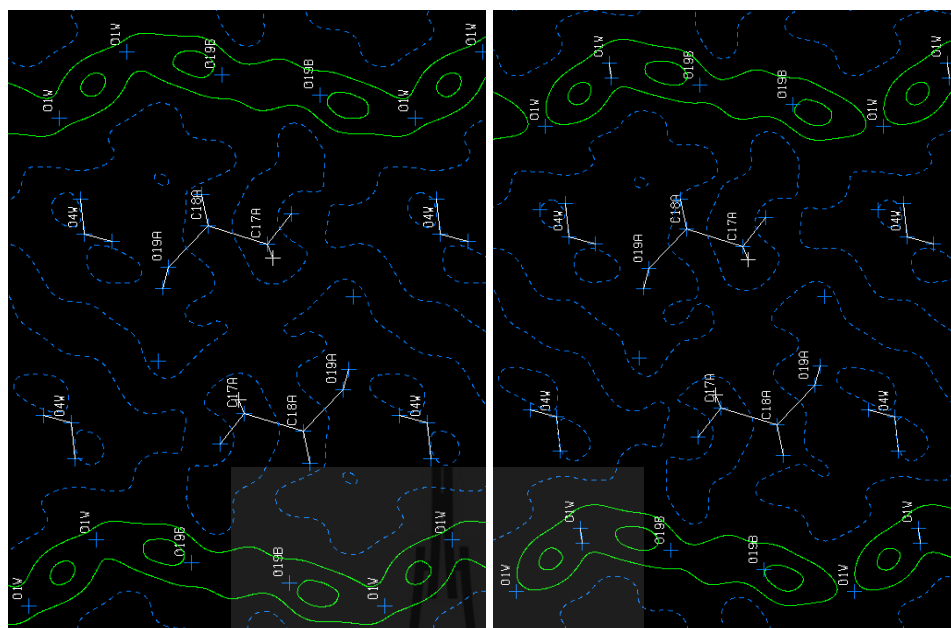
(a) (b)
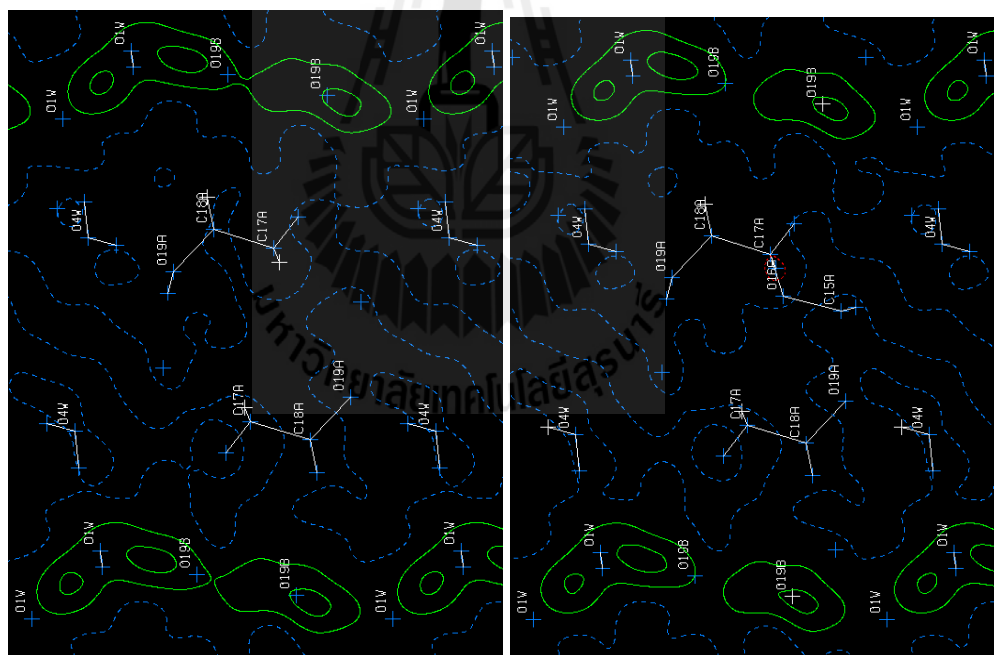
(c) (d)

Figure 5.8 The (F_o-F_c) maps of water systems without hydrogen atoms at 1.5 Å, 2.5 σ, used *ins* file, view is perpendicular to water region axis. a) Plane = 0.0, b) Plane = − 0.1, c) Plane = −0.2 and d) Plane = −0.3. The (F_o-F_c) maps were generated with *PLATON.*

The nonbonded contacts surrounding the regions exhibiting side chain disorder are shown in Figure 5.9 and Table 5.3.

(a)   (b)
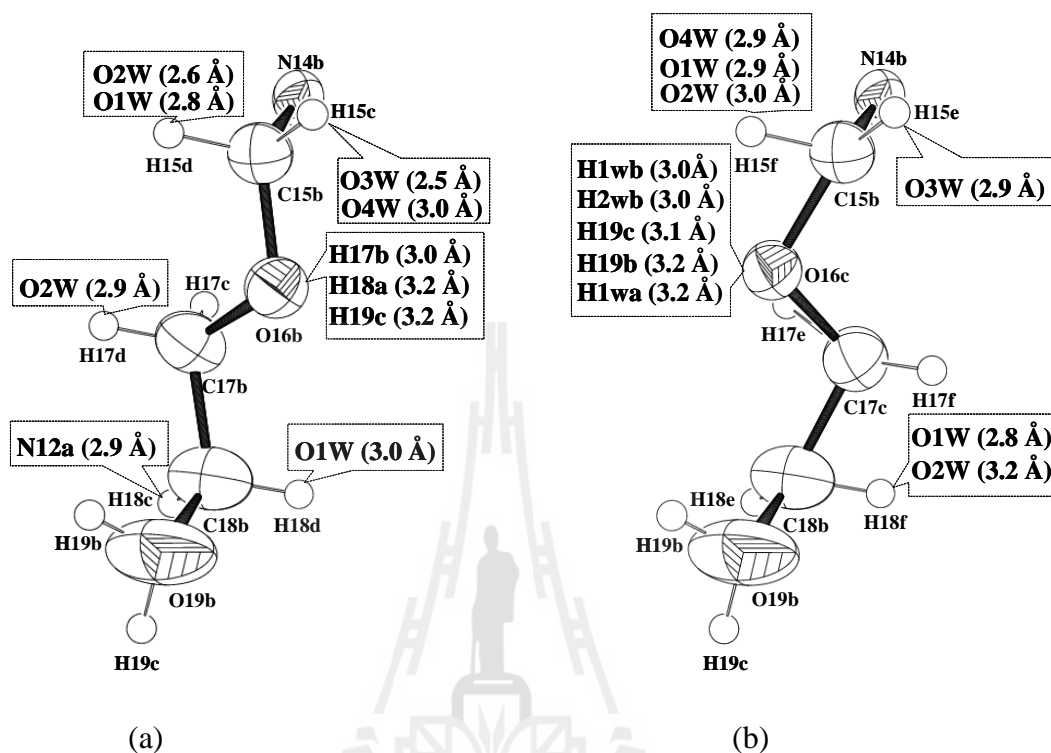
Figure 5.9 Intermolecular nonbonded contacts in the major and minor components of the side chain disorder (calculated by *ORTEP*-III to a search radius of 3.2 Å).

The N14b contacts for both components are the essentially same. The C−H···O contacts to water molecules at C15b strongly favor the major component, as do contacts to the A molecule at O16b (no A molecule contacts to O16c), while weaker contacts to O16c (to water) and to disordered hydrogen atoms at C18b favor the minor component. In addition the disordered water hydrogen position, H1wb, favors the minor component through a C−H···O hydrogen bond contact. There are no nonbonded contacts at C17c of the minor component, but one C−H···O contact to C17b of the major component. Taken together, these interactions are consistent with the preference for the major component as seen in the refinement of the structure.

Table 5.3 Intermolecular nonbonded contact for the major and minor components.

D–H···A	d[D–H]	d[H···A]	d[D···A]	∠[D–H···A]
	(Å)	(Å)	(Å)	(°)
Major component				
C15b–H15c···O3W[ii]	0.970	2.470	3.360	152.6
C15b–H15c···O4W[ii]	0.970	2.994	3.652	126.2
C15b–H15d···O2W[ii]	0.970	2.624	3.565	163.2
C15b–H15d···O1W[ii]	0.970	2.833	3.555	131.9
C17a[ii]–H17b[ii]···O16b	0.929	3.026	3.501	113.4
C18a[ii]–H18a[ii]···O16b	0.930	3.172	3.765	123.4
C17b–H17d···O2W[ii]	0.970	2.934	3.763	144.0
C17b–H17d···O19b[iv]	0.970	3.189	3.562	104.7
C18b–H18c···N12a[vi]	0.970	2.914	3.864	166.9
C18b–H18d···O1W[i]	0.971	2.987	3.705	131.6
Minor component				
C15c–H15e···O3W[ii]	0.969	2.912	3.360	109.4
C15c–H15f···O4W[iii]	0.970	2.909	3.652	134.2
C15c–H15f···O1W[iii]	0.970	2.921	3.555	124.0
C15c–H15f···O2W[iii]	0.970	3.040	3.565	115.3
C15c–H15f···O3W[iii]	0.970	3.095	3.360	97.4
O1W[ii]–H1Wa[ii]···O16c	0.820	3.146	3.418	102.4
O1W[ii]–H1Wb[ii]···O16c	0.830	2.985	3.418	114.9
O2W[ii]–H2Wb[ii]···O16c	0.826	3.072	3.238	94.2
O19b[iii]–H19b[iii]···O16c	0.820	3.156	3.300	92.8
O19b[iii]–H19c[iii]···O16c	0.820	3.091	3.300	97.5
C18b–H18f···O1W[ii]	0.970	2.790	3.705	157.4
C18b–H18f···O1W[v]	0.970	3.051	3.429	104.8
C18b–H18f···O2W[ii]	0.970	3.169	4.026	148.2

Symmetry codes: (i) = 1-x, 2-y, 2-z; (ii) = 1+x, 1+y, 1+z; (iii) = 1+x, y, 1+z; (iv) = x, 1+y, 1+z;

(v) = -x, 2-y, 2-z; (vi) = -x, 1-y, 2-z. [a] The distance values of original report are given in parentheses.

5.4 Conclusion

Tricyclic acyclovir, 3-[(2-hydroxyethoxy)-methyl]-6-methyl-3*H*-imidazolo[1,2-*a*]purin-9(5*H*)-one, has been reported as the dihydrate, $C_{11}H_{13}N_5O_3 \cdot 2H_2O$ and the complex hydrogen bond network of water and tricyclic acyclovir molecules suggested to be related to the solvation of the molecules in solution (Suwinska *et al*., 2001). The $Z = 2$ structure contains four independent solvent water molecules, forming an $(H_2O)_8$ cluster through a strong hydrogen bond (d[O···O] = 2.81 Å) between two water molecules across an inversion center. Three of the independent water molecules are ordered while the inversion center requires one hydrogen atom in the fourth to be statistically disordered. The second disordered hydrogen position is a strong donor to the 2-hydroxyl group of the side chain of one independent molecule of tricyclic acyclovir. The hydroxyl group in turn relates to an equivalent group on the next molecule through a strong hydrogen bond (d[O···O] = 2.67 Å) across another inversion center requiring statistical disordering of that hydroxyl hydrogen atom. The result of the hydrogen atom disorders is concerted chains propagating in opposite directions, which differ only in the placement of the hydrogen atoms. The $(H_2O)_8$ clusters are essentially perpendicular to the chains just described and create a 2D network with both independent tricyclic acyclovir molecules, using strong O–H···O water-water and water-drug, and O–H···N water-drug interactions. The supramolecular structure of tricyclic acyclovir is held together by extensive strong hydrogen bond interactions among the tricyclic acyclovir and water molecules extending in all directions.

The computational analysis of the 2-hydroxyethoxy-methyl side chain disorder of tricyclic acyclovir provides a rationalization of the nonstatistical disorder

previously reported. Intermolecular interaction of the 2-hydroxyethoxy-methyl side chain disorder in the (2-hydroxyethoxy)-methyl side chain strong favors contact to major component through supramolecular features of tricyclic acyclovir, implying that the competition of the C−H⋯O hydrogen bond interactions determines the packing of these disordered components.

5.5 References

Balzarini, J., Ostrowski, T., Goslinski, T. de Clercq, E., and Golankiewicz, B. (2002). Pronounced cytostatic activity and bystander effect of a novel series of fluorescent tricyclic acyclovir and ganciclovir derivatives in herpes simplex virus thymidine kinase gene-transduced tumor cell lines. **Gene Therapy**. 9: 1173–1182.

Boryski, J., Golankiewicz, B., and de Clerk, E. (1988). Synthesis and antiviral activity of novel N-substituted derivatives of acyclovir. **Journal of Medicinal Chemistry**. 31(7): 1351–1355.

Boryski, J., Golankiewicz, B., and de Clerk, E. (1991). Synthesis and antiviral activity of 3-substituted derivatives of 3,9-dihydro-9-oxo-5H-imidazo[1,2-a]purines, tricyclic analogs of acyclovir and ganciclovir. **Journal of Medicinal Chemistry**. 34(8): 2380–2383.

Bryn, S. R. (1982). Solid state chemistry of drugs. **Academic Press**, New York, 6–9.

Burnett, M. N. and Johnson, C. K. (1996). *ORTEP*-III: Oak ridge thermal ellipsoid plot program for crystal structure illustration, Report ORNL-6895, **Oak Ridge National Laboratory**. Tennessee, USA.

Chatkon, A. and Haller, K. J. (2002). 3rd National graduate student symposium, **Suranaree University of Technology**, Nakhon Ratchasima.

Etter, M. C., MacDonald, J. C., and Bernstein, J. (1990). Graph-set analysis of hydrogen-bond patterns in organic crystals. **Acta Crystallographica Section B**. 46: 256–262.

Fung, H.-L. and Nealon, T. (1974). Solvent effect on comparative dissolution of pharmaceutical solvates. **Chemical and Pharmaceutical Bulletin**. 22: 454‒458.

Grell, J., Bernstein, J., and Tinhofer, G. 1999. Graph set analysis of hydrogen bond Patterns. Some material concepts **Technical University of München**, Fak. f. Math, Report TUM M9908.

Haller, K. J. and Enemark, J. H. (1978). Structure chemistry of the $\{CoNO\}^8$ group. The structure of N,N′-ethylenebis(salicylideneiminato)nitrosylcobalt(II), Co-(NO)(salen). **Inorganica Chemica Acta**. 17(12): 3552–3558.

Moss, G. P. (1996). Basic terminology of stereochemistry (IUPAC Recommendations 1996). **Pure and Applied Chemistry**. 68: 2193–2220.

Levene P. A., Whitmore, F. C., and Hollingshead, J. P. (1943). **Organic Syntheses, Collective**. 2: 88.

Meepripruek, M. and Haller, K. J. (2010). Solvation in 3-[(2-Hydroxyethoxy)-methyl]-6-methyl-3*H*-imidazolo[1,2-*a*]Purin-9(5*H*)-one Dihydrate; $C_{11}H_{13}N_5O_3 \cdot 2H_2O$. **Proceedings of ANSCSE14**. Mae Fah Luang University, Chiang Rai, Thailand, p. 315.

Puntharod, R. and Haller, K. J. (2005). Preparation and characterization of $NiCl(NO)(PPh_3)_2$. **Acta Crystallographica Section A**. 61: C306.

Saenger, W., Betzel, Ch., Zabel, V., Brown, G.M., Hingerty, B.E., Lesyng, B., and Mason, S.A. (1985). Hydrogen bonding patterns and dynamics in the hydration of biological macromolecules. **Proceedings of the International Symposium on Biomolecular Structure and interactions. Supplement to Journal of Biosciences**. 8: 437–450.

Sheldrick, G.M. (1997). *SHELXL*-97 Program for the solution and refinement of crystal structures. **University of Göttingen**. Germany.

Steiner, T. (2002). The hydrogen bond in the solid state**. Angewandte Chemie International Edition**. 41: 48–76.

Suwińska, K., Golankiewicz, B., and Zielenkiewicz, W. (2001). Water molecules in the crystal structure of tricyclic acyclovir. **Acta Crystallographica Section C**. 57: 767–769.

Thanki, N., Thornton, J. M., and Goodfellow, J. M. (1988). Distributions of water around amino acid residues in proteins. **Journal of Molecular Biology**. 202(3): 637–57.

Werner, M. (2000). Crystal structure determination. **Marburg University**, Germany, 142–147.

Wenger, M. and Bernstein, J. (2006). Designing a cocrystal of γ-amino butyric acid. **Angewandte Chemie International Edition**. 45: 7966–7769.

CHAPTER VI

CONCLUSIONS

6.1 Conclusions

Crystal screening by a solvent based method using acyclovir separated from acyclovir drug provided a solid dihydrate form of acyclovir for which the structure has not been reported to the structure database. The dihydrate, $C_8H_{11}N_5O_3 \cdot 2H_2O$, crystallized as thin plates in the triclinic space group $P\bar{1}$, with cell dimensions, $a = 6.8996(6)$ Å, $b = 11.4170(9)$ Å, $c = 15.0806(13)$ Å, $\alpha = 82.595(7)°$, $\beta = 82.395(7)°$, $\gamma = 89.368(7)°$, $V = 1167.65(17)$ Å^3 at 293(2) K. The crystal lattice contains two crystallographically independent acyclovir molecules and four water molecules per asymmetric unit. The guanine ring systems of molecules A and B are approximately parallel with a dihedral angle of 1.600(1)°. The guanine bases of the two independent molecules join via C–H⋯O, N–H⋯N, and N–H⋯O hydrogen bonds into 1–D infinite wave-like chains. The chains interconnect to create 2–D sheet networks perpendicular to the a axis via bifurcated hydrogen bonds, C–H⋯O to the side chain of one of the independent acyclovir molecules. The adjacent 2–D sheet networks connect together to create 3–D networks through the guanine stacking with average distances of 3.2950(13) Å for A/B and 3.3925(18) Å for B/A. The guanine moieties stack with weak   C–H⋯π, N–H⋯π, and carbonyl-carbonyl dipole interactions in slipped parallel motif type. The glycosidic side chain is partially folded and almost perpendicular to the guanine ring, 90.2–93.3° and exhibits eclipsed conformation at

O2–C7–C8–O3 in both independent molecules. The water molecules form infinite serpentine chains of water molecules, $\cdot[\cdot O2–H\cdots O1–H\cdots O3–H\cdots O4–H\cdot]_\infty$, that propagate through channels in the network parallel to the a axis. The chains consist of alternating $R_5^5(10)$ motifs containing one oxygen atom of a carbonyl group and one hydroxyl group, respectively, to make stable pentagonal forms with average angles near the ideal pentagonal value of 108°. The F_o electron density maps at 1.5 Å resolution with water hydrogen atoms removed show rational positions for ordered water molecules in the acyclovir dihydrate structure.

The acyclovir derivative, tricyclic acyclovir, $C_{11}H_{13}N_5O_3$, has been reported as the dihydrate. The structure has been rerefined based on the literature data and an improved model describing additional hydrogen atom disorder is presented. Preliminary analysis of the hydrogen bonding indicated that the published structure did not completely model the disorder of the hydrogen bonded region. The new model induces a disordered hydrogen atom at O19B, modeled with a site occupancy factor of 0.5, and the side chain disorder at O16 and C17 with a refined site occupancy of 0.738(5) for major component and 0.262(5) for minor component. Discrepancy indices for the new refinement are $R[F^2>2\sigma(F^2)] = 0.056$ and wR (all of F^2 data) = 0.142. The bond distance in the water molecules is more ideal than those reported in the original report. The central hydrogen bond of the $(H_2O)_8$, cluster ($d[O\cdots O] = 2.81$ Å) is between two water molecules across an inversion center, requiring one hydrogen atom to be disordered. The second disordered hydrogen position is a strong donor to the 2-hydroxyl group of the side chain of one independent molecule of tricyclic acyclovir which in turn requires an equivalent disorder of the hydroxyl hydrogen atom through a strong hydrogen bond ($d[O\cdots O] = 2.67$ Å) across another inversion center.

The result of these hydrogen atom disorders is concerted chains propagating in opposite directions, which differ only in the placement of the hydrogen atoms. The region containing the disordered hydrogen atoms was examined in F_o–F_c maps which show the expected pattern of stronger and weaker peaks consistent with the relative occupancy factors. Furthermore, the peaks corresponding to the disordered positions extend along the respective O···O directions. The $(H_2O)_8$ clusters are essentially perpendicular to the chains just described and create a 2–D network with both independent tricyclic acyclovir molecules using strong O–H···O water-water and water-drug, and O–H···N water-drug interactions. The supramolecular structure of tricyclic acyclovir is held together by extensive, strong hydrogen bond interactions among the tricyclic acyclovir and water molecules extending in all directions to create a 3–D network. Intermolecular nonbonded contacts in the major and minor components of the side chain disorder at C15 and C17 strongly favor the major occupancy positions. Weaker contacts at C18 favor the minor component. The contacts at O16b and O16c seem approximately the same, implying that the competition of the C–H···O hydrogen bond interactions determines the packing of these disordered components. The intermolecular nonbonded contacts in the major and minor components of the side chain disorder are similar to those of the original report.

6.2 Suggestions for Further Work

The results of the screening experiments by the solution based method indicate many different crystalline materials form at the same time. It is expected that some of them may be new crystalline forms of the API, perhaps polymorphs or solvates. The

new acyclovir and tricyclic acyclovir materials should be characterized by using FT–IR, PXRD, melting point techniques, and single crystal X-ray crystallography or other techniques that are useful for evaluating the structure.

Further exploration for multicomponent materials of acyclovir with other compounds such as those classified generally recognized as safe (GRAS) is expected to provide additional interesting supramolecular networks. Particularly, in the case of similar new components or a large number of components, the solid materials thus isolated may provide insights that are useful for future pharmaceutical development.
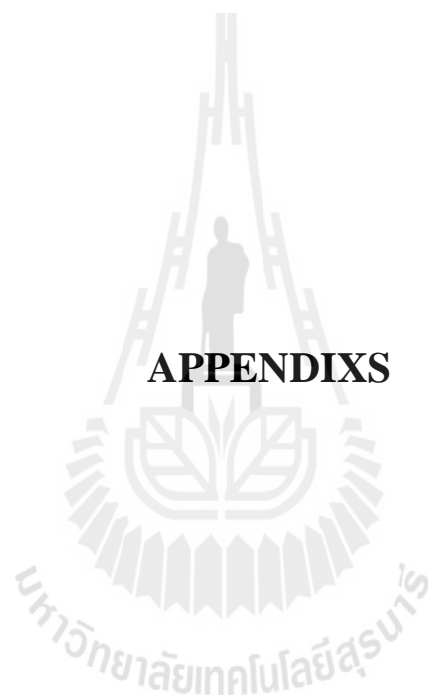
APPENDIXS

APPENDIX A

SUPPORTING INFORMATION CHAPTER III

Table A1 Fractional triclinic coordinates and equivalent atomic displacement parameters[a] ($Å^2$) for acyclovir, $C_8H_{11}N_5O_3 \cdot 2H_2O$.

Atoms	X	Y	Z	U_{eq}
Molecule A				
C1A	0.3713(3)	0.9390(16)	0.3444(12)	0.275(2)
C2A	0.4004(3)	0.7568(16)	0.3075(12)	0. 257(2)
C3A	0.3405(3)	0.7025(16)	0.3939(12)	0.273(2)
C4A	0.2846(3)	0.7739(16)	0.4634(12)	0.284(2)
C5A	0.3945(3)	0.5636(16)	0.3125(12)	0.336(2)
C6A	0.4805(3)	0.6800(16)	0.1571(12)	0.339(2)
C7A	0.1863(3)	0.6037(16)	0.1219(12)	0.414(3)
C8A	0.0071(3)	0.6388(16)	0.0792(12)	0.464(3)
N1A	0.3060(3)	0.8938(16)	0.4315(12)	0.288(19)
N2A	0.3789(3)	1.0572(16)	0.3260(12)	0.398(2)
N3A	0.4207(3)	0.8735(16)	0.2786(12)	0.280(19)
N4A	0.3375(3)	0.5808(16)	0.3960(12)	0.328(2)
N5A	0.4355(3)	0.6669(16)	0.2551(12)	0.297(2)
O1A	0.2212(3)	0.7419(16)	0.5432(12)	0.405(2)
O2A	0.3125(3)	0.7042(16)	0.1146(12)	0.353(19)
O3A	0.0569(3)	0.6638(16)	-0.0154(12)	0.557(3)
H1a	0.2749	0.9449	0.4709	0.320
H2a	0.4203	1.0941	0.2648	0.440
H2b	0.3430	1.1058	0.3737	0.440
H3a	-0.0399	0.6876	-0.0383	0.670
H5a	0.4069	0.4851	0.2927	0.370
H6a	0.5744	0.7438	0.1376	0.370
H6b	0.5399	0.6080	0.1390	0.370
H7a	0.1497	0.5734	0.1849	0.460
H7b	0.2542	0.5418	0.0920	0.460
H8a	-0.0886	0.5752	0.0931	0.510
H8b	-0.0504	0.7080	0.1031	0.510

[a] The standard deviations of the least significant digits are given in parentheses.

Table A1 (Continued).

Atoms	X	Y	Z	U_{eq}
Molecule B				
C1B	-0.1538(3)	0.6049(16)	0.3871(12)	0.284(2)
C2B	-0.1233(3)	0.7989(16)	0.3514(12)	0.259(2)
C3B	-0.1937(3)	0.8246(16)	0.4369(12)	0.269(2)
C4B	-0.2447(3)	0.7297(16)	0.5061(12)	0.279(2)
C5B	-0.1215(3)	0.9905(16)	0.3574(12)	0.321(2)
C6B	0.0091(3)	0.9224(16)	0.2062(12)	0.331(2)
C7B	-0.1612(3)	1.0568(16)	0.1114(12)	0.435(3)
C8B	-0.3360(3)	1.0613(16)	0.0624(12)	0.454(3)
N1B	-0.2205(3)	0.6211(16)	0.4744(12)	0.296(2)
N2B	-0.1425(3)	0.4932(16)	0.3690(12)	0.406(3)
N3B	-0.1020(3)	0.6925(16)	0.3217(12)	0.292(19)
N4B	-0.1921(3)	0.9457(16)	0.4395(12)	0.319(2)
N5B	-0.0756(3)	0.9059(16)	0.3006(12)	0.291(2)
O1B	-0.3042(3)	0.7349(16)	0.5872(12)	0.373(2)
O2B	-0.1343(3)	0.9370(16)	0.1479(12)	0.376(2)
O3B	-0.5148 (3)	1.0451(16)	0.1216(12)	0.448(2)
H1b	-0.2505	0.5569	0.5138	0.330
H2c	-0.1004	0.4779	0.3133	0.450
H2d	-0.1771	0.4341	0.4127	0.450
H3b	-0.5227	0.9646	0.1519	0.490
H5b	-0.1031	1.0754	0.3383	0.350
H6c	0.0940	0.9913	0.1950	0.360
H6d	0.0883	0.8543	0.1934	0.360
H7c	-0.0464	1.0853	0.0703	0.480
H7d	-0.1813	1.1063	0.1594	0.480
H8c	-0.3383	1.1371	0.0252	0.500
H8d	-0.3247	1.0004	0.0227	0.500
Water molecules				
O1W	0.5875(3)	0.3919(16)	0.1112(12)	0.593(3)
O2W	0.6511(3)	0.2791(16)	0.2751(12)	0.628(3)
O3W	0.2701(3)	0.2573(16)	0.0985(12)	0.562(3)
O4W	0.0598(3)	0.3056(16)	0.2660 (12)	0.719(4)
H1WA	0.6022	0.3606	0.1648	0.840(2)
H1WB	0.6963	0.3744	0.0769	0.840(2)
H2WA	0.7758	0.2805	0.2772	0.840(2)
H2WB	0.5976	0.0.2802	0.3299	0.840(2)
H3WA	0.3126	0.1865	0.1024	0.840(2)
H3WB	0.3716	0.3051	0.0938	0.840(2)
H4WA	0.1238	0.2865	0.2192	0.840(2)
H4WB	0.1276	0.2861	0.3121	0.840(2)

[a] The standard deviations of the least significant digits are given in parentheses.

Table A2 Least-squares mean plane[a] and deviations (Å) from the planes of acyclovir:

$C_8H_{11}N_5O_3 \cdot 2H_2O$.

Plane 1: Plane of molecule A (RMSD of fitted atoms = 0.0134 Å)
Plane 1: Plane of molecule B (RMSD of fitted atoms = 0.0169 Å)

Molecule A; 6.7591(5) x + 0.0433(28) y + 4.8975(47) z = 4.2359(26)

Molecule B; 6.7048(6) x - 0.1103(28) y + 5.3683(49) z = 0.9821(34)

Atoms	Molecule A	Molecule B
C1	0.0010(8)	−0.0018(8)
N1	−0.0152(8)	0.0184(8)
C2	0.0086(9)	−0.0110(9)
C3	0.0251(10)	−0.0264(10)
N3	0.0093(8)	−0.0155(8)
C4	−0.0098(8)	0.0137(8)
N4	0.0094(8)	−0.0150(8)
C5	−0.0141(9)	0.0129(9)
N5	−0.0143(8)	0.0246(8)
N2	−0.0292(15)	−0.0104(15)
O1[b]	−0.0484(14)	0.0495(14)
C6[b]	−0.1896(16)	0.0831(15)

[a] The standard deviations of the least significant digits are given in parentheses.
[b] Atom not used to define plane.

APPENDIX B

SUPPORTING INFORMATION CHAPTER IV

Table B1 Fraction triclinic coordinates and equivalent atomic displacement

parameters[a] (Å^2) for tricyclic acyclovir, $C_{11}H_{13}N_5O_3 \cdot 2H_2O$.

Atoms	X	Y	Z	U_{eq}
Molecule A				
C1A	-0.5280(3)	0.1796(2)	0.3236(16)	0.0510(6)
H1A1	-0.6394	0.1684	0.3231	0.0770
H1A2	-0.4679	0.1077	0.3195	0.0770
H1A3	-0.4817	0.2424	0.2703	0.0770
C2A	-0.5201(2)	0.2107(18)	0.4129(15)	0.0389(5)
N3A	-0.5959(2)	0.1406(15)	0.4999(12)	0.0397(4)
H3A	-0.6720(3)	0.0750(2)	0.5153(15)	0.0480
C4A	-0.5713(2)	0.1840(16)	0.5706(14)	0.0341(4)
N5A	-0.4756(19)	0.2842(14)	0.5284(11)	0.0344(4)
C6A	-0.4467(2)	0.2994(19)	0.4296(15)	0.0400(5)
H6A	-0.3872	0.3603	0.3839	0.0480
N7A	-0.6284(2)	0.1418(14)	0.6621(12)	0.0375(4)
C8A	-0.5781(2)	0.2090(17)	0.7106(14)	0.0357(4)
C9A	-0.4780(2)	0.3084(18)	0.6773(15)	0.0378(5)
C10A	-0.4177(2)	0.3533(17)	0.5790(15)	0.0374(5)
O11A	-0.3274(18)	0.4379(13)	0.5352(11)	0.0501(4)
N12A	-0.4558(2)	0.34980(17)	0.7529(13)	0.0479(5)
C13A	-0.5403(3)	0.2783(2)	0.8274(17)	0.0502(6)
H13A	-0.5474	0.2858	0.8888	0.060
N14A	-0.6181(2)	0.1910(16)	0.8079(12)	0.0430(4)
C15A	-0.7248(3)	0.0979(2)	0.8722(17)	0.0552(6)
H15A	-0.6990	0.0247	0.8522	0.0660
H15B	-0.7055	0.0854	0.9356	0.0660
O16A	-0.8903(2)	0.1256(16)	0.8749(12)	0.0612(5)
C17A	-0.9599(4)	0.1917(3)	0.9417(2)	0.0784(9)
H17A	-0.8923	0.2597	0.9328	0.0940
C18A	-1.1254(4)	0.2322(3)	0.9291(2)	0.0767(9)
H18A	-1.1653	0.2876	0.9680	0.0920
H18B	-1.1184	0.2742	0.8633	0.0920
H17B	-0.9665	0.1431	1.0055	0.0940

[a] The standard deviations of the least significant digits are given in parentheses.

Table B1 (Continued).

Atoms	X	Y	Z	U_{eq}
O19A	-1.2377(2)	0.1395(18)	0.9532(14)	0.0718(5)
H19A	-1.2500(4)	0.0960(3)	0.9030(2)	0.1080
Molecule B				
C1B	-0.1148(3)	0.5774(2)	0.3298(16)	0.0458(5)
H1B1	-0.2291	0.5614	0.3520	0.0690
H1B2	-0.0553	0.5041	0.3363	0.0690
H1B3	-0.0930	0.6198	0.2642	0.0690
C2B	-0.0639(2)	0.6498(18)	0.3864(14)	0.0369(5)
N3B	-0.1188(2)	0.6265(15)	0.4846(12)	0.0356(4)
H3B	-0.1850(3)	0.5720(2)	0.5218(15)	0.0430
C4B	-0.0537(2)	0.7042(16)	0.5194(14)	0.0313(4)
N5B	0.0437(19)	0.7778(13)	0.4417(11)	0.0332(4)
C6B	0.0355(3)	0.7432 (18)	0.3601(15)	0.0393(5)
H6B	0.0893	0.7787	0.2984	0.0470
N7B	-0.0773(19)	0.7094(14)	0.6084(11)	0.0334(4)
C8B	0.0083(2)	0.8003(16)	0.6152(13)	0.0319(4)
C9B	0.1093(2)	0.8795(16)	0.5422(14)	0.0333(4)
C10B	0.1348(2)	0.8729(17)	0.4470(14)	0.0348(4)
O11B	0.2198(18)	0.9347(13)	0.3751(10)	0.0476(4)
N12B	0.1735(2)	0.9596(14)	0.5785(12)	0.0393(4)
C13B	0.1130(3)	0.9297(18)	0.6694(15)	0.0399(5)
H13B	0.1357	0.9696	0.7116	0.0480
N14B	0.0115(2)	0.8328(15)	0.6969(11)	0.0369(4)
C15B	-0.0669(3)	0.7764(2)	0.7944(15)	0.0429(5)
H15C	-0.1228	0.8362	0.8251	0.0520
H15D	-0.1477	0.7201	0.7941	0.0520
O16B	0.0437(3)	0.7161(18)	0.8465(13)	0.0442(5)
C17B	0.1091(5)	0.6150(3)	0.8140(2)	0.0504(8)
H17C	0.1618	0.6392	0.7472	0.0610
H17D	0.0218	0.5611	0.8208	0.0610
O16C	0.0020(8)	0.6593(6)	0.8223(4)	0.0407(13)
C17C	0.1673(13)	0.6693(10)	0.8267(7)	0.0510(2)
H17E	0.1748	0.7243	0.8647	0.0610
H17F	0.2328	0.6997	0.7633	0.0610
C18B	0.2286(3)	0.5536(3)	0.8687(18)	0.0649(7)
H18C	0.2931	0.4998	0.8345	0.0780
H18D	0.3017	0.6118	0.8732	0.0780
O19B	0.1569(3)	0.4902(2)	0.9595(14)	0.0943(8)
H19B	0.0846	0.5302	0.9839	0.1410

[a] The standard deviations of the least significant digits are given in parentheses.

Table B1 (Continued).

Atoms	X	Y	Z	U_{eq}
Water molecules				
O1W	0.3884(12)	0.4140(8)	0.0598(6)	0.0563(4)
H1WA	0.3618	0.4275	0.1253	0.0850
H1WB	0.3004	0.4376	0.0373	0.0850
H1WC	0.4582	0.4614	0.0263	0.0850
O2W	0.2876(12)	0.4599(8)	0.2310(6)	0.0795(6)
H2WA	0.3363	0.5166	0.2383	0.1190
H2WB	0.2345	0.4190	0.2762	0.1190
O3W	0.2820(12)	-0.0214(8)	0.1755(6)	0.0824(6)
H3WA	0.3487	0.0345	0.1541	0.1240
H3WB	0.2664	-0.0369	0.2442	0.1240
O4W	0.4737(12)	0.1708(8)	0.0733(6)	0.0972(7)
H4WA	0.4524	0.2370	0.0581	0.1460
H4WB	0.5717	0.1748	0.0504	0.1460

[a] The standard deviations of the least significant digits are given in parentheses.
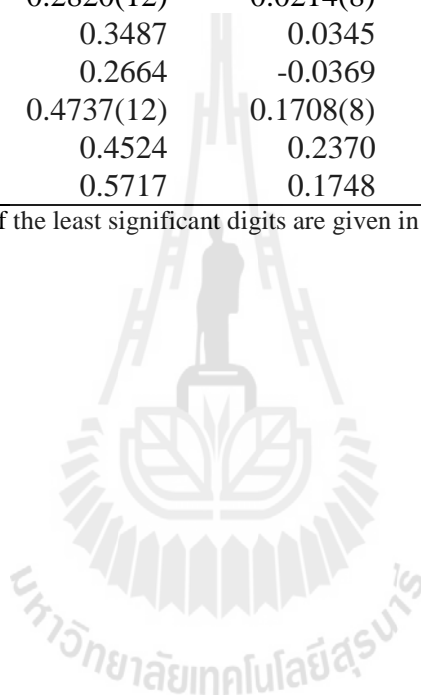
APPENDIX C

SUPPORTING INFORMATION CHAPTER V

Table C1 Fraction triclinic coordinates and equivalent atomic displacement

parameters[a] (Å^2) for tricyclic acyclovir, $C_{11}H_{13}N_5O_3 \cdot 2H_2O$.

Atoms	X	Y	Z	U_{eq}
Molecule A				
H1a1	-0.4862	0.2415	0.2722	0.077
H1a2	-0.6354	0.1662	0.3241	0.077
H1a3	-0.4667	0.1114	0.3188	0.077
H3a	-0.6532	0.0762	0.5079	0.049
H6a	-0.3871	0.3605	0.3840	0.049
H13a	-0.5473	0.2858	0.8887	0.061
H15a	-0.7000	0.0277	0.8531	0.067
H15b	-0.7064	0.0859	0.9330	0.067
H17a	-0.8947	0.2565	0.9330	0.095
H17b	-0.9657	0.1447	1.0026	0.095
H18a	-1.1634	0.2851	0.9668	0.093
H18b	-1.1192	0.2725	0.8664	0.093
H19a	-1.2320	0.1119	0.9074	0.110
Molecule B				
H1b1	-0.0762	0.6110	0.2656	0.070
H1b2	-0.2280	0.5741	0.3433	0.070
H1b3	-0.0733	0.5010	0.3453	0.070
H3b	-0.1870	0.5687	0.5195	0.043
H6b	0.0892	0.7783	0.2985	0.048
H13b	0.1358	0.9694	0.7115	0.048
H15c	-0.1238	0.8356	0.8249	0.052
H15d	-0.1471	0.7203	0.7936	0.052
H17c	0.1616	0.6393	0.7471	0.060
H17d	0.0216	0.5612	0.8208	0.060
H18c	0.2928	0.4998	0.8350	0.078
H18d	0.3017	0.6122	0.8732	0.078
H19b	0.0567	0.5006	0.9689	0.144

[a] The standard deviations of the least significant digits are given in parentheses.

Table C1 (Continued).

Atoms	X	Y	Z	U_{eq}
Molecule C				
H15e	-0.0524	0.8239	0.8361	0.052
H15f	-0.1827	0.7691	0.7993	0.052
H17e	0.1734	0.7243	0.8654	0.066
H17f	0.2326	0.7005	0.7639	0.066
H18e	0.2263	0.5035	0.8264	0.078
H18f	0.3419	0.5641	0.8680	0.078
H19c	0.2260	0.4648	0.9895	0.144

[a] The standard deviations of the least significant digits are given in parentheses.

Table C2 Least-squares mean plane[a] and deviations from the planes (Å) for tricyclic

acyclovir, $C_{11}H_{13}N_5O_3 \cdot 2H_2O$.

Plane 1: Plane of molecule A (RMSD of fitted atoms = 0.0206 Å)	
Plane 2: Plane of molecule B (RMSD of fitted atoms = 0.0064 Å)	

Molecule A; - 6.8373(37) x + 6.2359(59) y - 1.3304(46) z = 4.3111(33) Molecule B; -

6.6607(33) x + 6.4645(43) y - 2.2105(57) z = 3.7648(39)

Atoms	Molecule A	Molecule B
C2	0.0107(17)	0.0061(17)
N3	−0.0231(15)	0.0047(14)
C4	−0.0173(18)	−0.0037(17)
N5	0.0094(15)	−0.0038(15)
C6	0.0393(17)	0.0066(17)
N7	−0.0104(15)	−0.0074(14)
C8	0.0008(18)	−0.0060(17)
C9	−0.0200(19)	−0.0053(17)
C10	−0.0229(17)	−0.0084(16)
N12	−0.0149(17)	0.0023(15)
C13	0.0175(20)	0.0123(17)
N14	0.0310(16)	0.0027(15)
C1A[b]	−0.0129(29)	0.0039(27)
O11A[b]	−0.0545(24)	−0.0148(23)
C15A[b]	0.0938(33)	−0.0570(27)

[a] The standard deviations of the least significant digits are given in parentheses.
[b] Atom not used to define plane. The angle to previous plane = 4.43(7) Å.

APPENDIX D

PUBLICATION AND CONFERENCE PRESENTATIONS

D.1 Publication

Montha Meepripruk and Kenneth J. Haller (2011). Rerefinement of tricyclic acyclovir: $C_{11}H_{13}N_5O_3 \cdot 2H_2O$. *Acta Cryst.* (2011) A**67,** C761-C762.

D.2 Conference Presentation

D.2.1 Proceeding

1. Montha Meepripruk and Kenneth J. Haller.

    "Side chain disorder in 3-[(2-Hydroxyethoxy)-methyl]-6-methyl-3*H*-imidazolo[1,2-*a*]Purin-9(5*H*)-one dihydrate; $C_{11}H_{13}N_5O_3 \cdot 2H_2O$"

    International Annual Symposium for Computational Science and Engineering, ANSCSE15. March 30 – April 2, 2011, Bangkok, Thailand.

D.2.2 Oral Presentation

1. Montha Meepripruk and Kenneth J. Haller

    Solvation in 3-[(2-hydroxyethoxy)-methyl]-6-methyl-3*H*-imidazolo[1,2-*a*]purin-9(5*H*)-one dihydrate; $C_{11}H_{13}N_5O_3 \cdot 2H_2O$.

    International Annual Symposium for Computational Science and

Engineering, ANSCSE14. March 23–26, 2010. Mae Fah Luang University, Chiang Rai, Thailand.

2. Montha Meepripruk and Kenneth J. Haller.

"Side chain disorder in 3-[(2-Hydroxyethoxy)-methyl]-6-methyl-3*H*-imidazolo[1,2-*a*]Purin-9(5*H*)-one dihydrate; $C_{11}H_{13}N_5O_3 \cdot 2H_2O$"

at International Annual Symposium for Computational Science and Engineering, ANSCSE15. March 30–April 2, 2011, Bangkok, Thailand. Proceeding.

3. Montha Meepripruk and Kenneth J. Haller.

"Tricyclic acyclovir: concerted disorder through the water region"

to at the Young Crystallographers Satellite meeting, YCG. April 16th–17th, 2012. University of Warwick, England.

D.2.2 Poster Presentation

1. Montha Meepripruk and Kenneth J. Haller

Concerted disorder through the hydrate region of tricyclic acyclovir: $C_{11}H_{13}N_5O_3 \cdot 2H_2O$. The 10th Conference of the Asian Crystallographic Association, AsCA2010. October 31st–November 3rd, 2010. Busan, Korea.

2. Montha Meepripruk and Kenneth J. Haller

Supramolecular features of the antiherpes agent tricyclic acyclovir. The 2nd Conference of the NanoThailand 2010, November 18th–20 th, 2010, Pathumthani, Thailand.

3. Montha Meepripruk and Kenneth J. Haller.

 "Rerefinement of tricyclic acyclovir: $C_{11}H_{13}N_5O_3 \cdot 2H_2O$" to the

 International Union of Crystallography, IUCr. August 22th–30th, 2011,

 Spain, Won hydrogen bond award of G.A. Jeffery.

4. Montha Meepripruk and Kenneth J. Haller.

 "Supramolecular network of water molecules in acyclovir antiviral

 drugs" to the Pure and Applied Chemistry International, PACCON.

 January 11th–13th, 2011, Chiang Mai, Thailand.

5. Montha Meepripruk and Kenneth J. Haller.

 "Tricyclic acyclovir: concerted disorder through the water region"

 to at the Young Crystallographers Satellite meeting, YCG. April

 16th–17th, 2012. University of Warwick, England.

6. Montha Meepripruk and Kenneth J. Haller.

 "Water Structure in Two Acyclovir Systems" to the British

 Crystallographic Association Spring Meeting, BCA. April 17th–19th,

 2012, University of Warwick, England.

CURRICULUM VITAE

MONTHA MEEPRIPRUK

Date of Birth   16 November 1971

Place of Birth   Mueang, Kamphang Phet

Education

2004   M.Sc., Natural Resources and Environmental Management, Naresuan
            University, Thailand.

1994   B.Sc., Chemistry, Naresuan University, Thailand.

Publications

> **Montha Meepripruk** and Kenneth J. Haller (2011). Rerefinement of
> Tricyclic Acyclovir: $C_{11}H_{13}N_5O_3 \cdot 2H_2O$. *Acta Cryst.* (2011) A**67,** C761–
> C762.

Awards

2010   Bursary Student Awards from the 10th Conference of the Asian
            Crystallographic Association, 2010, Korea.

2011   G.A. Jeffery Student Travel Award from Pittsburgh Diffraction Society
            at the International Union of Crystallography, 2011, Spain.

Grants and Fellowships

> Kamphang Phet Rajabhat University Grant, Thailand, 2009.

Position and Place of Work

2005–Now   Lecturer, Kamphang Phet Rajabhat University, Kamphang Phet,
            Thailand.